The evolution of neuronal progenitor cell division in mammals: The role of the abnormal spindle-like microcephaly associated (Aspm) protein and epithelial cell polarity

Dissertation for the attainment of the academic degree of *Doctor rerum naturalium*
Given by the Fakultät *Mathematik und Naturwissenschaften* of the Technische Universität Dresden

Jennifer Fish

Born on the 7th of May, 1972 in Mansfield, Ohio (USA)

Table of contents

Summary

Summary

Among mammals, primates are exceptional for their large brain size relative to body size. Relative brain size, or encephalization, is particularly striking among humans and their direct ancestors. Since the human-chimp split 5 to 7 million years ago, brain size has tripled in the human lineage (Wood & Collard 1999). The focus of this doctoral work is to investigate some of the cell biological mechanisms responsible for this increase in relative brain size. In particular, the processes that regulate symmetric cell division (ultimately generating more progenitors), the constraints on progenitor proliferation, and how neural progenitors have overcome these constraints in the process of primate encephalization are the primary questions of interest. Both functionally analyses in the mouse model system and comparative neurobiology of rodents and primates are used here to address these questions.

Using the mouse model system, the cell biological role of the Aspm (abnormal spindle-like microcephaly associated) protein in regulating brain size was investigated. Specifically, Aspm function in symmetric, proliferative divisions of neuroepithelial (NE) cells was analyzed. It was found that *Aspm* expression in the mouse neuroepithelium correlates in time and space with symmetric, proliferating divisions. The Aspm protein localizes to NE cell spindle poles during all phases of mitosis, and is down-regulated in cells that undergo asymmetric (neurogenic) cell divisions. *Aspm* RNAi alters the division plane in NE cells, increasing the likelihood of premature asymmetric division resulting in an increase in non-NE progeny. At least some of the non-NE progeny generated by *Aspm* RNAi migrate to the neuronal layer and express neuronal markers. Importantly, whatever the fate of the non-NE progeny, their generation comes at the expense of the expansion of the proliferative pool of NE progenitor cells.

These data have contributed to the generation of an hypothesis regarding evolutionary changes in the regulation of spindle orientation in vertebrate and mammalian neural progenitors and their impact on brain size. Specifically, in contrast to invertebrates that regulate the switch from symmetric to asymmetric division through a rotation of the spindle (horizontal versus vertical cleavage), asymmetric NE cell division in vertebrates is accomplished by only a slight deviation in the cleavage plane away from the vertical, apical-basal axis. The requirement for

the precise alignment of the spindle along the apical-basal axis in symmetric cell divisions may have contributed to selection on spindle "precision" proteins, thus increasing the number of symmetric NE cell division, and contributing to brain size increases during mammalian evolution.

Previous comparative neurobiological analyses have revealed an increase in basally dividing NE cells in the brain regions of highest proliferation and in species with the largest brains (Smart 1972a,b; Martinez-Cerdeno et al. 2006). The cell biological characteristics of these basally dividing cells are still largely unknown. We found that primate basal progenitors, similar to rodent apical progenitors, are Pax6+. This suggests that primate basal progenitors may share other properties with rodent apical progenitors, such as maintenance of apical contact. Our previous finding that artificial alteration of cleavage plane in NE cells affects their ability to continue proliferating supports the hypothesis that the apical membrane and junctional complexes are cell fate determinants (Huttner & Kosodo 2005). As such, the need to maintain apical membrane contact appears to be a constraint on proliferation (Smart 1972a,b; Smart et al. 2002). Together, these data favor the hypothesis that primate basally dividing cells maintain apical contact and are epithelial in nature.

I. Introduction

I Brain Size and Evolution

Mammals are a class of vertebrates recognized for their elaborate social behaviors and intelligence (Figure 1A). Correspondingly, large brain size relative to body size, or encephalization, has evolved in multiple mammalian lineages. The evolution of relatively large brains is particularly evident in the primate lineage, especially among humans and their recent ancestors. The human brain is roughly 3 times as large as the chimp brain, which is remarkable given the similar body size of these two species (Figure 1B). The evolutionary mechanisms responsible for this dramatic increase in brain size have been the basis of scientific research for decades. To fully understand the pattern and process of brain size evolution, it is useful to consider this question in its historical context. The mechanisms involved in the development of the vertebrate central nervous system (CNS) have provided the foundation for subsequent evolutionary change. From this basis, the cell biological processes regulating proliferation, as well as proliferative constraints, can be interpreted in order to understand the evolutionary changes that have generated the exceptional human brain.

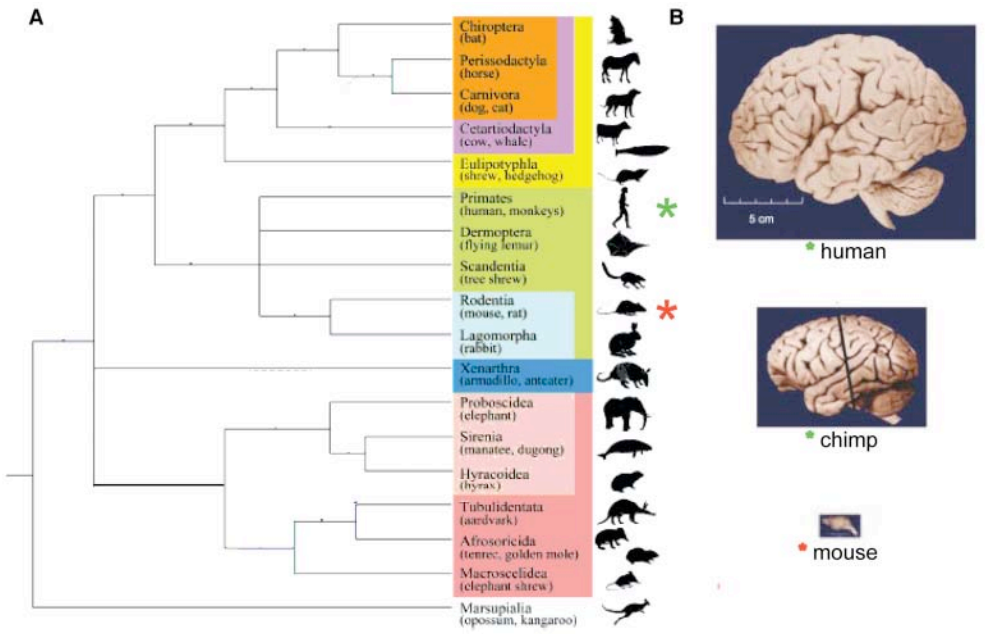

Figure 1: Evolution and brain size in mammals. **A**, Mammalian phylogeny showing the evolutionary relationships of the mammalian orders. Primates (green asterisk) and Rodentia (red asterisk), the primary orders discussed in this thesis, are highlighted. Image modified from Nishihara et al. 2006. **B**, Lateral views of adult human, chimp and mouse brains showing their relative size. Green and red asterisks reflect the position of these species on the phylogeny presented in **A**. Scale bar, 5 cm. Images modified from Hill & Walsh 2005.

I – 1. Development of the Vertebrate Brain

I – 1.1. From neural plate to neural tube

The first recognizable manifestation of the brain in the developing vertebrate embryo is the neural plate. The neural plate is induced from the underlying mesoderm, and progressively differentiates along a rostral to caudal gradient. Initially, the neural plate consists of a monolayer of cuboidal neuroepithelial (NE) cells exhibiting both apical-basal polarity and planar cell polarity (Strutt 2003; Wang et al. 2006). Apical-basal polarity in NE cells is manifested by apical and basolateral membrane compartments with distinct lipid and protein content that are separated by tight junctions (Aaku-Saraste et al. 1996).

At the onset of neurulation, the neural plate invaginates, creating the neural groove. The lateral margins of this groove extend outward into neural folds. These lateral neural folds initially grow convexly into a bulge that faces opposite to the direction of neural tube closure. Convexity is reversed, at least in part, by the elongation of NE cells which reduces their apical area (Jacobson & Tan 1982). This process lengthens and narrows NE cells, leading to convergent extension of the neural plate, resulting in neural tube closure and internalization of the central nervous system. Signaling via the Sonic hedgehog and non-canonical Wnt pathways are required for convergent extension and neural tube closure (Copp et al. 2003; Doudney & Stainer 2005; Wang et al. 2006; Ybot-Gonzalez et al. 2007).

Fusion of the neural tube involves a change in the expression of cell adhesion molecules (CAMs). After neural induction, NE cells up-regulate N-cadherin and N-CAM (Thiery et al. 1982). This change in cell-adhesive properties mediates homotypic interaction between NE cells and inhibits their fusion with the adjacent mesodermal cells. Neural tube closure is also associated with a down-regulation of some of the epithelial characteristics of NE cells, such as the loss of functional tight junctions (Aaku-Saraste et al. 1996).

Although NE cells of the neural plate are proliferating (undergoing symmetric divisions that generate two progenitor cells), they are neither homogenous nor static. At the one-somite stage, prior to neural tube closure, the three primary vesicles of the mouse brain can already be distinguished (Figure 2). From rostral to caudal, these are the prosencephalon (the forebrain), the mesencephalon (midbrain), and the

rhombencephalon (the hindbrain). The prosencephalon is later subdivided into two structures, the diencephalon and the larger, more anterior telencephalon. The rhombencephalon also divides into the metencephalon (pons) and the mylencephalon (medulla). The boundaries between these vesicles are molecularly characterized by the nested expression of the paired-box containing transcription factors Pax2/5 and Pax6 (Walther & Gruss 1991; Rowitch & McMahon 1995; Schwarz et al. 1999).

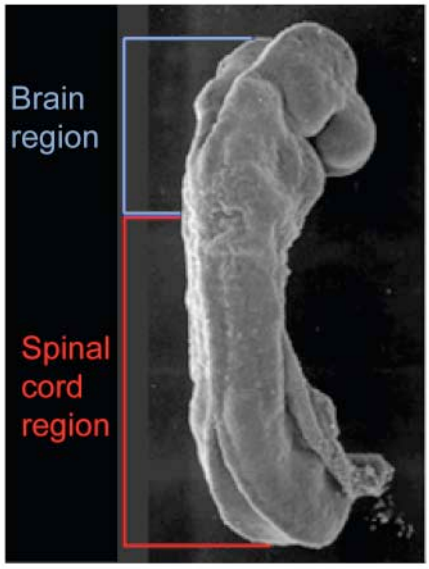

Figure 2: The primary vesicles of the developing brain. Scanning electron micrograph of an E8.5 mouse embryo, prior to completion of neural tube closure, and showing the two major regions of the developing CNS, the brain region in blue and the spinal cord region in red. The primary vesicles of the developing brain can be clearly distinguished at this developmental time point. Image modified from www.med.unc.edu.

I – 1.2. From neural tube to neurogenesis

In the mouse, neural tube closure occurs in approximately 12 hours, beginning at the 6-somite stage (~E8.25) in the cervical region at the boundary of the prospective brain and spinal cord, and completing by the 19-somite stage (~E8.75; Jacobson & Tam 1982). After neural tube closure, the neuroepithelium appears as a thin sheet of cells lining the ventricles of the prospective brain (Figure 3A). The apical surface of NE cells is exposed to the ventricles whereas their basal processes adhere to the basement membrane.

As development proceeds, NE cells proliferate and elongate, progressively forming a pseudo-stratified tissue with multiple cell nuclei occupying different positions over the apical membrane (Figure 3B). Pseudo-stratification of the neuroepithelium is mediated by interkinetic nuclear migration (INM), a cell-cycle

coordinated nuclear movement across the epithelium (Sidman & Rakic 1973). Progenitor cell nuclei migrate from the apical surface to the basal pia in G1 of the cell cycle, replicate their DNA in S-phase at the basal side of the neuroepithelium, and finally return to the apical surface during G2 where they will undergo mitosis (Figure 3C).

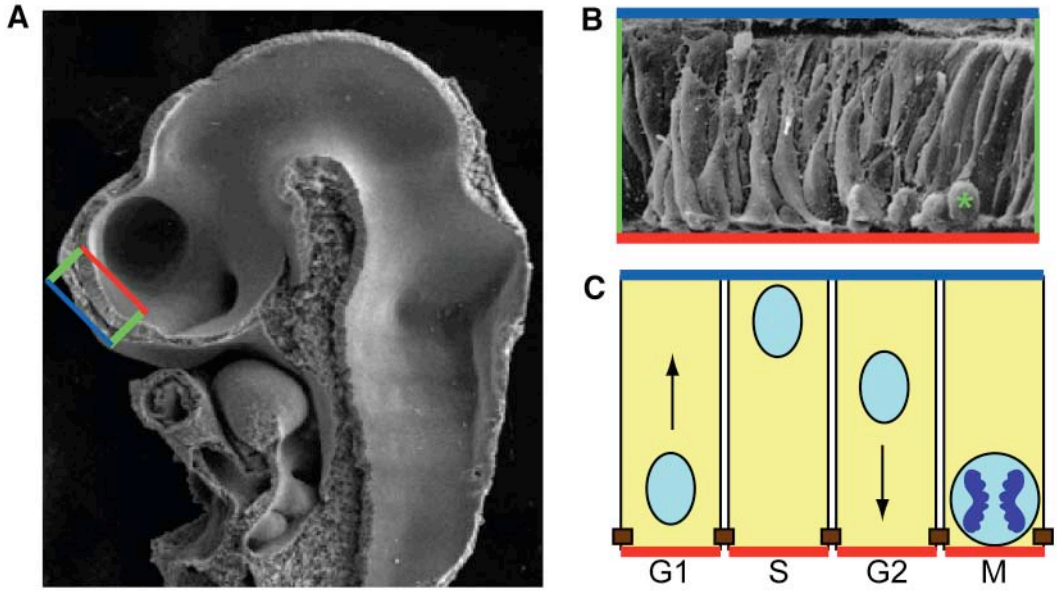

Figure 3: The neuroepithelium and NE cells. **A**, Scanning electron micrograph of a sagittal section through an E9.5 mouse embryo showing the neuroepithelium and the lumen of the neural tube. The area highlighted by the rectangle is enlarged in **B**. **B**, Scanning electron micrograph of the neuroepithelium from the telencephalon of an E9.0 mouse embryo. The upper, blue border of the rectangle signifies the basal pole of the neuroepithelium and the lower, red border of the rectangle marks the apical side. The green asterisk identifies a mitotic cell at the apical surface. Images in **A** and **B** are modified from www.med.unc.edu. **C**, A schematic cartoon representing the interkinetic nuclear migration of NE cells. Cell nuclei, shown in light blue, migrate from the apical surface (red line) to the basal pia (blue line) in G1 of the cell cycle, replicate their DNA in S-phase at the basal side of the neuroepithelium, and finally return to the apical surface during G2 where they will undergo mitosis. Image concept following from A. Attardo, unpublished.

NE cells experience three basic types of cell division. A symmetric, proliferative NE cell division generates two NE progenitors, resulting in amplification of the progenitor pool (Figure 4A). Shortly after neural tube closure, a subset of NE cells begin to divide asymmetrically, generating one progenitor and one post-mitotic neuron (Figure 4B). Finally, neural progenitors are consumed in symmetric, neurogenic divisions (Figure 4C). The onset of neurogenesis begins in the hindbrain and proceeds through the central nervous system (CNS) in a wave-like fashion. The telencephalon, which occupies the most anterior position in the CNS, is the last region to initiate neurogenesis, doing so around E10.5.

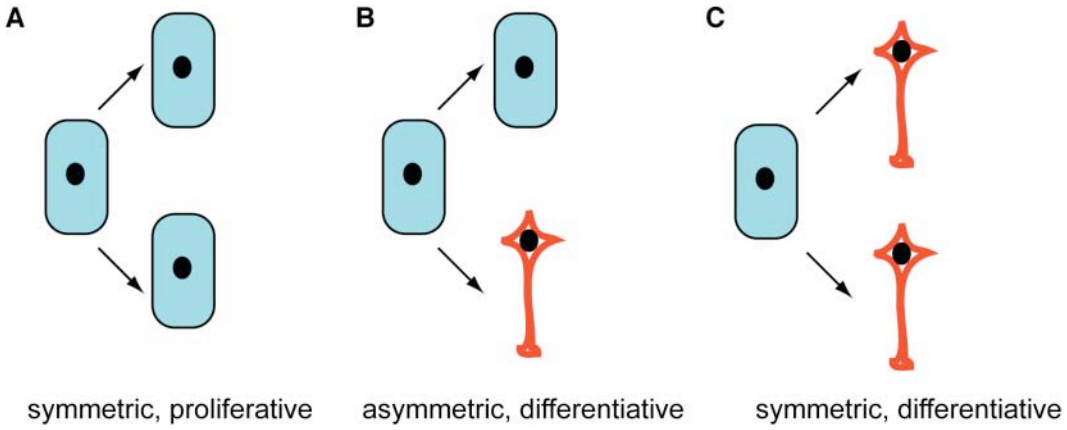

Figure 4: Divisions of NE cells. NE cells experience three basic types of cell division. A, Symmetric, proliferative NE cell division generates two NE progenitors, resulting in amplification of the progenitor pool. B, Asymmetric, differentiative divisions generate one progenitor and one post-mitotic neuron. C, Symmetric, differentiative divisions generate two post-mitotic neurons. Image concept following from Götz & Huttner 2005.

I – 1.3. The vertebrate telencephalon

The telencephalon ultimately gives rise to the cerebral hemispheres, the region of the brain that has experienced the greatest evolutionary increase in size and complexity (Figure 5). In mammals, the telencephalon can be subdivided into 4 structures: the isocortex (also referred to as neocortex), the hippocampus, and the olfactory cortex, which constitute the dorsal telencephalon, and the striatum (ganglion eminences) of the ventral telencephalon. Amphibians have the simplest brain organization of all vertebrates, with no large cell masses and little neuronal migration. Reptilian brains are slightly more complex, having a three-layered cortex, but are still relatively small. The medial and dorsomedial regions of the reptilian brain are homologous to the mammalian hippocampus, the lateral cortex corresponds to the olfactory cortex, and the dorsal cortex is the homologue of the mammalian isocortex (Aboitiz et al. 2002).

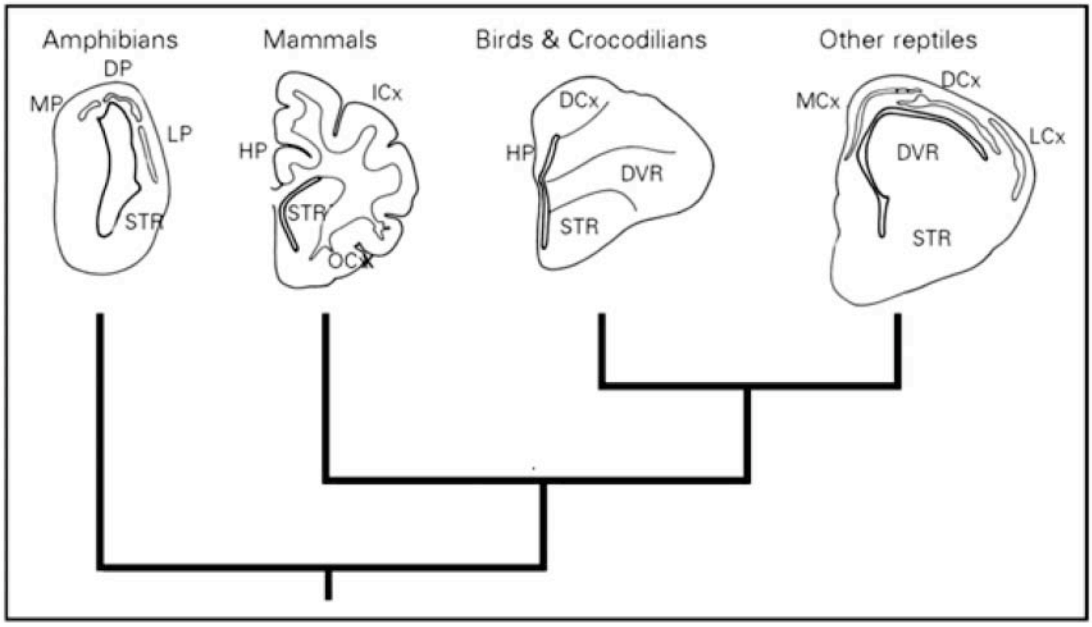

Figure 5: Major regions of the cerebral cortex in terrestrial vertebrates. A cladogram of the major classes of terrestrial vertebrates, showing a schematic drawing of a cerebral hemisphere from a representative species. DCx: Dorsal cortex; DP: Dorsal pallium; DVR: Dorsal ventral ridge; HP: Hippocampus; ICx: Isocortex; LCx: Lateral cortex; LP: Lateral pallium; MCx: Medial cortex; MP: Medial pallium; OCx: Olfactory cortex; STR: striatum. Image modified from Aboitiz et al. 2002.

It is the evolution and expansion of the isocortex, in particular, that is often associated with the intelligence and social complexity of mammals. The isocortex is a derived feature of the mammalian brain that can be distinguished from the less complex areas of the dorsal telencephalon (the hippocampus and olfactory cortex) as well as the reptilian cortex by two critical features (Aboitiz et al. 2001). First, the mammalian isocortex is characterized by a six-layered architecture, which develops from an inside-out neurogenic gradient. In contrast, the reptilian dorsal cortex is a three-layered structure that develops from an outside-in gradient. Non-isocortical regions of the mammalian dorsal telencephalon have an intermediate structure: the hippocampus and dentate gyrus both have only three layers, but the hippocampus develops inside-out whereas the dentate gyrus retains the ancestral outside-in gradient.

A second unique feature of the mammalian isocortex is the tremendous increase in surface area it has undergone in the mammalian lineage. For example, the surface area of the human cortex is 1000 fold greater than that of a mouse, but is only 3-5 times as thick (Rakic 1995). This pattern of morphological change indicates that brain size increases have resulted from a lateral, rather than radial, expansion of the neuroepithelium.

I – 2. Development of the Mammalian Isocortex

I – 2.1. Origin and migration of cortical neurons

The mammalian isocortex is composed of two basic types of neurons, inhibitory local circuit interneurons and excitatory pyramidal neurons (Anderson et al. 1999). Inhibitory interneurons, also called GABAergic interneurons, form local synaptic connections and release the neurotransmitter Gamma Amino Butirric Acid (GABA) (Gupta et al. 2000). Importantly, the vast majority of GABAergic interneurons are not born in the isocortex, but migrate tangentially into the dorsal telencephalon from their point of origin in the ganglionic eminences (Anderson et al. 1997; Letinic et al. 2002). This migration is dependent upon the expression of the homeodomain proteins Dlx-1 and Dlx-2 (Anderson et al. 1997). In rodents, interneurons comprise only 15-30% of all isocortical neurons (Parnavelas et al. 1977).

Pyramidal neurons, also often referred to as projection neurons or glutamergic neurons, project their axons to distant targets and excite via the neurotransmitter glutamate. Pyramidal neurons are born locally in the isocortex and migrate basally to the cortical plate (Rakic 1988; Tan et al. 1998). Although all pyramidal neurons migrate to the cortical plate along the processes of radial glia, they derive from several distinct progenitors that occupy different germinal layers in the isocortex.

I – 2.2. Isocortical germinal layers

The mammalian isocortex is composed of two germinal layers: the ventricular zone (VZ), and the subventricular zone (SVZ), which lies basal to the VZ (Figure 6). The VZ contains at least two molecularly distinct progenitors, NE cells and radial glia (RG) cells. Both NE and RG cells have apical and basal processes, however, NE cell processes do not always contact the pia (Götz & Huttner 2005). Progenitors of the SVZ lack processes, and as a consequence, are rounded and randomly organized (Miyata et al. 2004; Attardo et al. in prep.). Until recently, progenitors of the SVZ were thought to give rise to glia, not neurons (Altman & Bayer 1990; Takahashi et al. 1995). Recent imaging and lineage analyses have revealed that SVZ progenitors can also produce neurons (Haubensak et al. 2004; Miyata et al. 2004; Noctor et al. 2004).

These basal progenitors, or intermediate progenitor cells (IPCs), typically divide only once in a symmetric division that generates two neurons (Noctor et al. 2004; Attardo et al. in prep.).

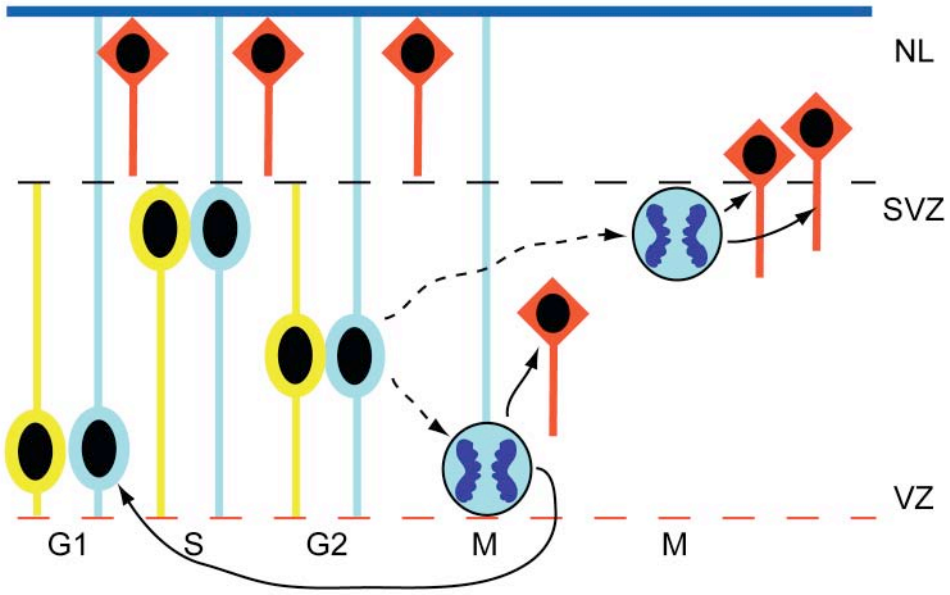

Figure 6: Progenitors and germinal layers of the neuroepithelium. The mammalian neuroepithelium has two germinal layers, the ventricular zone (VZ) and the subventricular zone (SVZ). NE cells (shown in yellow) and radial glia (RG) cells (shown in blue) have elongated processes and divide at the apical surface. Asymmetric NE or RG cell divisions can generate either one RG/NE progenitor and one post-mitotic neuron (shown in red), or one RG/NE progenitor and one intermediate progenitor (IPC) that will divide in the SVZ to generate two post-mitotic neurons. Apical cell divisions are only shown for the blue RG cell, but are similar for the yellow NE cell. The red dashed line represents the apical membrane, the solid blue line represents the basal pia, and the black dashed line separates the germinal layers from the neuronal layer (NL). Image concept following from A. Attardo, unpublished.

Given these data, the contribution of IPCs to different cortical layers and their general role in brain size and evolution has been a topic of much interest. The molecular identity of IPCs suggests that they contribute neurons predominantly to the upper, supergranular layers of the cortical plate. In particular, *Svet1* and *Cux2*, which have been shown to be reliable markers of upper layer neurons, are initially expressed in the SVZ (Tarabykin et al. 2001; Zimmer et al. 2004). Similarly, Englund and colleagues (2005) have shown that Tbr2 is a molecular marker of IPCs. Importantly, their data suggests a distinct molecular identity for IPCs. In contrast to apically dividing NE cells expressing Pax6, basal neurogenic progenitors are characterized by Tbr2 expression (Englund et al. 2005). Since *Tbr2* is also predominantly expressed in the SVZ, this correlation has contributed to the hypothesis that IPCs generate upper layer neurons. It should be noted, however, that IPCs are present in the telencephalon

from the onset of neurogenesis (Haubensak et al. 2004). Additionally, Miyata and colleagues (2004) concluded that IPCs were the major source of deep layer neurons, and that their early generation may be important for the initial development of the cortical plate.

I – 2.3. Isocortical layering

The first neurons to settle in the isocortex form the loosely arranged preplate, or primordial plexiform layer (PPL), a prominent and transient association of cells. Subsequent waves of radially migrating neurons give rise to the cortical plate, which will become the mature six-layered isocortex. The preplate consists of Cajal-Retzius (C-R) cells, GABAergic neurons, pioneer neurons, and predecessor neurons (Meyer et al. 2000; Bystron et al. 2006). Most preplate neurons are derived from the ventral telencephalon and migrate tangentially into the isocortex. Although these cell populations largely disappear late in development due to apoptosis, they have important roles during corticogenesis, particularly for radial migration.

The cortical plate forms within the preplate, splitting it into a superficial marginal layer, which is the future layer 1, and a deeper subplate. The cortical plate forms in an inside-out gradient, with early born neurons occupying the deep layers, and later born neurons migrating past them to settle in more superficial layers (Figure 7A). The most predominant cells of the preplate are the C-R cells, which secrete Reelin, an extracellular matrix protein that is believed to stop migrating neurons and detach them from radial glia (D'Arcangelo et al. 1995). In reeler mutant mice, in which Reelin is not expressed, the preplate fails to split and neurons are arranged inversely, in an outside-in gradient (Figure 7B; Caviness 1973; Rakic & Caviness 1995; Lambert de Rouvroit & Goffinet 1998).

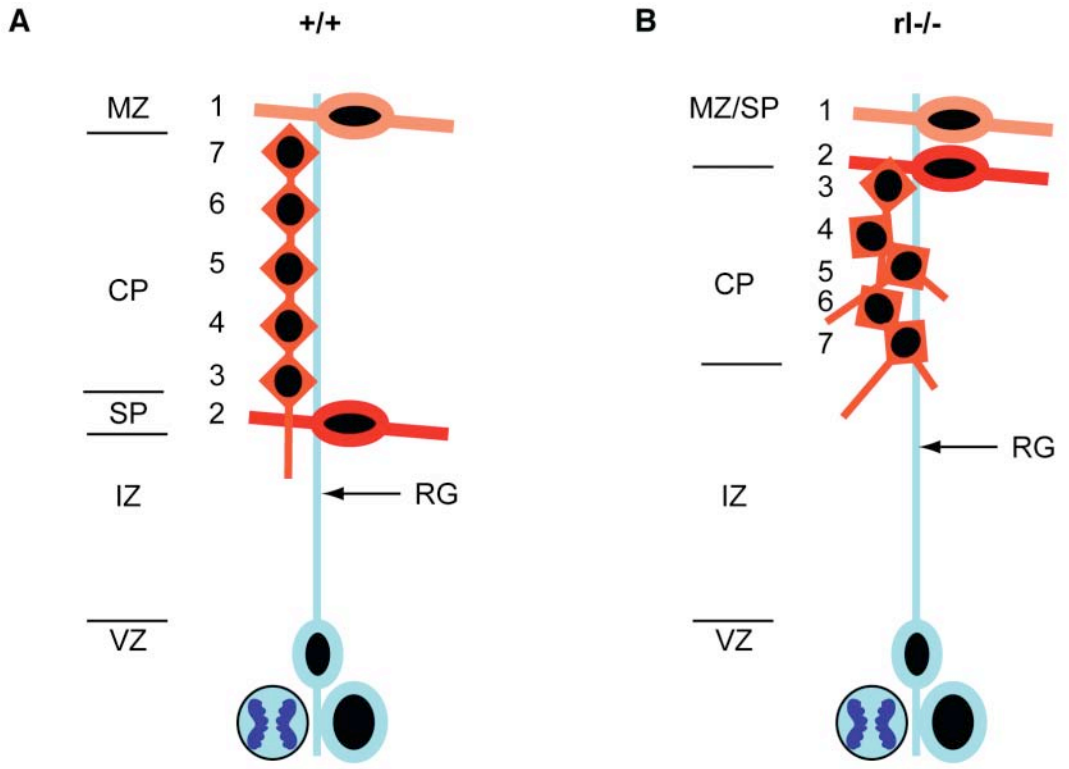

Figure 7: Cortical layering in normal, A, and reeler mutant, B, mice. **A**, Wild-type mouse cortex (+/+). The first neurons to arrive in the isocortex form the marginal zone and sub-plate. Subsequent neurons born at the ventricular surface migrate basally along radial guides and settle in the cortical plate in an inside-out gradient. The birthdate of the neurons is represented by the number on their left. Late born neurons migrate past earlier born neurons and settle in the upper layers of the cortex. **B**, Reeler mutant cortex (rl –/–). Radially migrating neurons are disorganized, fail to split the sub-plate and align inversely to wildtype, with late born neurons occupying the deep layers of the cortical plate. CP: cortical plate; IZ: intermediate zone; MZ: marginal zone; RG: radial glia; SP: sub-plate; VZ: ventricular zone. Image modified from Aboitiz et al. 2001.

Reelin is necessary but not sufficient for the formation of the inside-outside neurogenic gradient. Reelin is secreted into the extracellular matrix by C-R neurons of the MZ. The response to the Reelin signal by migrating neurons in the cortical plate requires at least one of two lipoprotein receptors, the VLDLR (very low density lipoprotein receptor) or ApoER2 (apolipoprotein E receptor type-2) and the intracellular adaptor, Dab1 (Disabled 1) (Trommsdorff et al. 1999; Howell et al. 1997; Sheldon et al. 1997; Ware et al. 1997). Reelin binds to the ligand binding domains of VLDLR or ApoER2. Subsequently, Dab1 binds to the cytoplasmic tails of the lipoprotein receptors and initiates the signal transduction pathway (Trommsdorff et al. 1998, 1999). VLDLR and ApoER2 are expressed by migrating neurons in the cortical plate in a partially redundant manner, and are both capable of responding to the stop signal conferred by Reelin, which tells neurons to detach from their radial guide and prevents them from invading layer 1 (Trommsdorff et al. 1999).

I – 3. Evolution of the Mammalian Isocortex

I – 3.1. Evolutionary increase in the SVZ and upper layer neurons

The SVZ is non-existent or rudimentary in lizards (Goffinet 1983), turtles (Martinez-Cerdeno et al. 2006), and chick (Molnar et al. 2006). In mammals, the size of the SVZ correlates with brain size, a trend that is particularly evident in primates (Figure 8, right panel). The increase in SVZ cellular density correlates with increasing thickness of the upper neuronal layers. In rodents and primates, neuronal layers V and VI are similar in thickness. In contrast, layers II, III, and IV of the primate cortex are obviously thicker than their rodent counterparts (Figure 8B,C). These comparative neuroanatomical data suggest that the SVZ is a mammalian specific germinal zone, and that SVZ expansion may have been an important contributor to brain size evolution (Molnar et al. 2006). Expansion of the SVZ in primates is such that the SVZ can be sub-divided into the inner SVZ (ISVZ) and the outer SVZ (OSVZ) (Figure 8D; Smart et al. 2002).

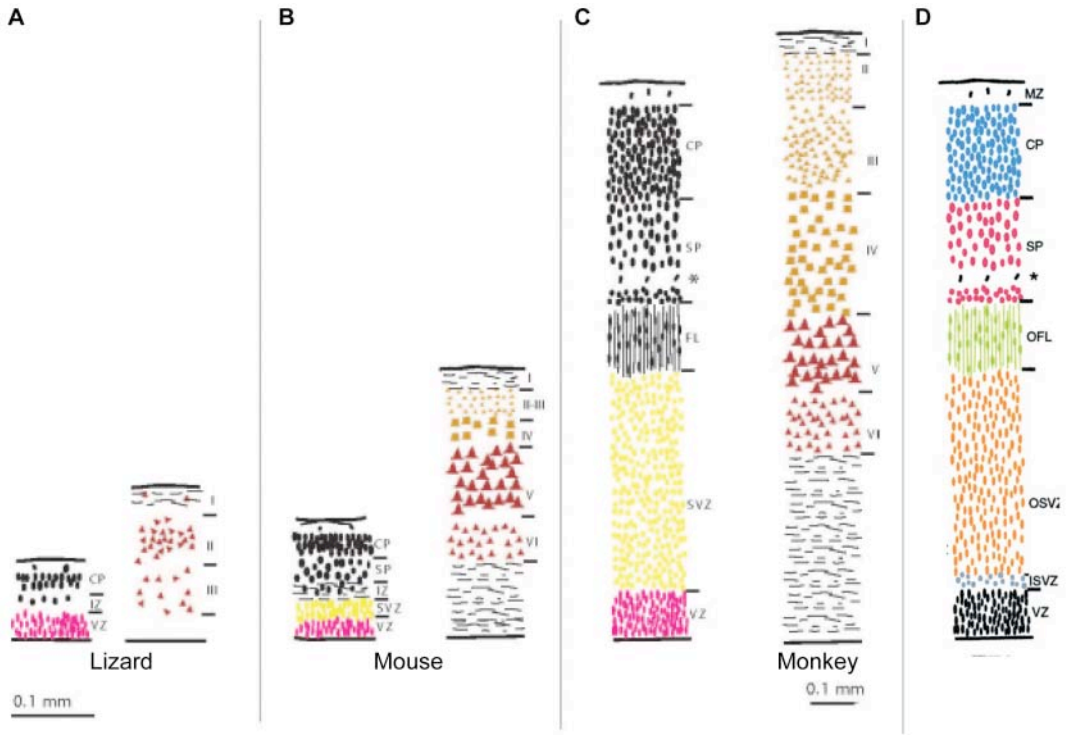

Figure 8: The SVZ and upper layer neurons. The relationship between SVZ density and cortical thickness and complexity in a lizard (**A**), mouse (**B**), and monkey (**C**). The images represent the germinal layers during mid-neurogenesis (left panels) and the cortical layers of an adult brain (right panels). Note that the increasing thickness and diversity of the adult neuronal layers correlates with the increasing density of the SVZ (yellow cells) during development. **D**, The neuroepithelium of a monkey at mid-neurogenesis, showing the SVZ sub-divided into the ISVZ and the OSVZ. Image in **A**, **B**, and **C**, modified from Molnar et al. 2006. Image in **D** modified from Smart et al. 2002.

I – 3.2. Evolutionary increase in cortical interneurons

Recent experimental data from primate species reveal the increasing importance of GABAergic interneurons to brain size and function. During primate evolution, GABAergic interneurons have increased in number, complexity, and proportion relative to projection neurons (Hendry et al. 1994; Jones 1993; Letinic et al. 2002). In contrast to rodents where 95% of GABAergic interneurons tangentially migrate into the dorsal telencephalon, in humans, only 35% of GABAergic interneurons are born in the GE and arrive to the cortical plate via radial migration (Letinic et al. 2002). This change in origin is reflected by a change molecular identity. Similar to rodents, GABAergic interneurons of the human isocortex express DLX1/2, however, the subpopulation of interneurons that are born in the dorsal telencephalon also express MASH1 (Letinic et al. 2002).

These data indicate the increasing importance of the radial migration of neurons generated locally from the progenitors in the VZ/SVZ for the evolution of brain size in primates, which is also reflected by changes in regulation of the Reelin signaling pathway. The inside-out neurogenic gradient is unique to mammals, but Reelin expression is not. Reelin positive neurons are present in all vertebrates examined, irrespective of isocortex architecture and neuronal migration patterns (Molnar et al. 2006). Rather, the importance of Reelin in cortical evolution is indicated by the increasing intensity of its expression with increasing cortical complexity (Bar et al. 2000). C-R cells increase in number and morphological complexity during mammalian evolution (Molnar et al. 2006). In particular, the human marginal zone expresses an exceptionally high level of Reelin signal (Meyer et al. 2000).

Despite the relative increase in number of radially migrating neurons in primate corticogenesis, tangentially migrating neurons also play an important evolutionary role. In rodents, generation of layer 1 neurons occurs only during a limited time early in neurogenesis. In contrast, neurons of layer 1 are continuously generated throughout primate corticogenesis (Zecevic & Rakic 2001; Rakic & Zecevic 2003; Smart et al. 2002). These neurons are born in the ventral telencephalon and are likely immune to the Reelin signaling pathway, allowing them to integrate into the superficial layer 1 (Zecevic & Rakic 2001).

I – 3.3. Evolutionary increase in surface area

The above data highlight critical morphological changes that have occurred during the evolution of the mammalian isocortex. In particular, changes in preplate (layer 1) structure and function and the appearance of the inside-out neurogenic gradient provided the basis for the evolution of cortical size. However, these changes largely reflect the organization of cortical neurons and the thickness of the cortical plate. So then, what are the changes that produced more cortical neurons and resulted in the lateral expansion of the cortex?

Early in development, NE cells proliferate via symmetric cell divisions. At the onset of neurogenesis, NE cells generate neurons through asymmetric divisions (see Figure 4). Whereas symmetric divisions result in an exponential expansion of progenitor cells, asymmetric divisions result in a linear increase in neuronal number while maintaining the progenitor population. Consequently, a delay in the timing of the switch between symmetric, proliferative and asymmetric, differentiative divisions will affect the final number of neurons generated (Figure 9). Delayed differentiation, as a mechanism to generate more progenitors, forms the basis of several prominent hypotheses offered to explain lateral expansion, however, there are important differences in the hypothesized processes responsible for this delay.

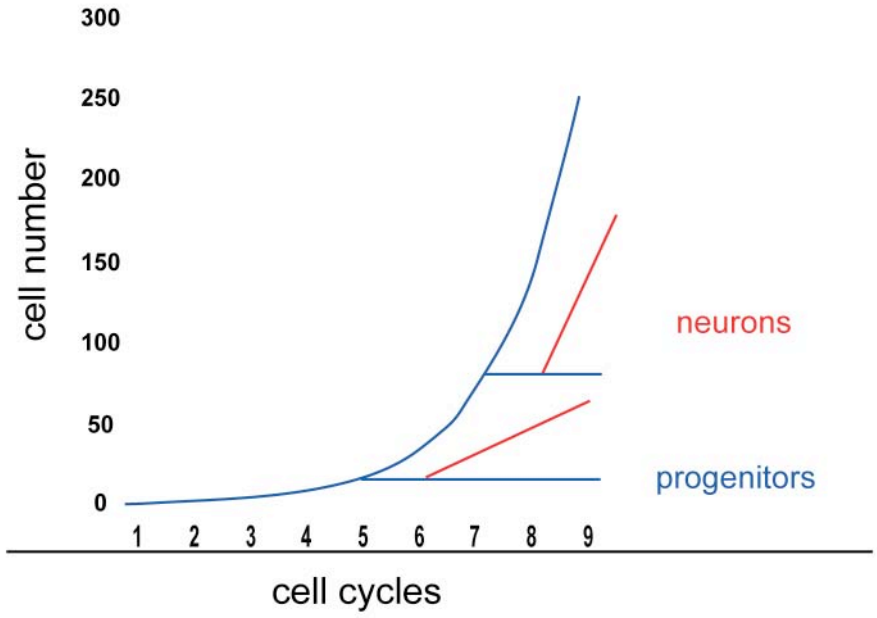

Figure 9: The number of neurons generated within a given number of cell cycles depends on the timing of the switch between symmetric and asymmetric cell divisions. Initially, NE cell progenitors increase exponentially via symmetric cell division (represented by the blue line). At the onset of neurogenesis, asymmetric divisions generate one progenitor and one neuron (represented by

the red line), resulting in maintenance of the progenitor population and a linear increase in neurons. An early switch from symmetric to asymmetric divisions generates fewer neurons than a late switch. Image modified from W. B. Huttner, unpublished.

I – 4. Lateral Expansion: Hypotheses and Processes

I – 4.1. The radial unit hypothesis and Smart's two rules

In the early 1970's, Ian Smart specifically addressed the question of how the CNS generates more cells, and offered the following two rules: 1) In order to produce the maximum number of nerve cells in a given number of generations differentiation must be delayed, and 2) Given the pseudostratified nature of the ependymal layer, proliferation without a corresponding increase in area of the central canal will lead to a disproportion between cell number and canal surface such that cell production will decrease unless the apical migration of mitotic figures characteristic of the layer is discontinued and nuclei are free to go into mitosis away from the central canal surface (Smart 1972a,b).

Echoing Smart's first rule, Pasko Rakic considered neural proliferation to occupy two phases. The first is the proliferative phase where symmetric divisions predominate, and the second reflects the period of asymmetric, differentiative divisions (Rakic 1995). His hypothesis is that the length of the first phase establishes the number of radial units in the cortex (Figure 10A), and the length of phase two determines column thickness (Figure 10B). The emphasis here is on the number of precursors, or founder cells, generated before the onset of neurogenesis, each of which will generate one cortical column.

Rakic's "radial unit" hypothesis and Smart's two rules essentially agree on the primary issue that differentiation must be delayed. There are, however, two other important points embedded in these hypotheses. First, Rakic uses the term radial unit to emphasis the highly organized, radial structure of the cortical plate. He also emphasizes the obvious, but not trivial, morphological feature of the cortex that it develops as a sheet, rather than as a lump. The radial unit hypothesis accounts for this morphological feature. The second point comes from Smart's second rule, which emphasizes his observation that the number of basal mitoses increases in areas of higher cell production. He explicitly notes the possibility that apical membrane space may act as a constraint on cell proliferation.

The suggestion that apical membrane space acts as a constraint on cell proliferation has been elaborated on in two opposing hypotheses. The first comes from Smart himself, and is based on comparisons between rodent and primate neuroepithelia. Smart and colleagues (2002) noticed that the SVZ in primates, while vastly increased compared to rodents, actually consists of two distinct cell types (see Figure 8d). The first, the ISVZ consists of randomly organized cells and appears similar to the SVZ of rodents. The second layer, the OSVZ, consists of more organized, radially aligned cells, similar to those of the VZ. Based on this observation, Smart and colleagues (2002) have hypothesized that the OSVZ may derive from progenitors of the VZ that no longer move their nucleus inter-kinetically. Consequently, NE cells of the OSVZ may maintain their epithelial characteristics, including radial alignment and contact to both the apical membrane and basal pia. By dividing basally, OSVZ nuclei avoid mitotic congestion at the apical surface, allowing more progenitors to accumulate per apical membrane area (Smart et al. 2002).

I – 4.2. The intermediate progenitor hypothesis

More recently, Kriegstein and colleagues (2006) hypothesized that the important evolutionary change behind cortical evolution was an increase in non-epithelial progenitors. It has been noted that approximately 10% of the IPCs rodents do not divide only once in a symmetric, consumptive manner, but appear capable of multiple cell divisions (Haubensak et al. 2004; Noctor et al. 2004). In their "intermediate progenitor hypothesis," Kriegstein and colleagues propose that lateral expansion occurs via an increase in symmetric, proliferative divisions of these non-epithelial progenitors (Figure 10C). In contrast to Smart and colleagues, Kriegstein and colleagues argue that constraints imposed by apical membrane space are overcome by an increase in non-epithelial neural progenitors.

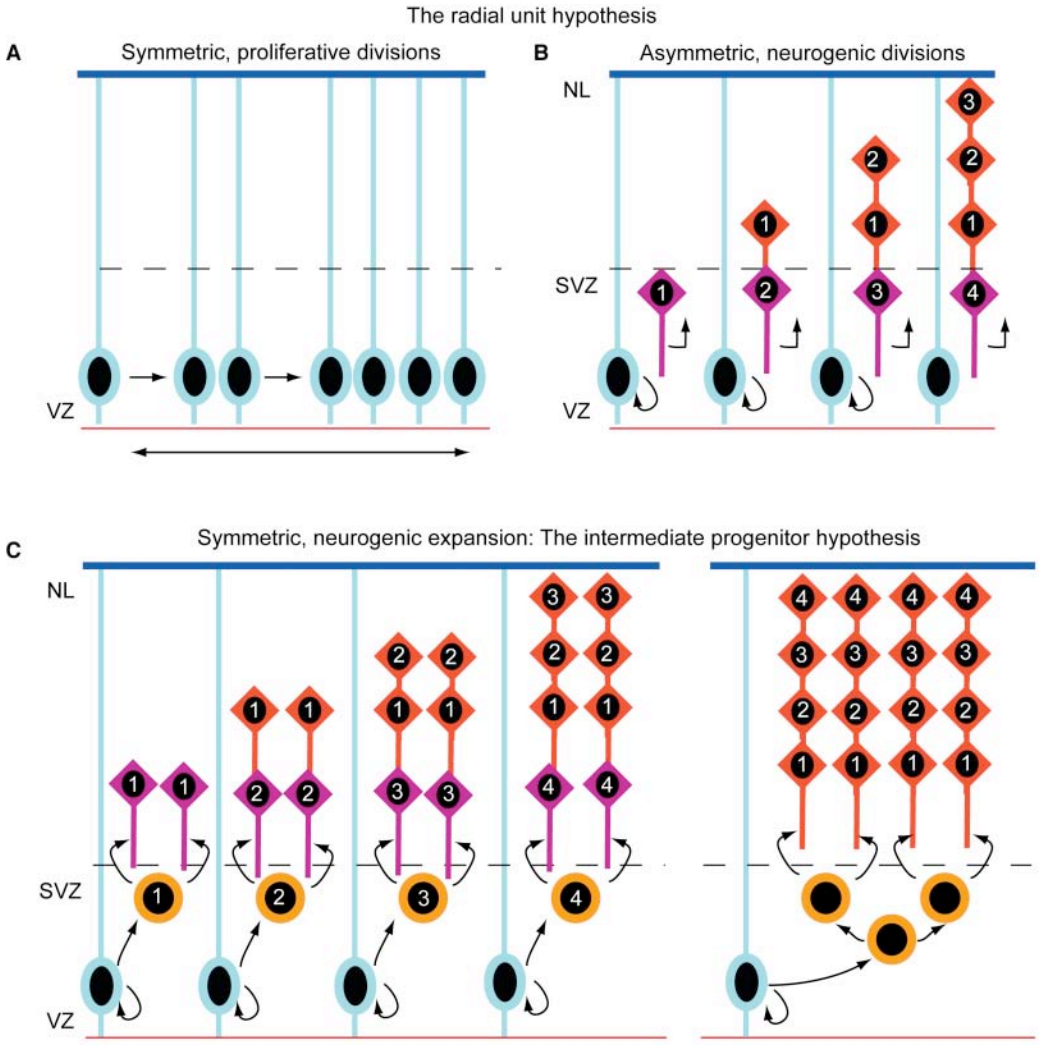

Figure 10: The radial unit and intermediate progenitor hypotheses. **A**,**B** The radial unit hypothesis. **A**, Symmetric proliferative divisions of NE/RG cells lead to an exponential increase in "radial units." **B**, Asymmetric neurogenic divisions generate neurons that migrate to the cortical plate in an inside-out gradient. The radial unit hypothesis predicts that the number of divisions shown in **A** will determine the lateral expansion of the cortex whereas the number of divisions shown in panel **B** determine the thickness of the cortex. **C**, The intermediate progenitor hypothesis suggests that neurons are produced predominantly from non-epithelial, basally dividing "intermediate progenitors." In this model, evolutionary lateral expansion of the cortex results from an increase in these non-epithelial precursors, largely driven by their self-amplification. Numbers **B**, **C** represent the order of cell birth. New-born neurons are presented in purple; Neurons that have already settled in the cortical plate are presented in red. Image concept following from Kriegstein et al. 2006.

I – 4.3. Cellular processes implicated in lateral expansion

Although important evolutionary changes in cortical thickness and layering of the isocortex have occurred in mammalian evolution, it is the lateral expansion of the isocortex that is predominantly responsible for an increase in brain size. Thus, evolutionary expansion of the brain must be due, at least in part, to an increase in the number of progenitors (generated by symmetric, proliferative cell divisions) in the

developing neuroepithelium (Kornack and Rakic 1998). Evidence in favor of this hypothesis includes the development of a gyrencephalic rodent brain upon constituent overexpression of beta-catenin, which induces cell cycle re-entry (Chenn and Walsh 2002).

Similarly, the duration of the cell cycle is an important factor involved in NE cell proliferation. The cell cycle of NE cells lengthens as development proceeds (Takahashi et al. 1995). Calegari and colleagues (2003, 2005) showed more specifically that the cell cycle is longer in NE cells undergoing neurogenic division than in proliferating NE cells. These data suggest that a fast cell cycle is important to maintain NE cell proliferation. This observation was also reported by Lukaszewicz and colleagues (2005), however, they also noted that the cell cycle in primate neural progenitors is longer than that of rodent progenitors. The authors propose that a longer cell cycle in primates is an adaptive mechanism for fine-tuning differentiation programs. Consistent with this model, primate embryonic stem cells have a longer cell cycle than their rodent counterparts (Fluckiger et al. 2006), suggesting that lengthening of the cell cycle could be a general aspect of evolutionary change between the Primate and Rodent orders.

Another important cellular factor implicated in cell proliferation is the cleavage plane of neuronal progenitors. Due to the importance of these mechanisms to the results reported in this thesis, factors related to cleavage plane and spindle orientation will be discussed in greater detail in the following section.

I – 5. Regulation of Symmetric Versus Asymmetric Cell Division

Up to this point, I have distinguished symmetric from asymmetric cell division based on the fate of the daughter cells. However, the symmetry of division can also be described in cell biological terms. Much research has been dedicated to understanding the cell biological factors that regulate differences in daughter cell fate. Because of their accessibility to genetic manipulation, *Drosophila* have proven to be an excellent model for this question. Importantly, this system has contributed to our understanding of how the symmetry (or asymmetry) of division is a consequence of the symmetric (or asymmetric) segregation of cell fate determinants between daughter cells.

In contrast to vertebrates that internalize their CNS by invagination to form the neural tube, *Drosophila* (and other invertebrates) internalize the CNS by delamination. *Drosophila* neural progenitors, called neuroblasts (NBs), lose their adherens junctions and delaminate from the overlying layer of neuroecotodermal epithelial cells, also called epidermoblasts. As NBs delaminate, they form a transient apical stalk, which is lost once NBs begin asymmetric cell division. Unlike epidermoblasts that divide symmetrically to produce two daughter epidermoblasts, NBs divide asymmetrically to generate another NB and a ganglion mother cell (GMC). The GMC will divide once more in a symmetric, consumptive manner and give rise to either two neurons or two glia.

I – 5.1. Cell polarity in *Drosophila* neuroblasts

Despite losing their epithelial characteristics during delamination, NBs remain polarized along the apical-basal axis. The PAR/aPKC apical protein complex is essential for regulating apical-basal polarity in both NBs and epidermoblasts. Members of the PAR/aPKC complex include *bazooka*, *atypical protein kinase C*, *DaPKC*, and *DmPAR-6* (Müller and Wieschaus 1996; Wodarz et al. 2000; Petronczki & Knoblich 2001; Wodarz & Huttner 2003). This protein complex directs the asymmetric localization of cell fate determinants in NBs, Prospero and Numb.

Prospero (Pros; Hirata et al. 1995; Knoblich et al. 1995; Spana & Doe 1995) and Numb (Knoblich et al. 1995), as well as their adaptor proteins Miranda (Ikeshima-Kataoka et al. 1997; Shen et al. 1997) and Partner of Numb (Pon; Lu et al. 1998), localize to the basal cortex of NBs, ensuring their exclusive inheritance by the GMC where they promote differentiation. Prospero is required for the transcription of GMC specific genes and also suppresses cell cycle regulators, leading to cell cycle exit (Doe et al. 1991). The ability of the apical PAR/aPKC complex to regulate basal localization of cell fate determinants is achieved by its interaction with the cytoskeletal protein Lethal giant larvae (Lgl). LGL directs Miranda binding to the cell cortex. At the apical cortex, aPKC inhibits Lgl by phosphorylation, thus restricting Lgl activity to the basal pole of the cell, where it promotes association of Miranda to the cell cortex (Betschinger et al. 2003).

Cortical polarity in NBs, is established by the Pins-Gαi protein complex (Cai et al. 2003; Yu et al. 2003). The apical localization of the Inscuteable (Insc), Partner

of Inscuteable (Pins), and heterotrimeric G-proteins in NBs is also regulated by the PAR/aPKC complex (Kraut et al. 1996; Kaltschmidt et al. 2000; Schaefer et al. 2000, 2001; Yu et al. 2000). During NB delamination, Insc associates with the apical stalk in a Bazooka dependent manner via binding of its PDZ domains (Schaefer et al. 2000). Maintenance of Insc apical localization after delamination requires both Bazooka and Pins (Yu et al. 2000). Work in Drosophila suggests a biochemical pathway whereby G-proteins recruit Pins to the apical cortex (Schaefer et al. 2000). Pins, in turn, is required with Bazooka to localize to the apical stalk during NB delamination.

I – 5.2. Regulation of spindle orientation in the *Drosophila* CNS

Asymmetric division of *Drosophila* NBs requires the coordination of spindle alignment with the axis of polarity. In contrast to epidermoblasts that divide vertically along the planar axis, *Drosophila* NBs align their mitotic spindle along the apical-basal axis, resulting in a horizontal cleavage plane (Figure 11). This process involves two major components: establishment of cortical polarity followed by alignment of the spindle with the cortical polarity cues.

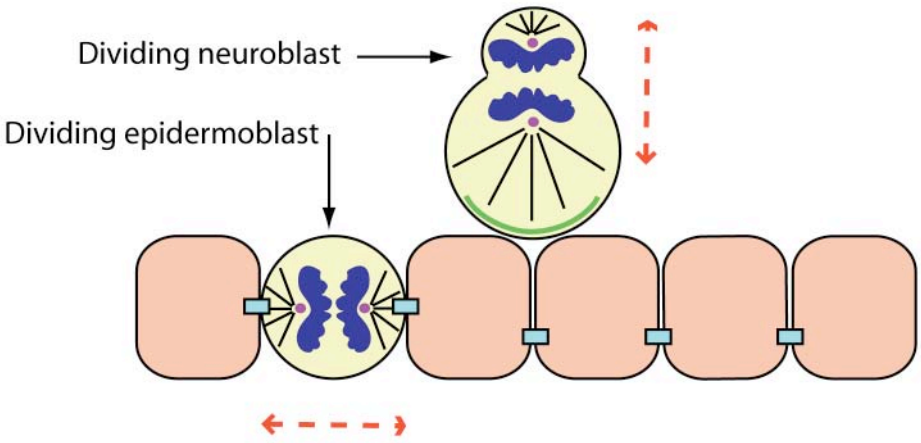

Figure 11: Spindle orientation in asymmetric divisions of *Drosophila* neuroblasts. *Drosophila* epidermoblasts divide along the planar axis with a cleavage plane vertical to the lumen. In neuroblasts, Insc (represented by the green line) directs a 90° rotation of the spindle, aligning it along the apical-basal axis and generating a cleavage plane horizontal to the lumen. Spindle alignment is represented by the red dashed line. The plane of cleavage will be perpendicular to spindle alignment. Image concept following from Buchman and Tsai 2006.

At NB delamination during interphase, the Par/Insc pathway coordinates Pins-Gαi localization with CNS tissue polarity (Cai et al. 2003). Communication between the cortically localized Pins-Gαi complex and spindle microtubules is mediated by the NuMA-related Mushroom body defect (Mud) protein (Izumi et al. 2006; Siller et al. 2006; Bowman et al. 2006). Cortical localization of the Pins-Gαi complex in NBs is mediated by Insc, which is necessary and sufficient for spindle rotation (Kraut et al. 1996; Kaltschmidt et al. 2000). In *Drosophila*, Insc is expressed specifically in NBs, and its ablation leads to randomization of spindle orientation (Kaltschmidt et al. 2000). Moreover, ectopic expression of Insc in epidermoblasts which normally divide vertically, leads to spindle rotation and horizontal cleavage (Kraut et al. 1996).

In the absence of the Par/Insc pathway, astral microtubules can also align the Pins-Gαi complex into cortical crescents over one spindle pole during metaphase (Siegrist & Doe 2005). This "microtubule-to-cortex" signaling pathway can align the spindle to cortical polarity cues (Pins-Gαi), however, in the absence of Insc, cortical polarity is not properly aligned with apical-basal polarity. As a consequence, the cleavage plane in NBs is randomized.

I – 5.3. Cell polarity in mammalian NE cells

Consistent with their epithelial nature, NE cells also exhibit apical-basal polarity. NE cells (including radial glia cells) contact both the apical and basal membranes through extended processes. The apical process forms an endfoot at the ventricular lumen. The apical and basolateral membranes have distinct protein and lipid contents which are separated by junctional complexes. The *Drosophila* PAR/aPKC apical protein complex, which in mammals includes ZO-1, ASIP/PAR-3/Bazooka, PAR-6, aPKC, and Cdc42, is functionally conserved and localizes to the junctions. Integral components of the apical plasma membrane include the transmembrane protein Prominin-1 (Weigmann et al. 1997). The apical membrane of NE cells also contains protrusions such as microvilli and a primary cilium, which is anchored from the apically localized centrosome (Chenn et al. 1998).

One important difference between *Drosophila* and mammalian (vertebrate) neural development is that mammalian NE progenitors do not delaminate from the epithelium at the onset of differentiation. Thus, whereas *Drosophila* progenitors and

stem cells are segregated into stratified layers, vertebrate progenitors undergoing asymmetric, neurogenic division are junctionally connected to proliferating, symmetrically dividing progenitors within a single, pseudo-stratified cell layer.

I – 5.4. Regulation of spindle orientation in the mammalian CNS

The eloquence of the *Drosophila* model has tempted many researchers to investigate if spindle orientation and daughter cell fate are similarly correlated in the mammalian neuroepithelium. However, the vast majority of NE cells in mammals divide with a vertical cleavage plane (i.e., perpendicular to the ventricular surface) irrespective of daughter cell fate (Smart 1972,1973; Zamenhof 1976; Silva 2002; Kosodo 2004; Stricker et al. 2006), suggesting that cleavage plane itself is not sufficient to predict cell fate (Figure 12). Instead, it was recently discovered that vertical cleavage planes can result in both symmetric and asymmetric cell division (Kosodo et al. 2004).

This was achieved by evaluating the apical plasma membrane distribution in proliferating NE cell divisions versus neuron-generating cell divisions. Neurogenic cell divisions were distinguished from proliferating divisions by the presence of *Tis21*, an anti-proliferative gene that is specifically expressed in NE cells that are undergoing neurogenic divisions (Iacopetti et al. 1999). Utilizing a transgenic mouse in which GFP is expressed under the control of the *Tis21* promoter, cells that are undergoing symmetric, proliferative divisions can be distinguished from those that are undergoing asymmetric, neurogenic divisions because the former are GFP–negative while the latter are GFP–positive (Haubensak et al. 2004). It was shown that the cleavage plane of proliferating NE cells bisects the apical membrane, symmetrically distributing it to both daughter cells (Figure 12A). In contrast, the cleavage plane of neuron-generating cells bypasses the apical membrane, resulting in its asymmetric distribution to only one of the daughter cells (Figure 12B; Kosodo et al. 2004).

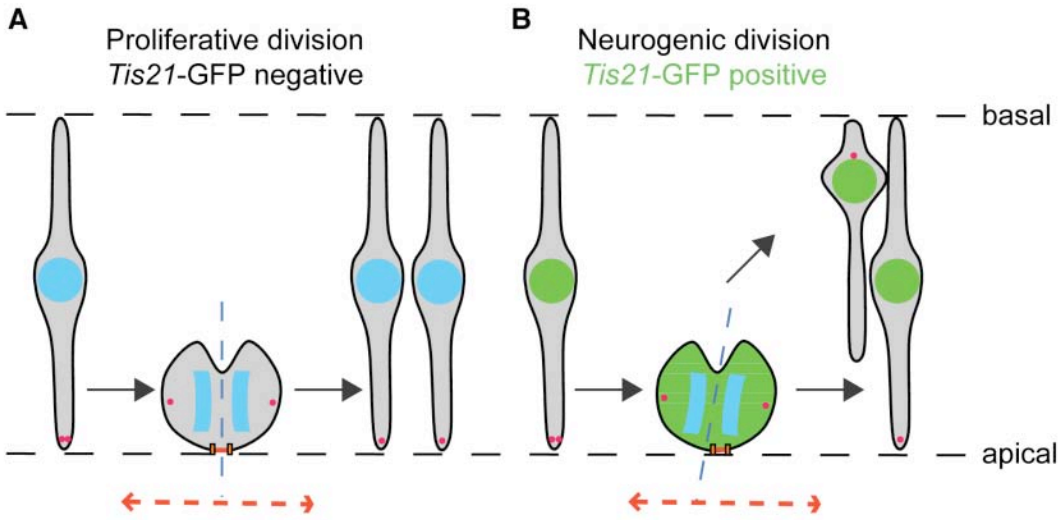

Figure 12: **Spindle orientation in mammalian NE cell divisions.** In mammals, the spindle of both (**A**) symmetrically dividing (*Tis21*-GFP negative) and (**B**) asymmetrically dividing (*Tis21*-GFP positive) NE cells is vertically aligned along the planar axis. In these cells, the switch from symmetric, proliferative to asymmetric, neurogenic is accompanied by only a slight deviation of the cleavage plane from the apical-basal orientation, but nonetheless results in the apical membrane (shown in red) and junctional complexes (brown boxes) being bypassed, as in **B** (rather than bisected, as in **A**) by the cleavage furrow. Spindle alignment is represented by the red dashed line. The plane of cleavage will be perpendicular to spindle alignment. Image modified from Y. Kosodo, unpublished.

As a result of this finding, a refined model of neurogenesis was proposed in which inheritance of the apical plasma membrane maintains a cell in the proliferative state while loss of the apical plasma membrane contributes to cell differentiation (Huttner &Kosodo 2005). Nonetheless, despite the absence of spindle rotation in mammals, spindle alignment is controlled at the cell cortex in a similar manner to *Drosophila*. NuMA is recruited to the cell cortex during mitosis via a cell cycle dependent interaction with LGN and Gαi proteins, which are homologous to the Pins-Gαi complex in *Drosophila* (Du & Macara 2004). A major question, then, is what regulates asymmetric division in mammalian NE cells? Further, how might this regulation be subject to evolutionary change? The recent discovery that some primary microcephaly genes code for proteins that localize to the mitotic spindle, has led to the hypothesis that these genes regulate brain size by controlling some aspect of NE cell division (Bond et al 2002; Woods et al. 2005). Further investigation of the cell biological function these candidates may therefore provide insight into the relationship between asymmetric division and brain size in mammals.

I – 6. The abnormal spindle-like microcephaly associated (Aspm) Protein

I – 6.1. Primary microcephaly

Autosomal recessive primary microcephaly (MCPH) is a neurodevelopmental disorder characterized by a small but architecturally normal brain (Woods 2004). Brain size of affected patients is at least 4 standard deviations below the age and sex adjusted mean (Woods et al. 2005). The greatest reduction in size occurs in the cerebral cortex, the region of the brain associated with cognitive function (Figure 13; Bond et al. 2002). Correspondingly, microcephalic individuals suffer from mental retardation, but lack any other abnormalities. Primary microcephaly is distinguished from secondary microcephaly in that the brain is smaller at birth. This is likely due to a deficit in neuronal production, since the vast majority of neurons are produced in the first 21 weeks of gestation (Sidman & Rakic 1973; O'Rahilly & Müller 1999). Although the microcephalic brain is smaller, it appears to have normal cortical thickness and morphology, also suggestive of a reduction in neural progenitors (Mochida and Walsh 2001). In contrast, individuals with secondary microcephaly are born with normal brain size, but develop microcephaly progressively from a lack of dendritic growth post-natally (Woods 2004).

There are at least 7 MCPH loci, of which 4 genes have been identified: *Microcephalin* (MCPH1), *CDK5RAP2* (MCPH3; cyclin-dependent kinase 5 regulatory subunit-associated protein 2), *ASPM* (MCPH5; abnormal spindle-like microcephaly associated), and *CENPJ* (MCPH6; centromere protein J) (see Table 1). The molecular function in neurogenesis is unknown for all four of these genes, but some functional inferences can be made. The protein products of the latter three genes have been shown to localize to the centrosome during mitosis, suggesting that they may be involved in cell division (Bond et al. 2005; Kouprina et al. 2005; Zhong et al. 2005). *Microcephalin* has been proposed to be involved in cell cycle regulation through its BRCT domains (Evans et al. 2004a). Irrespective of the details of their molecular function, at the tissue level, microcephaly genes appear to regulate brain size, specifically lateral expansion of the brain.

MCPH loci	Gene	Subcellular localization	Predicted functions	References
MCPH 1	Microcephalin	unknown	DNA damage response, Cell cycle control, Telomerase regulation	Jackson et al. 2002 Evans et al. 2004 Evans et al. 2005
MCPH 2	unidentified	unknown		Woods 2004
MCPH 3	CDK5RAP2	Spindle poles	Enhance centrosomal microtubule production	Bond et al. 2005
MCPH 4	unidentified	unknown		Woods 2004
MCPH 5	ASPM	Spindle poles Central spindle	Microtubule bundling and cross-linking	Bond et al. 2002 Kouprina et al. 2005 Zhong et al. 2005
MCPH 6	CENPJ	Spindle poles	Regulation of microtubule nucleation and depolymerization	Bond et al. 2005 Basto et al. 2006
unassigned	unidentified	unknown		Woods 2004

Table 1: Microcephaly genes. The identified microcephaly loci are listed along with the genes, subcellular localization and predicted functions, where known. Table concept follows from Woods 2004.

I – 6.2. ASPM mutations

Mutations in the *ASPM* (abnormal spindle-like microcephaly associated) gene are the most common cause of primary microcephaly in humans. ASPM is a large protein consisting of 28 exons and 3477 amino acids (3123 in mouse) with a N-terminal microtubule binding domain, two calponin-homology domains, multiple isoleucine-glutamine (IQ) calmodulin-binding repeats, and a C-terminal domain of unknown function (Figure 13A). To date, there are 30 known *ASPM* mutations, occurring throughout the length of the gene (Roberts et al. 2002; Bond et al 2003; Kumar et al.2004; Pichon et al 2004; Gul et al. 2006). There is no correlation between the location of the mutation and degree of microcephaly (Bond et al. 2003), suggesting that all the mutations result in a functional null protein. It has been hypothesized that non-sense mediated decay is the mechanism behind the phenotype (Bond et al. 2003; Woods et al, 2005). However, western blots of a cell line produced

from a patient with a frameshift mutation in *ASPM* revealed that a truncated protein was produced (Kouprina et al. 2005).

Further, at least one non-truncating pathogenic mutation has been identified, a missense mutation occurring within the IQ repeat region (Gul et al. 2006). This mutation occurs within a region of the IQ repeats that is conserved between rodents and primates and is predicted to be important for forming higher-order trimer repeats (HOR) that may be essential for calmodulin binding and ASPM function (Kouprina et al 2005; Gul et al. 2006). Taken together, these results indicate that multiple domains (at least some IQ repeats and the C-terminus) are necessary for the function of ASPM in the developing brain.

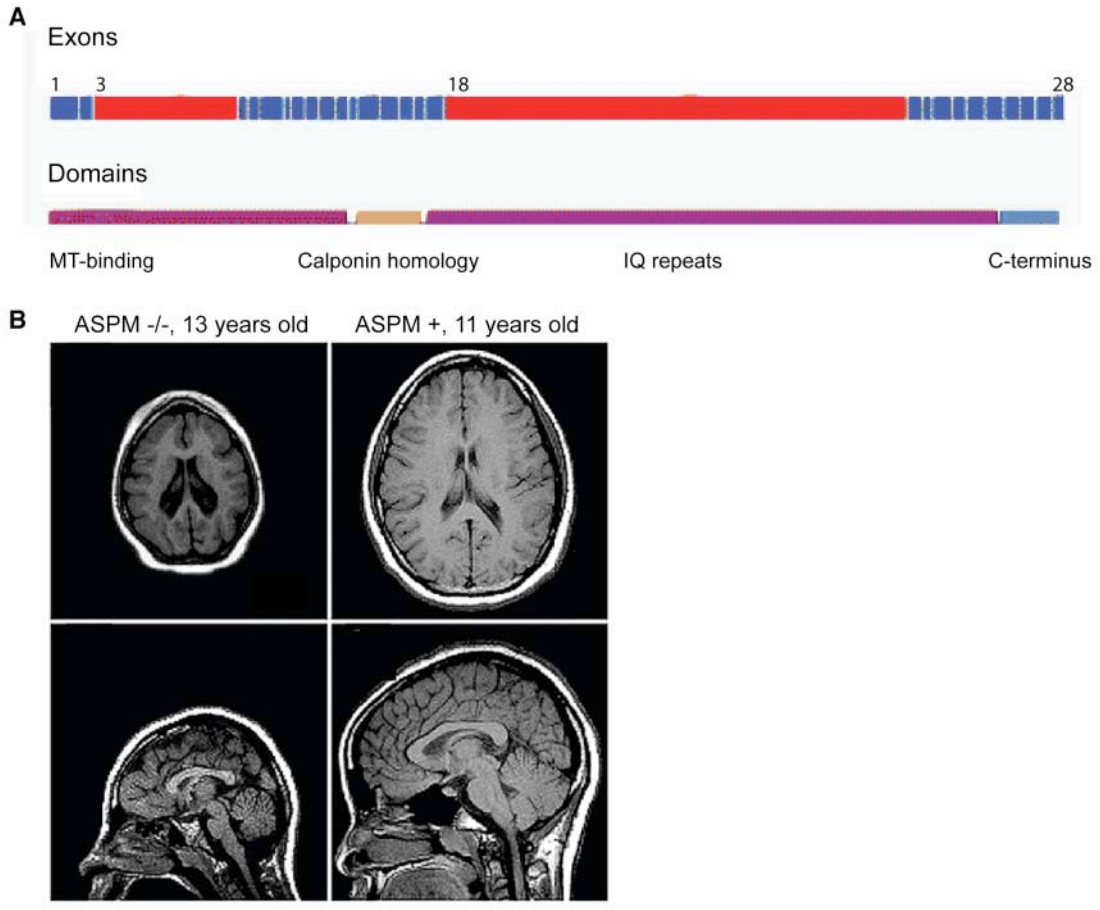

Figure 13: ASPM: Structure and phenotype. A, The ASPM protein has 28 exons and 4 major domains: an N-terminal microtubule binding domain, a calponin homology domain, multiple IQ calmodulin binding repeats, and a C-terminal domain of unknown function. Image modified from Ponting and Jackson 2005. **B,** Human patients with homozygous mutations in ASPM have brains >3 standard deviations below the age and sex average. The left panels show an 11 year-old mutant individual. The brain of a normal 13 year-old individual is shown in the right panels. Image taken from Bond et al. 2002.

I – 6.3. *Aspm/ASPM* expression in development, adult tissues, and cancer

The expression of *Aspm* in mammals was first reported by *in situ* hybridization on embryonic mouse tissue. In the developing mouse brain, *Aspm* expression was observed in the VZ of the neuroepithelium during mid-neurogenesis (E14, E16) and shown to be down-regulated post-natally (Bond et al. 2002). Luers et al. (2002) reported a more broad expression both temporally and spatially, with *Aspm* (also known as *Calmbp1*) expression observed in the VZ at E11.5 and later in the SVZ and cortical plate at E16.5. These differences may be attributed to the choice of *in situ* probes: Bond and colleagues hybridized using an N-terminal probe whereas Luers and colleagues generated a C-terminal probe corresponding to the cDNA of Calmbp1 (later identified as homologous to the C-terminal region of *Aspm*). Expression of *Aspm* was also found in the fetal liver and spleen, but was absent in adult tissues with the exception of the testis (Luers et al. 2002).

Aspm expression in the developing mouse embryo was re-evaluated by Kouprina and colleagues (2005), confirming that *Aspm* is not a brain specific gene. Expression detected by *in situ* hybridization was found in the embryonic liver, heart, lungs, and kidney. A similar pattern was observed for *ASPM* expression in human fetal tissues. RT-PCR from cDNA libraries of human fetal tissue revealed *ASPM* expression in fetal brain, bladder, colon, heart, liver, lungs, muscle, skin, spleen, and stomach (Kouprina et al. 2005). This near ubiquitous expression is present, but reduced, in all examined adult human tissues except for the brain. That is, *ASPM* expression is maintained in those tissues that continue to proliferate into adulthood. Additionally, *ASPM* is up-regulated in multiple types of cancer cells (Kouprina et al. 2005; Zhong et al. 2005), including glioblastoma, a tumor of the brain (Horvath et al. 2006). Taken together, *ASPM* expression correlates with cell proliferation: it is high in dividing cells and is low or absent in post-mitotic cells.

I – 6.4. Adaptive evolution of *ASPM*

Positive selection indicates increased organismal fitness resulting from modifications in a DNA segment (Kreitman 2000; Zhang et al. 2002). A common method for identifying positive selection is to compare the ratio of the rate of nonsynonymous nucleotide substitutions (K_a) to synonymous substitutions (K_s).

Since most nonsynonymous mutations are deleterious, K_a/ K_s in most functional genes is less than 1. When advantageous nonsynonymous mutations are fixed by positive selection, the value of this ratio increases (Kreitman 2000). *ASPM* sequences in humans and several other primate and mammal species have been evaluated for signs of evolutionary change by several groups. In all cases, strong evidence for positive selection acting on *ASPM* within the human lineage has been found (Zhang 2003; Evans et al. 2004b; Kouprina et al. 2004). In ape lineages leading to humans, the K_a/ K_s ratio of ASPM is nearly one, whereas in other lineages (e.g., monkeys, carnivores, artiodactyls, rodents) the ratios are less than 0.5. This data suggests that the increased K_a/ K_s ratio represents positive selection on *ASPM* that is specific to the ape lineages (Evans et al. 2004).

More compelling evidence indicates positive selection on *ASPM* in the terminal human lineage (i.e. since the human-chimp split) and comes from the McDonald-Kreitman test. If a gene is evolving neutrally or under constant purifying selection, the K_a/ K_s ratio between species should be similar to the K_a/ K_s ratio within a species (McDonald & Kreitman 1991). Evans and colleagues (2004b) sequenced 40 humans representing a world-wide distribution to determine the polymorphism distribution of *ASPM* among modern human populations. They found that the number of nonsynonymous polymorphisms within the human species is significantly less than the number of nonsynonymous substitutions occurring between humans and their last common ancestor with chimpanzees (Evans et al. 2004b). Interestingly, nonsynonymous changes within the ASPM protein are variable; most substitutions occur within the N-terminal microtubule binding domain and the IQ repeat region, while the calponin-homology domain and the C-terminal region are more conserved (Evans et al. 2004b; Kouprina et al. 2004).

Evidence for positive selection on *ASPM* exists at two branches in the primate lineage: along the terminal human linage after the human-chimp split, and at the base of the hominoid lineage. There is disagreement, however, about whether this occurs after the great apes split from the lesser apes (Evans et al. 2004b) or after the African apes split from orangutans (Kouprina et al. 2004). Nonetheless, the consensus is that strong positive selection on the *ASPM* locus correlates with brain size increases in the primate lineage.

I – 6.5. Asp, the *Drosophila* ortholog of ASPM

Because *ASPM* mutations result in microcephaly, it can be inferred that *ASPM* regulates brain size. However, the molecular and cellular mechanism of this regulation is unknown. The function of ASPM in mammalian neurogenesis is largely inferred from its *Drosophila* ortholog, Asp, which exerts a critical role at spindle poles during both mitosis and meiosis (Ripoll et al. 1985; Casal et al. 1990; Avides & Glover 1999). Asp is a 220-kDa microtubule-associated protein (MAP) that localizes to the polar regions of the mitotic spindle in *Drosophila* embryos and larval NBs (Saunders et al. 1997; Avides & Glover 1999).

Biochemical studies have shown that the N-terminal region of Asp has a strong affinity for microtubules. The Asp N-terminal region binds microtubules with very high affinity and is not removed at salt concentrations that disassociate most MAPs (Saunders et al. 1997). The central region (containing the calponin homology, actin-binding domain) binds microtubules poorly. The microtubule binding ability of the C-terminal domain is unknown because it is unstable in bacterial and insect expression systems. Additionally, the N-terminal domain of Asp is an excellent substrate for phosphorylation by Polo kinase, the central region is a poor substrate, and it is unknown for the C-terminal region (Avides el at. 2001).

The mitotic function of *asp* has been predominantly studied in Drosophila NBs. Asp associates with the spindle poles during all phases of mitosis, but during late anaphase and telophase, Asp is also found on the central spindle (Saunders et al. 1997; Wakefield et al. 2001). This localization may be mediated dynein-dynactin since Asp is partially mis-localized when dynein-dynactin is depleted (Morales-Mulia & Scholey 2005). It has been suggested that Asp organizes the γ–tubulin ring complex within the PCM to form a microtubule nucleating center, rather than directly nucleating microtubules itself (Avides & Glover 1999).

Further investigation of Asp in other mutant backgrounds indicates that Asp is required for the aggregation of microtubules into focused spindle poles, independently of its microtubule nucleating activity (Wakefield et al. 2001). Dividing *asp* mutant NBs frequently arrest in metaphase, likely due to the activation of a spindle integrity checkpoint (Gonzalez et al. 1990; Avides & Glover 1999). Most arrested *asp* NBs have bipolar spindles with a normal chromosome complement, but with broad, unfocused microtubules at the spindle poles (Gonzalez et al. 1990; Avides & Glover

1999). The lack of a stringent spindle checkpoint in meiosis allows *asp* mutant spermatids to proceed through mitosis. As a consequence, *asp* mutants exhibit a high incidence of non-disjunction, resulting in aneuploidy and nuclei of variable size in spermatids (Casal et al. 1990). This is caused, at least in part, by the dissociation of centrosomes from the chromatids during meiosis (Gonzalez et al. 1990). In the absence of Asp, "free" centrosomes are observed in both mitotic NBs and meiotic spermatocytes (Gonzalez et al. 1990; Wakefield et al. 2001).

Taken together, these data indicate that Asp functions specifically during cell division to focus both the spindle poles and the central spindle. Asp appears to mediate spindle pole integrity by bundling microtubule minus ends and operating as a link between the microtubule minus ends at the centrosome. In the absence of Asp, NB cell division is arrested, inhibiting proliferation.

I – 6.6. Aspm function in mammals

Similar to Asp, ASPM in non-neural human cells has been shown to localize to spindle poles, suggesting that it may be involved in some aspect of cell division in mammalian cells (Kouprina et al. 2005; Zhong et al. 2005). Bioinformatics and structural modeling predict that ASPM directly interacts with the cytoskeleton and can form a rod-like conformation upon interaction and binding with calmodulin (Cox et al. 2006). The N-terminal domain of ASPM has also been identified as a member of the ASH (ASPM, SPD-2, Hydin) family of proteins (Pointing 2006). The ASH domain is predicted to have a fundamental role in cilia formation. Pointing (2006) suggests that the essential function of ASPM in the developing neuroepithelium may not be during mitosis, but rather be related to cilia. In this regard, he postulates that ASPM may have a ciliary role either in neuronal migration or in directing movement of cerebral spinal fluid (Pointing 2006).

The only data about Aspm function in mammals comes from a study on the calmodulin binding protein, Sha1 (Craig & Norbury 1998). *Sha1* was isolated from a murine cDNA library and shown to disrupt normal spindle function when over-expressed in yeast, a phenotype that was suppressed by simultaneous over-expression of calmodulin. It is now known that *Sha1* is a partial *Aspm* cDNA corresponding to the C-terminal region of the gene (Bond et al. 2002). Still, the study by Craig and Norbury (1998) is important because it indicates a potential role for calmodulin in the

regulation of Aspm function. This finding is particularly relevant since ASPM has the highest number of the IQ repeats of any known calmodulin binding protein (Kouprina et al. 2005).

To date, there is not much known about Aspm function in mammals or how it might regulate brain size. From what is known about Asp and the limited information available from mammals suggest that Aspm may control an aspect of mitotic spindle function that is crucial for maintaining symmetric, proliferative divisions of the highly elongated, polarized NE cells, thereby allowing the lateral expansion of the neocortex. In the present study, we have investigated a possible role of Aspm in regulating cleavage plane orientation and symmetric, proliferative *versus* asymmetric, neurogenic divisions of NE cells in the mouse embryonic telencephalon.

I – 7. Aims of this Study

Given the importance of symmetric cell division to the lateral growth of the isocortex, we are interested in cell biological mechanisms involved in the switch from symmetric, proliferative NE cell divisions to asymmetric, differentiative NE cell divisions. In particular, we aim to test the hypothesis that maintenance of epithelial characteristics, including apical membrane attachment, is important for lateral expansion of the isocortex. We have chosen two approaches to for this investigation: a candidate approach and a comparative analysis.

I – 7.1. Candidate analysis: Aspm

In the developing neuroepithelium, the primary progenitor cells of the central nervous system are the neuroepithelial (NE) cells, which characteristically exhibit apical-basal polarity. A key feature of proliferative divisions of NE cells is that cleavage occurs along their apical-basal axis, which ensures the symmetric distribution of polarized cell fate determinants to the daughter cells. The switch of NE cells from symmetric, proliferative to asymmetric, neurogenic divisions is accompanied by a deviation of the cleavage plane from the apical-basal orientation. This deviation is often only relatively small, but nonetheless results in the apical plasma membrane of NE cells being bypassed by the cleavage furrow, and hence being inherited by only one of the daughter cells. Our hypothesis is that some factors must exist to tightly maintain spindle position in symmetrically dividing cells and that these factors are down-regulated at the onset of neurogenesis, allowing the spindle to wobble and thus increasing the likelihood of asymmetric cell division. We are interested in the role of the Aspm (abnormal spindle-like microcephaly associated) protein in controlling this process.

Aspm was chosen as a candidate for analysis because human patients with homozygous mutations in *ASPM* have brains severely reduced in size, but with apparently normal cortical patterning and organization (Bond et al. 2002). Additionally, ASPM has shown accelerated evolution within the primate lineage (Bond et al. 2003; Evans et al. 2004; Kumar et al. 2004; Kouprina et al. 2005). Finally, the *Drosophila* ortholog of Aspm, Asp, is essential for normal cell division

(Avides & Glover 1999). Following from these data, we generated two hypotheses about the role of Aspm in NE cell division:

1. Aspm stabilizes mitotic spindle position, promoting symmetric, proliferative cell division by ensuring inheritance of apical membrane by both daughter cells.
2. Loss of Aspm causes premature asymmetric division, increasing the generation of non-NE cells, and thereby inhibiting expansion of the proliferating cell population.

Predictions following from these two hypotheses about the function of Aspm will be evaluated in the mouse model system. Subsequently, the evolutionary implications of the data will be discussed.

I – 7.1. Comparative analysis: Primate and rodent progenitors

The increase in basal mitotic cells during developmental and evolutionary time has been widely noted. This trend is exceptional in primates where the majority of neurons are generated from basally dividing progenitors (Lukazewicz et al. 2005). In rodents, basal progenitors can be distinguished from apical progenitors in at least two ways. First, basal progenitors in rodents lack apical membrane (Miyata et al. 2004). Second, basal progenitors express the transcription factor Tbr2, in contrast to apical progenitors that express Pax6 (Englund et al. 2005). In primates, the characteristics of basally dividing cells are largely unknown. In particular, the epithelial nature of primate basal progenitors is debated, and has become central to evolutionary hypotheses (c.f., Kriegstein et al. 2006). Therefore, we aim to evaluate the epithelial characteristics of primate basal progenitors. We will test the following two questions:

1. Do primate basal progenitors express Tbr2 or Pax6?
2. Do primate basal progenitors maintain apical contact?

These two questions will be evaluated in fixed tissue specimens from monkey and human developing neuroepithelia.

II. Results

II – 1. Candidate Analysis: Aspm

II – 1.1. Expression and localization of Aspm in the mouse neuroepithelium

Previous reports on *Aspm* expression, as revealed by *in situ* hybridization in the developing mouse brain, gave somewhat inconsistent results. Luers and colleagues (2002) found expression of *Aspm* in the VZ of the telencephalon from the onset of neurogenesis (E11.5) and continuing until late neurogenesis (E16.5), in both the VZ and SVZ. Interestingly, they also described *Aspm* expression in the neuronal layer. Bond and colleagues (2002) looked at mid- (E14) and late- (E16) neurogenic embryos, as well as post-natal brains and found that *Aspm* expression was limited to the germinal layers and decreased over time. To resolve the issue of whether or not *Aspm* expression was specific to proliferating NE cells, or also expressed by post-mitotic cells, we preformed *in situ* hybridization on the mouse forebrain from E8.5 (prior to the onset of neurogenesis) to E17.5 (when neurogenesis is largely complete).

In situ hybridization (Figure 14) confirmed previous observations that *Aspm* mRNA is expressed in the ventricular zone (VZ) of the murine embryonic forebrain. Interestingly, *Aspm* expression in NE cells was highest when these cells underwent symmetric, proliferative divisions and exhibited a highly (rather than only moderately) elongated shape. Specifically, *Aspm* expression (i) was still comparatively rare at early developmental stages (E8.5), when NE cells are not yet highly elongated; (ii) was detected in most, if not all, VZ cells around the onset of neurogenesis (E9.5-E11.5), when symmetric, proliferative divisions of NE cells prevail; and (iii) declined progressively at later stages of neurogenesis (E13.5-E17.5), when an increasing proportion of VZ cells have switched to asymmetric, neurogenic divisions. We did not observe Aspm expression in the neuronal layer, suggesting that it is specific to proliferating cells. Given these observations, we decided to explore the possibility that Aspm may function specifically in the symmetric, proliferative divisions of NE cells.

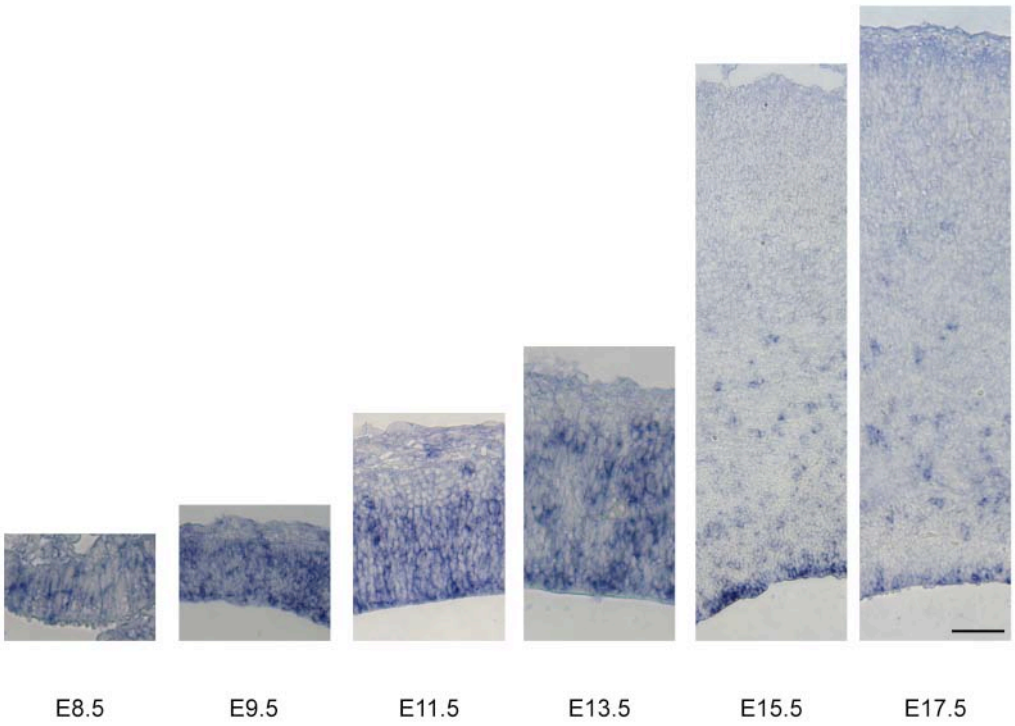

Figure 14: ***Aspm*** **expression in the embryonic mouse brain is highest in the VZ and when symmetric, proliferative NE cell divisions prevail.** *In situ* hybridization for *Aspm* mRNA in the dorsal telencephalon at the indicated developmental stages. The apical surface of the VZ is down. Scale bar in right panel, 100 μm. Image modified from supplemental data, Fish et al. 2006.

In order to determine the sub-cellular localization of Aspm in NE cells, an antibody raised against a recombinantly expressed fragment of mouse Aspm ($Aspm_{150\text{-}263}$), corresponding to exon three of this gene, was generated (see methods for details). The affinity-purified antibody was tested by Western blot analysis of two different cell extracts. First, Aspm exon 3 tagged with GFP was over-expressed in Cos7 cells. The fusion construct was detected on western blots of Cos7 cell extracts using antibodies directed against either GFP or Aspm (Figure 15A). Both antibodies detected a similar band of approximately 78kDa, the predicted size of the fusion construct. Second, we checked for the presence of the full-length protein in protein extracts from the heads of E12.5 mice (Figure 15B). Surprisingly, multiple bands from the *in vivo* extract were found. A band larger than 250kDa, likely corresponding to the full-length protein predicted to be 364kDa was identified. The other bands are likely splice variants as human non-neuronal cells express several, the largest predicted to be 218 kDa with multiple variants between 150 and 110 kDa (Kouprina et al. 2005).

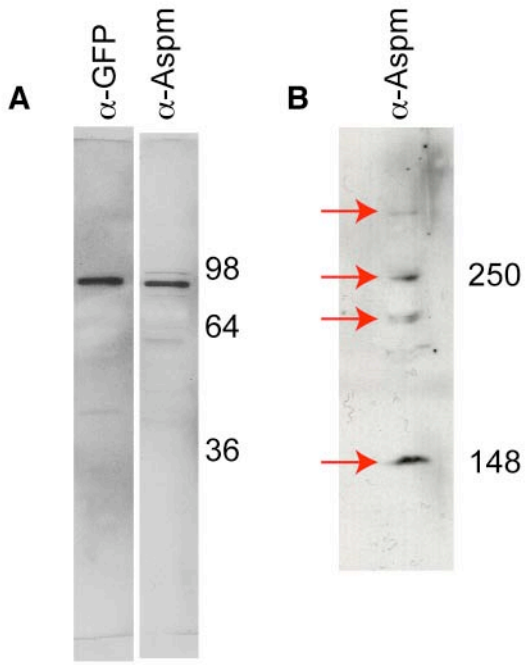

Figure 15: Western blot of Aspm antibody. **A,** Aspm exon 3 was over-expressed as a GFP fusion protein in Cos7 cells. Protein extracts were run on 12% acrylamide gels and blotted using antibodies generated against Aspm exon 3 (right lane) and against GFP (left lane). Both antibodies recognize a band between 98 and 64 kDa which is consistent with the expected size of the fusion protein (78kDa). **A,** Protein extracts from E12.5 mouse heads were run on a 4% acrylamide gel, followed by western blot analysis. Red arrows point to four bands recognized by our Aspm antibody. The largest band (~364 kDa) is likely the full-length protein. See text for details.

Immunostaining of mitotic NE cells in the E12.5 mouse telencephalon showed that Aspm was concentrated at the poles of the mitotic spindle (Figure 16). Specifically, Aspm immunoreactivity was clustered in the immediate vicinity of, but did not overlap with, the γ-tubulin staining of centrosomes. Association of Aspm with the spindle poles was observed during all phases of mitosis, with an apparent decrease in the intensity of immunostaining in telophase (Figure 16D). However, Aspm did not appear to be associated with centrosomes during interphase (see Figure 19, arrows). The association of Aspm with the spindle poles of NE cells is consistent with previous observations on the subcellular localization of Asp in mitotic *Drosophila* NBs (Avides & Glover 1999) and of ASPM in mitotic non-neural human cells in culture (Kouprina et al. 2005; Zhong et al. 2005).

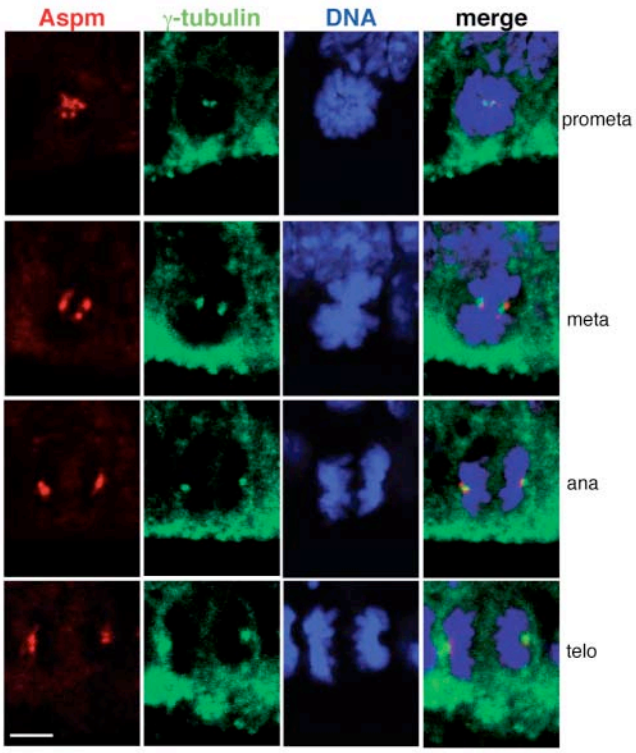

Figure 16: Aspm is concentrated at the spindle poles during mitosis. Dorsal telencephalon of E12.5 *Tis21*-GFP knock-in mice was stained with DAPI (DNA, blue) to reveal NE cells in prophase, metaphase, anaphase and telophase, and immunostained for Aspm (red) and γ-tubulin (green). All cells analyzed were *Tis21*-GFP–negative (not shown). Note the concentration of Aspm in the immediate vicinity of the γ-tubulin–stained centrosomes. Image modified from Fish et al. 2006.

II – 1.2. *Aspm* is down-regulated in NE cells undergoing neurogenic divisions

The spatio-temporal pattern of *Aspm* expression revealed by our *in situ* hybridization analysis correlates with the incidence of symmetric, proliferative NE cell divisions. Further, the localization of Aspm at spindle poles is consistent with a factor involved in cleavage plane orientation. Together, these data suggest that Aspm may have a critical function in maintaining spindle orientation during symmetric, proliferative NE cell divisions. If this is true, it predicts that Aspm is more highly expressed in proliferating rather than neuron-generating NE cells.

To test this prediction, we utilized the *Tis21*-GFP knock-in mouse line (Haubensak et al. 2004) to compare Aspm immunoreactivity between these two cell populations. To do so, neighboring NE cells in the same mitotic phase (prophase or metaphase as revealed by DAPI staining) were compared in E14.5 *Tis21*-GFP knock-in mice. In each comparison, at least one cell was *Tis21*-GFP–negative and one was *Tis21*-GFP–positive. For example, three neighboring metaphase NE cells are shown in Figure 17A, stained for DAPI (upper panel), Aspm (middle panel), GFP (lower

panel). For each mitotic cell, the centrosome-specific Aspm immunostaining was evaluated relative to the non-specific background staining and then given a relative intensity assessment (strong, medium, or weak) independently of the GFP channel. Each mitotic cell was then scored separately for *Tis21*-GFP expression as positive or negative. The percentage of cells from each relative intensity of Aspm immunoflourescence was then plotted against GFP expression. As shown in Figure 17B, *Tis21*-GFP–negative NE cells, which undergo proliferative divisions, tended to exhibit more intense Aspm immunostaining at spindle poles than *Tis21*-GFP–positive NE cells, which undergo neurogenic divisions. This trend is consistent with a down-regulation of *Aspm* in NE cells concomitant with their switch from proliferative to neurogenic divisions. Further, it suggests that the function of Aspm is more critical in symmetric divisions than asymmetric divisions.

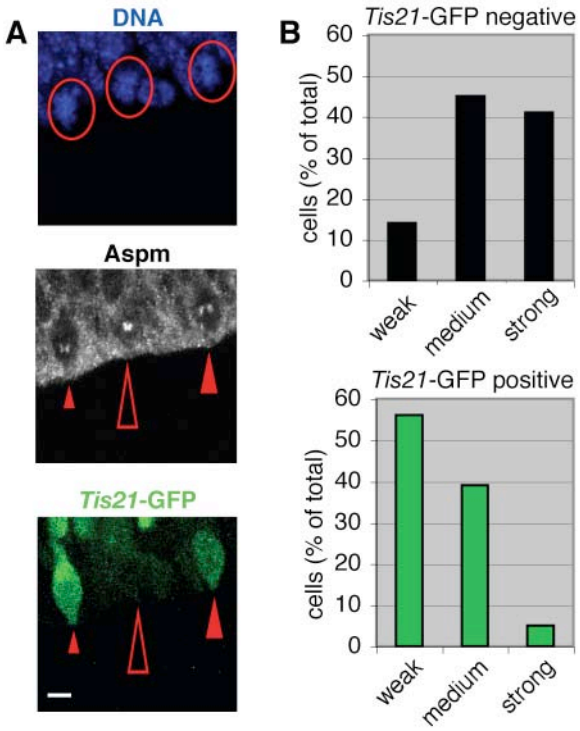

Figure 17: *Aspm* is down-regulated in NE cells undergoing neurogenic divisions. **A**, Comparison of Aspm immunoreactivity at spindle poles in metaphase *Tis21*-GFP–negative NE cells (proliferative divisions, open triangles) *versus* *Tis21*-GFP–positive NE cells (neurogenic divisions, closed triangles) in the dorsal telencephalon of an E14.5 *Tis21*-GFP knock-in mouse. Upper, DNA staining using DAPI (blue); circles indicate the three metaphase cells analyzed. Middle, Aspm immunoreactivity (white); the small, medium and large triangles indicate weak, medium and strong Aspm immunoreactivity at spindle poles, respectively. Lower, *Tis21*-GFP fluorescence (green). **B**, Quantification, in the dorsal telencephalon of E14.5 *Tis21*-GFP knock-in mice, of pro- or metaphase *Tis21*-GFP–negative (black columns, 22 cells) and *Tis21*-GFP–positive (green columns, 18 cells) NE cells showing either weak, medium, or strong Aspm immunoreactivity at spindle poles, expressed as percent of total (weak+medium+strong). Data are from 19 cryosections which originate from at least four brains. **A**, The apical surface of the VZ is down. Image modified from Fish et al. 2006.

II – 1.3. Knock-down of *Aspm* results in its loss from spindle poles

Functional analysis of Aspm was performed using RNA interference-mediated gene depletion. We chose to use endoribonuclease-prepared short interfering RNAs (esiRNAs), an approach combining multiple different short-interfering RNAs (siRNA) that target a broad region of the mRNA. This approach is more specific for a particular target gene, with less off target effects than gene depletion by a single siRNA construct (Kittler et al. 2007). Our esiRNAs were generated against the entire coding region of exon 3, a region within the N-terminal microtubule binding domain (Figure 13), shared by all known splice-variants of *Aspm* (Kouprina et al. 2005). Knock-down was mediated by electroporation of the esiRNAs into the telencephalon of developing embryos, followed by at least 24 hours of development (Figure 18). We injected the telencephalon with esiRNAs and a monomeric red fluorescent protein (mRFP) reporter construct (Roger Tsien, University of California, San Diego). The nucleic acids were then directionally electroporated so that only one telencephalic vesicle received them. This method allows us to use the non-targeted vesicle as a control for the manipulation. As an additional control, we electroporated buffer containing mRFP alone into some embryos.

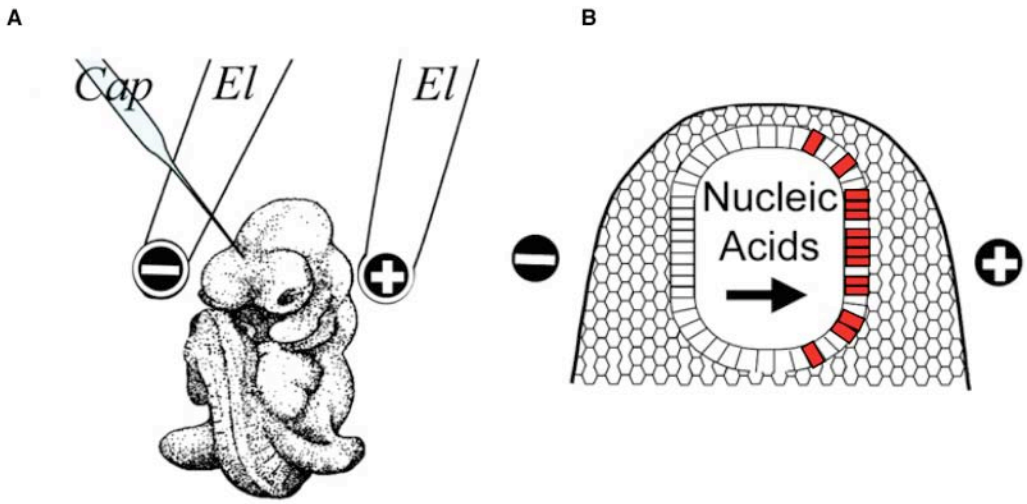

Figure 18: Procedure for *Aspm* knock-down. A, The mouse telencephalon is injected with nuclei acids (a reporter plasmid with or without *Aspm* esiRNAs) via glass capillary (Cap). The nucleic acids are then directionally electroporated into one half of the telencephalon with electrodes (El). **B,** Diagram showing the neural tube after electroporation in which the targeted side expresses the injected nucleic acids, represented by the red cells, whereas the non-targeted side does not. Image modified from Calegari et al. 2002.

We used two different methods to mediate *Aspm* down regulation: whole embryo culture (WEC) and *in utero* electroporation (IUP). For WEC experiments, embryos were removed from the uterus and cultured *ex utero*, with an open yolk sac, in oxygenated rat serum (Eto & Osumi-Yamashito 1995; Calegari et al. 2004). Embryos were dissected and electroporated at E10.5 (around the onset of neurogenesis in the mouse telencephalon), followed by 24 hours of development in culture.

IUP experiments involve a surgical procedure on the pregnant mother to open the peritoneum. Embryos are injected through the uterine wall while the mother is anesthetized. After injection and electroporation, the peritoneum is closed, and the embryos develop *in utero* (Takahashi et al. 2002). We used E12.5 embryos for IUP, and allowed them to develop for 24 to 48 hours after electroporation.

We determined the efficiency of our knock-down protocol at the tissue level by *in situ* hybridization and at the cellular level by immunohistochemistry. Figure 19a shows the telencephalic hemispheres of an embryo electroporated at E10.5 and followed by 24 hours WEC, with the targeted side presented in the lower panel. The electroporated region was identified in a consecutive section by mRFP expression (Figure 19B). *Aspm* mRNA levels were significantly reduced in the targeted hemisphere compared to the non-targeted side (Figure 19A). The reduction in Aspm mRNA levels was associated with a loss of spindle pole-associated Aspm protein (Figure 19C). Red arrowheads point to the spindle-poles of an RFP-negative cell from the non-targeted hemisphere, indicating Aspm association with the centrosomes (Figure 19C, upper panel). In contrast, little to no Aspm is seen on RFP-positive mitotic centrosomes from the targeted region (Figure 19C, lower panel). From these data, we concluded that our esiRNA electroporation and culture system resulted in sufficient knock-down of *Aspm* mRNA leading to loss of Aspm function from the spindle-poles during mitosis.

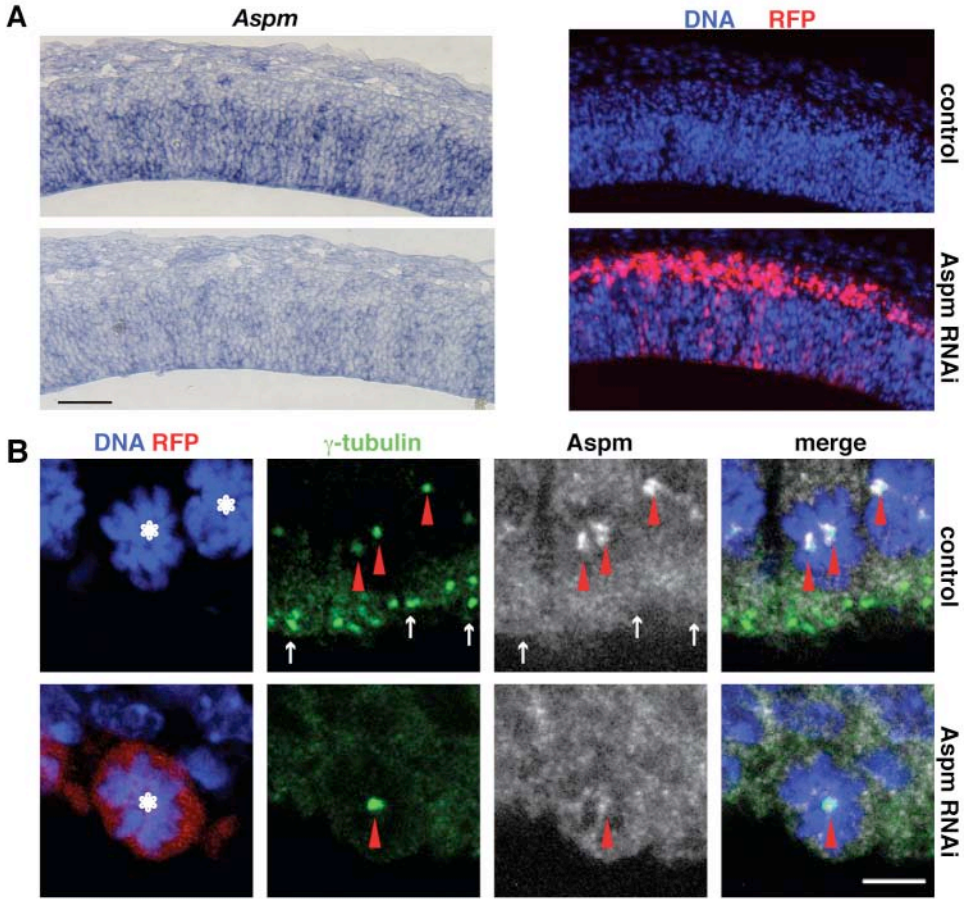

Figure 19: Knock-down of *Aspm* results in its loss from centrosomes in mitosis. **A**, RNAi of *Aspm* mRNA. Mouse E10.5 dorsal telencephalon was co-electroporated with Aspm esiRNAs and mRFP plasmid followed by 24 h whole-embryo culture, and consecutive cryosections were analyzed by *in situ* hybridization for *Aspm* mRNA (left) and RFP fluorescence (right). Non-targeted (control, top) and targeted (Aspm RNAi, bottom) hemispheres are from the same cryosections. The apical surface of the VZ is down. **B**, Knock-down of Aspm. Mouse E12.5 dorsal telencephalon was co-electroporated with Aspm esiRNAs and mRFP plasmid followed by 24 h *in utero* development, and cryosections were analyzed for mitotic NE cells (asterisks) by DNA staining using DAPI (blue), RFP fluorescence (red), and γ-tubulin (green) and Aspm (white) immunofluorescence. Single optical sections are shown. Top, non-targeted hemisphere serving as control; bottom, targeted hemisphere subjected to Aspm RNAi. Note the loss of Aspm immunoreactivity from the spindle poles (arrowheads) upon Aspm knock-down. The cell shown is representative of all targeted cells of the electroporated hemisphere. Arrows indicate centrosomes of adjacent NE cells in interphase, which lack Aspm. The apical surface of the VZ is down. Image modified from Fish et al. 2006.

II – 1.4. Knock-down of *Aspm* perturbs vertical cleavage plane orientation

Following from our previous results, we were particularly interested in the consequence of Aspm depletion during symmetric NE cell divisions. Therefore, we examined targeted mitotic cells. The first thing we noticed is that *Aspm* knock-down had severe effects on centrosome localization in mitotic NE cells, as shown in Figure 20. The upper panel shows a control cell that has been electroporated with mRFP only. In this cell, the centrosomes are properly positioned near the chromatids (red

arrowheads), which are aligned vertically to the ventricular surface. In contrast, a cell targeted with mRFP and Aspm esiRNAs shown in the lower panel, appears to have "free" centrosomes that are not associated with the chromatids. At the same time, the chromatids are mis-aligned and oblique to the ventricular surface.

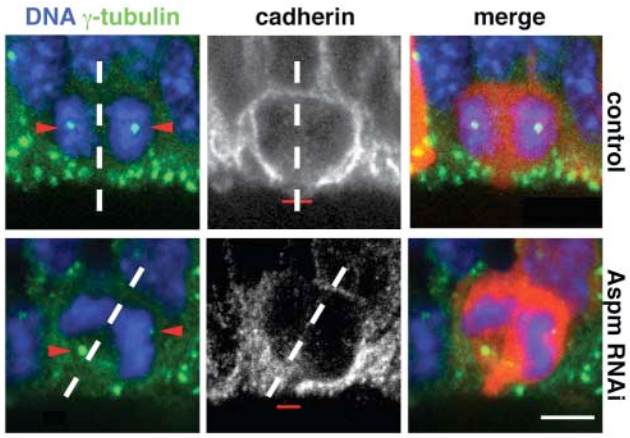

Figure 20: Knock-down of *Aspm* alters the cleavage plane of NE cells. Mouse E12.5 dorsal telencephalon was either electroporated with mRFP plasmid only (top) or co-electroporated with Aspm esiRNAs and mRFP plasmid (bottom), followed by 24 h *in utero* development, and cryosections were analyzed for NE cells in anaphase or telophase by DNA staining using DAPI (blue), RFP fluorescence (red), and γ-tubulin (green) and cadherin (white) immunofluorescence. The cleavage plane (dashed lines) was deduced from the orientation of the sister chromatids. Note the aberrant position of the γ-tubulin–stained centrosomes (arrowheads, stack of optical sections) in the targeted cell and the oblique cleavage plane which bypasses the cadherin hole (red bar, single optical section), upon Aspm knock-down. The apical surface of the VZ is down. Experiment done in collaboration with Y. Kosodo. Image modified from Fish et al. 2006.

Notably, *Aspm* knock-down did not perturb the localization of centrosomes in interphase NE cells, which remained associated with the apical cell cortex (Figure 21). The apical endfeet of the processes of two cells in either G1 or G2 phase contain centrosomes (Figure 21A). Similarly, Aspm knock-down did not disrupt the apical localization of centrosomes in S-phase cells in which the nucleus is at the basal side of the VZ (Figure 21B).

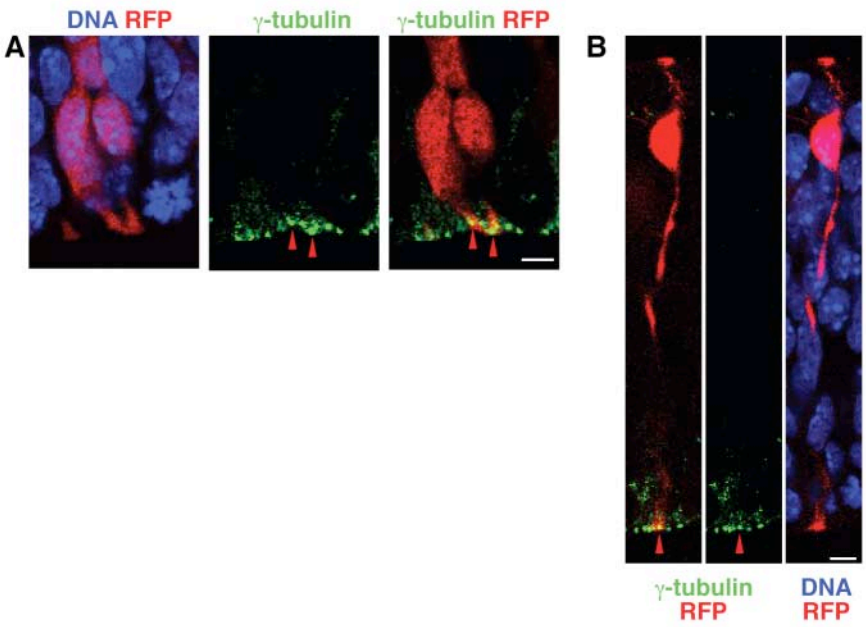

Figure 21: *Aspm* knock-down does not affect the apical localization of centrosomes of interphase NE cells. Mouse E10.5 dorsal telencephalon was co-electroporated with Aspm esiRNAs and mRFP plasmid followed by 24 h whole-embryo culture, and cryosections were analyzed for DNA staining using DAPI (blue), RFP fluorescence (red), and γ-tubulin immunofluorescence (green). Note the apical localization of centrosomes (arrowheads) in the targeted NE cells in interphase of two NE cells in G1/G2 (**A**) and in an S-phase NE cell (**B**). The apical surface of the VZ is down. Image modified from Fish et al. 2006.

From these data, we conclude that the free centrosome phenotype was specific to Aspm loss of function during mitosis. This phenomenon was particularly evident in telophase cells and was not observed prior to anaphase. This suggests that *Aspm* may have a vital function during the metaphase to anaphase transition. One possibility is that Aspm may maintain the attachment of microtubules to the centrosome, buffering forces generated during sister chromatid separation.

What initially interested us most was the related phenotype also pictured in Figure 20. That is, upon *Aspm* knock-down there is an alteration in chromatid orientation that is associated with a change in the predicted plane of cleavage. The dashed lines in Figure 20 represent the predicted cleavage plane orientation as determined by the mid-line of the separating chromatids (see methods for details). Upon immunostaining for cadherin, a constituent of the lateral NE cell plasma membrane, the apical plasma membrane of mitotic NE cells, identified by the presence of the apical marker prominin-1, appears as a small, unstained segment of the cell surface, referred to as the "cadherin hole" (Figure 20, middle panel). Symmetric versus asymmetric distribution of the apical plasma membrane to the

daughter cells can be predicted from the orientation of the cleavage plane relative to the cadherin hole (Kosodo et al. 2004).

In the control condition, represented in the upper panel, the cleavage plane is predicted to bisect the cadherin hole which would result in a symmetric distribution of the apical membrane and junctional complexes to both daughter cells. In contrast, in the lower panel, there is a significant alteration in the orientation of the cleavage plane. This corresponds with a cleavage plane that is predicted to bypass the cadherin hole, resulting in an asymmetric distribution of apical membrane and junctional complexes to the daughter cells.

This observation was striking for two reasons. First, at such early stages in neurogenesis, the vast majority of cells have vertical cleavage planes, i.e. perpendicular or nearly perpendicular to the ventricular surface of the neuroepithelium. Second, most NE cells at this developmental time point are *Tis21*-GFP–negative, which tend to bisect the cadherin hole upon cell division even if the cleavage plane is slightly oblique.

II – 1.5. Loss of Aspm promotes asymmetric cell division

Therefore, we sought to quantify the effect of *Aspm* knock-down on cell division in *Tis21*-GFP–negative NE cells. First, we deduced the cleavage plane from the orientation of the sister chromatids of NE cells in anaphase / early telophase. In agreement with previous observations (Kosodo et al. 2004), nearly all mitotic *Tis21*-GFP–negative NE cells in the control condition showed a vertical cleavage plane orientation (Figure 22A, black columns). Upon Aspm knock-down, however, almost half of the cleavage planes of *Tis21*-GFP–negative NE cells deviated significantly from the normal, vertical orientation (Figure 22A, white columns).

This data indicates that loss of Aspm disrupts the normal cleavage orientation in proliferating NE cells. However, in mammalian NE cells, cleavage plane orientation and symmetry of division are not correlated (Smart 1972a,b; Haydar et al. 2003; Kosodo et al. 2004). Therefore, we investigated whether or not the alteration in cleavage plane angle might also affect the symmetry of division in terms of distribution of apical plasma membrane to the daughter cells.

The distribution of the apical plasma membrane upon division of *Tis21*-GFP–negative NE cells was evaluated by determining the cleavage plane relative to the cadherin hole. In the control condition, consistent with previous observations, 80% of the cleavage planes were predicted to bisect the apical membrane, resulting in its symmetric distribution to the daughter cells (Figure 22B, control). In contrast, almost half of the cleavage plane orientations observed upon Aspm knock-down were predicted to bypass the apical membrane, resulting in its asymmetric distribution (Figure 22B, Aspm RNAi). Such effects on cleavage plane orientation have not been noticed upon RNA interference using esiRNAs for various other proteins expressed in neuroepithelial cells (F. Calegari, L. Farkas, A. Grzyb, A.-M Marzesco and W.B.H., unpublished data), indicating that the present phenotype was specifically due to *Aspm* esiRNAs.

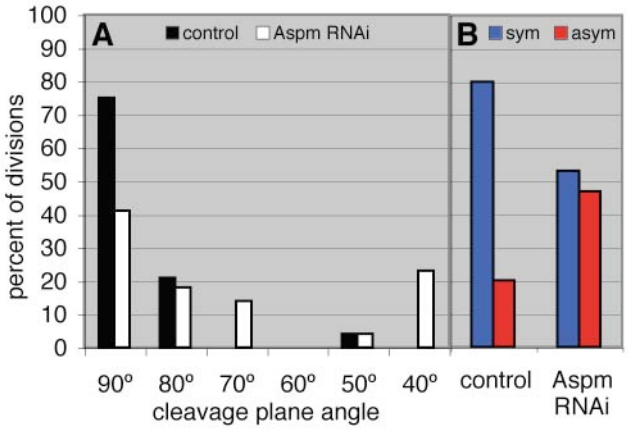

Figure 22: Cleavage plane and cadherin hole analysis. Quantification of cleavage plane orientation (**A**) and cadherin hole distribution (**B**). Dorsal telencephalon of E10.5 *Tis21*-GFP knock-in mice was either electroporated with mRFP plasmid only (control) or co-electroporated with mRFP plasmid and Aspm esiRNAs (Aspm RNAi) followed by 24 h whole-embryo culture, and *Tis21*-GFP–negative, mRFP-expressing NE cells in anaphase or telophase were analyzed for cleavage plane orientation and the position of the cadherin hole as in Figure 20. **A**, Orientation of the cleavage plane relative to the radial, apical-basal axis of the neuroepithelium (defined as 90°), expressed as percentage of all divisions for either the control (black columns, n=24) or Aspm RNAi (white columns, n=22) condition. Groups of cleavage plane angle are ±5°. **B**, Quantification of cadherin hole distribution. Cleavage planes bisecting (symmetric, blue columns) or bypassing (asymmetric, red columns) the cadherin hole, expressed as percentage of all divisions for either the control (n=15) or Aspm RNAi (n=15) condition. Image modified from Fish et al. 2006.

II – 1.6. Increased non-NE fate of NE cell progeny after *Aspm* knock-down

In normal mouse brain development, an asymmetric distribution of the apical plasma membrane upon division of NE cells is highly correlated with these divisions being neurogenic (Kosodo et al. 2004), as reflected by *Tis21*-GFP expression. The

cleavage plane of *Tis21*-GFP–positive NE cells, despite the fact that it is usually vertical, tends to bypass the cadherin hole. This correlation suggests that the apical plasma membrane and junctional complexes are important cell fate determinants. Given the increase in cleavage plane orientations leading to an asymmetric apical membrane distribution in dividing NE cells upon Aspm knock-down, we explored whether this would also cause a change in cell fate. That is, would the loss of Aspm cause *Tis21*-GFP–negative divisions to become neurogenic, rather than proliferative.

We first tried to identify newborn neurons in the VZ by βIII-tubulin immunoreactivity, which is reported to be an early neuronal marker (Fanarraga et al. 1999). However, we did not observe a significant increase in βIII-tubulin–positive cells in the VZ after *Aspm* knock-down (data not shown). This result was not too surprising given other observations in our lab about the onset of βIII-tubulin expression in newborn neurons. Results of live imaging of telencephalic neuroepithelium of transgenic mouse embryos expressing GFP under the control of the βIII-tubulin promoter imply that βIII-tubulin expression in the majority of cells born at the ventricular surface occurs relatively late, that is, after these cells have left the ventricular zone (A. Attardo et al., manuscript in preparation).

Because we needed a very early indication of neuron generation, we chose to use a cellular, rather than molecular, marker. To identify neuron-like cells in the VZ irrespective of whether they have already turned on neuron-specific gene expression, we used abventricular centrosomes as a marker. In contrast to NE cells whose centrosomes are located at the ventricular (apical) surface (Chenn et al. 1998), one of the characteristics of their non-NE progeny, which lack apical plasma membrane, is the abventricular localization of their centrosome (see Figure 11). For example, in neurons, centrosomes are located in the vicinity of the nucleus, both when they are migrating through the VZ (Tanaka et al. 2004; A. Attardo personal communication) and after they have reached the neuronal layers.

Both newborn neurons and basal progenitors are predicted to have abventricular centrosomes due to their non-epithelial nature. To support the use of abventricular centrosomes as a marker of newborn neurons distinct from basal progenitors, we wanted to confirm that abventricular centrosomes in the VZ were associated with post-mitotic cells. Bromodeoxyuridine (5-bromo-2-deoxyuridine, BrdU) is a synthetic nucleoside which is an analogue of thymidine and can be used to

detect cells that are synthesizing DNA. We labeled E11.5 NE cells in S-phase by exposing embryos to BrdU for 30 minutes prior to sacrificing them. After immunolabeling with γ-tubulin, we observed that NE cells in the VZ with abventricular centrosomes in the vicinity of their nucleus indeed lacked BrdU incorporation (Figure 23).

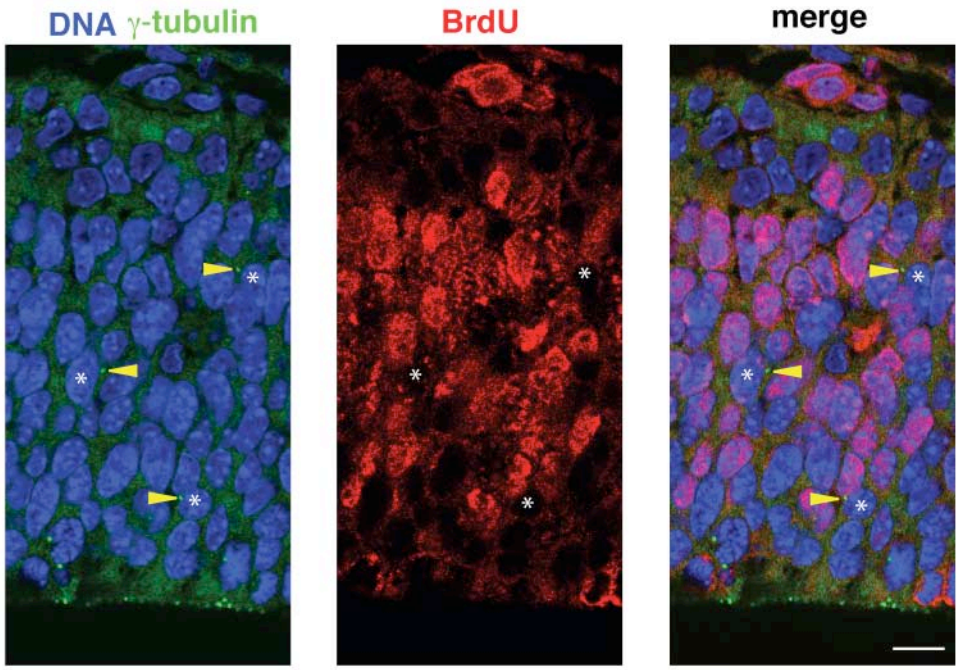

Figure 23: **Abventricular centrosomes in the VZ are associated with BrdU-negative cells.** Cryosections of mouse E11.5 midbrain labeled for 30 min with BrdU were analyzed for DNA staining using DAPI (blue), and γ-tubulin (green) and BrdU (red) immunofluorescence. Arrowheads, abventricular centrosomes; asterisks, abventricular centrosome-associated nuclei, which lack BrdU incorporation. Scale bar in right panel, 10 µm. Experiment done in collaboration with Y. Kosodo. Image modified from supplemental data, Fish et al. 2006.

In order to determine if *Aspm* knock-down had an affect on the number of abventricular centrosomes, we compared the VZ of the targeted telencephalic hemisphere to the opposite, non-targeted hemisphere in the same embryo (Figure 24). After identification of the electroporated region via RFP fluorescence, abventricular γ-tubulin–immunostained centrosomes in the VZ of the targeted and non-targeted side were counted within a 200x50 μm field which excluded the strip containing the apical mitotic cells and the βIII-tubulin–immunostained neuronal layers (e.g., the area between the yellow and white lines in Figure 24). The ratio of abventricular centrosomes in the VZ of the targeted over non-targeted side was then calculated.

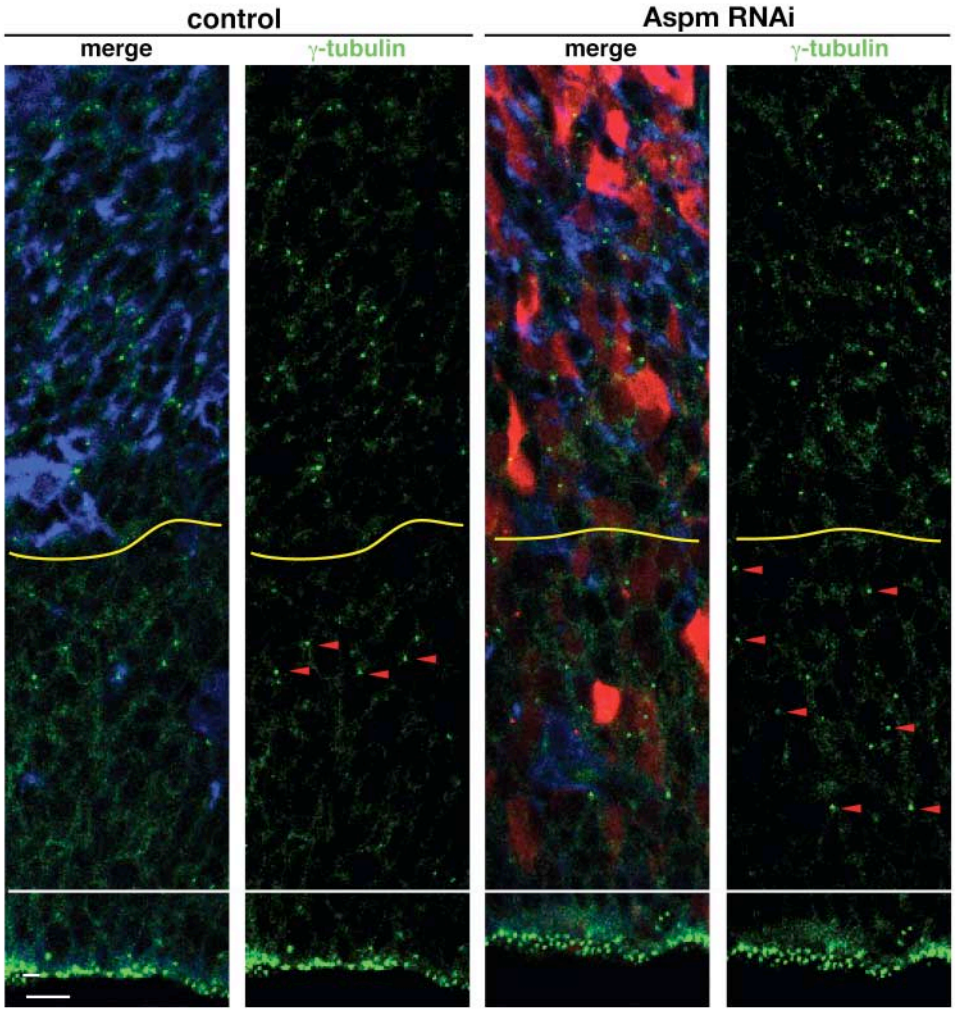

Figure 24: Knock-down of *Aspm* increases the generation of non-NE cells. Mouse E12.5 dorsal telencephalon was either co-electroporated with Aspm esiRNAs and mRFP plasmid or electroporated with mRFP plasmid only, followed by 48 h *in utero* development. Cryosections of the non-targeted (control) and targeted (Aspm RNAi) hemispheres were analyzed for RFP fluorescence (red), and γ-tubulin (green) and βIII-tubulin (blue) immunofluorescence. Note the increase in abventricular centrosomes (arrowheads) upon *Aspm* knock-down. The yellow lines indicate the boundary between the VZ/SVZ and the neuronal layers. The white line indicates the apical boundary for counting abventricular centrosomes in order to exclude interphase centrosomes. The apical surface of the VZ is down. Experiment done in collaboration with Y. Kosodo. Image modified from Fish et al. 2006.

We observed a significant increase in abventricular centrosomes in the VZ of the targeted hemisphere (Figure 24, right panels) compared to the non-targeted hemisphere (Figure 24, left panels) 48 h after initiation of Aspm knock-down in E12.5 mice. This increase was 1.6-fold over the abventricular centrosomes observed in the VZ under control conditions (Figure 25, Aspm RNAi), which is what would be expected, given (i) the efficiency of targeting of NE cells upon in utero electroporation (<50%), (ii) the normal abundance of abventricular centrosomes (cf. Figure 25, left), (iii) the proportion of NE cells undergoing proliferative divisions at

this developmental stage, and (iv) the increase in asymmetric NE cell divisions upon Aspm knock-down (Figure 22B), among other parameters. The increase in abventricular centrosomes was due to the presence of Aspm esiRNAs as no such increase was observed upon electroporation of the mRFP reporter plasmid only (Figure 25, control).

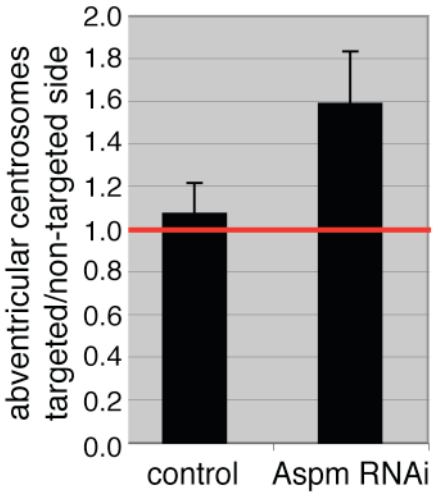

Figure 25: Knock-down of *Aspm* increases the generation of non-NE cells. Numbers of centrosomes per 10,000 μm^2 counted in γ-tubulin–immunostained cryosections are expressed as a ratio of targeted/non-targeted hemispheres for mRFP plasmid only (control) and mRFP plasmid plus Aspm esiRNAs (Aspm RNAi) electroporation. Data are the mean of 5 cryosections from 3 different embryos each; bars indicate S.D. Image modified from Fish et al. 2006.

As Aspm knock-down did not perturb the apical localization of centrosomes in interphase NE cells (Figure 21), we conclude from the increase in abventricular centrosomes that knock-down of Aspm causes an increase in the generation of non-epithelial (non-NE) cells. Because neurons are not the only non-NE cells in the developing telencephalon, this result by itself does not allow us to conclude that NE cells to switch from proliferative to neurogenic divisions upon *Aspm* knock-down. Therefore, we characterized the non-NE cells generated by *Aspm* knock-down in more detail.

II – 1.7. Increased neuron-like fate of NE cell progeny after *Aspm* knock-down

To begin with, we analyzed the neuronal layer of the targeted hemisphere of *Tis21*-GFP knock-in mouse embryos identified by βIII-tubulin immunofluorescence (Figure 26). Consistent with previous observations (Haubensak et al. 2004), in the

control condition (electroporation of mRFP only), less than half of the young neurons in the neuronal layer lacked GFP fluorescence (Figure 26B, left column). *Aspm* knock-down resulted in a significant increase in the proportion of GFP-negative/RFP-positive cells in the neuronal layer (Figure 26B, right column), suggesting an increasing contribution of progeny derived from NE cells lacking *Tis21*-GFP expression. Remarkably, almost all of the GFP-negative/RFP-positive cells in the neuronal layer observed upon *Aspm* knock-down showed βIII-tubulin expression, as exemplified in Figure 26A. From these results, we conclude that at least some of the non-NE progeny generated by *Aspm* knock-down migrate to the neuronal layer and express neuronal markers.

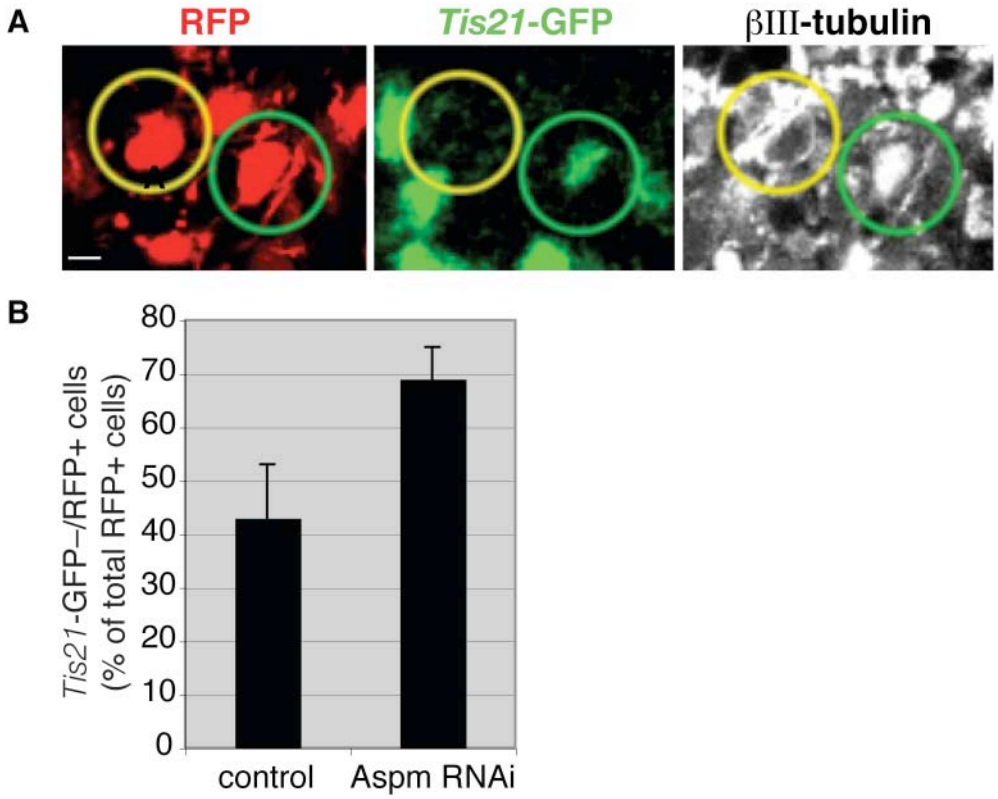

Figure 26: The increase in non-NE cells correlates with an increase in *Tis21*-GFP- cells in the neuronal layer. Dorsal telencephalon of E10.5 *Tis21*-GFP knock-in mice was either co-electroporated with Aspm esiRNAs and mRFP plasmid (Aspm RNAi) or electroporated with mRFP plasmid only (control), followed by 24 h whole-embryo culture. **A**, Representative example of two neighboring RFP-positive cell bodies (red) in the neuronal layer, with one being positive (green circles) and one negative (yellow circles) for *Tis21*-GFP fluorescence (green) but both exhibiting βIII-tubulin immunofluorescence (white). Scale bar in left panel, 5 μm. **B**, Cryosections were analyzed for the proportion of RFP-positive cells in the neuronal layer that lacked *Tis21*-GFP fluorescence. Data are the mean of 3 cryosections from 2-3 different embryos each (control, 70 cells; Aspm RNAi, 74 cells); bars indicate S.D. Image modified from Fish et al. 2006.

In the telencephalon, neurons arise from NE and radial glia cells dividing at the ventricular surface and from progenitors dividing basally in the VZ and SVZ (Haubensak et al. 2004; Miyata et al. 2004; Noctor et al. 2004). Given that the centrosomes of the basal progenitors are also abventricular, we examined whether the increase in abventricular centrosomes in the VZ upon *Aspm* knock-down reflected an increase in basal progenitors. However, no obvious increase in abventricular mitotic cells was observed upon *Aspm* RNAi (Figure 27). This lack of increase in basal progenitors in turn suggests that the neuron-like cells observed in the neuronal layer after *Aspm* knock-down were generated directly by NE cells.

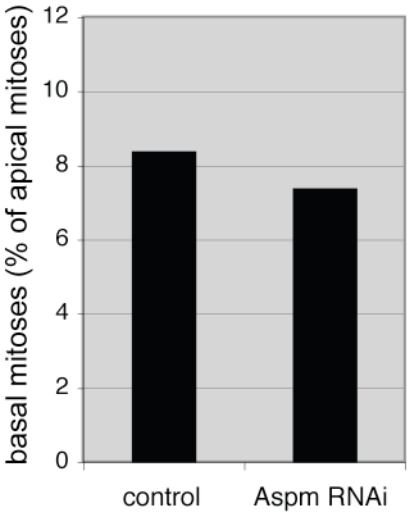

Figure 27: ***Aspm* knock-down does not result in an increase in basal progenitors.** Mouse E10.5 dorsal telencephalon was co-electroporated with Aspm esiRNAs and mRFP plasmid, followed by 24 h whole-embryo culture. Cryosections of the non-targeted (control) and targeted (Aspm RNAi) hemispheres were analyzed for mitotic cells in the basal region *versus* apical surface of the VZ, using phosphohistone H3 immunofluorescence. Basal mitotic cells are expressed as a percentage relative to apical mitotic cells, whose frequency of occurrence was similar for the control (244 cells per total reference area) and Aspm RNAi (219 cells per total reference area) condition. Data are the sum of 18 cryosections, each with the same size field for the non-targeted (control) and targeted (Aspm RNAi) hemisphere, from 3 different embryos. Image modified from supplemental data, Fish et al. 2006.

Taken together, our observations indicate that *Aspm* knock-down in NE cells increases the probability of their progeny adopting a non-NE fate. This includes a neuron-like fate (migration to neuronal layers, expression of neuronal markers). We do not know whether the neuron-like cells observed develop into functional neurons, and we cannot exclude that the progeny generated by the *Aspm*–knocked-down NE cells, including the neuron-like cells, eventually undergo apoptosis. However, we can conclude that whichever fate the progeny ultimately adopt, it is a non-NE fate, which

in any case implies a reduction in the NE progenitor pool relative to control.

II – 1.8. Loss of Aspm affects mitotic cells in anaphase

Having made some conclusions about the cellular function of Aspm, we wanted to dissect the molecular mechanism of this function in a little more detail. In our earlier analysis, we noticed that the deviation in chromatid alignment of cells lacking Aspm only became apparent after anaphase. Initially, our quantification of cleavage plane orientation only considered cells in anaphase or telophase. Now, we have expanded that analysis to include NE cells in metaphase. In these experiments, a reporter plasmid (pCAGGS-Cherry) was co-electroporated with either Aspm esiRNAs or PBS. As before, cleavage plane orientation was predicted from chromatid alignment relative to the ventricular surface. Representative cells electroporated with *Aspm* esiRNAs in metaphase (upper panel) and telophase (lower panel) are shown in Figure 28A.

In contrast to cells in anaphase or telophase, *Aspm* knock-down does not affect metaphase cells which align perpendicular to the ventricular surface in the vast majority of the cases (Figure 28C, blue bars). The increasing tendency for chromatids to deviate from a vertical orientation during anaphase and telophase (Figure 28C, red bars) suggests that Aspm is particularly important in stabilizing spindle orientation throughout the metaphase to anaphase transition. This indicates that *Aspm* is not important for spindle position (which is determined by the end of metaphase by regulators at the cell cortex, as discussed in the introduction), but rather for ensuring the precision of spindle precision through cytokinesis.

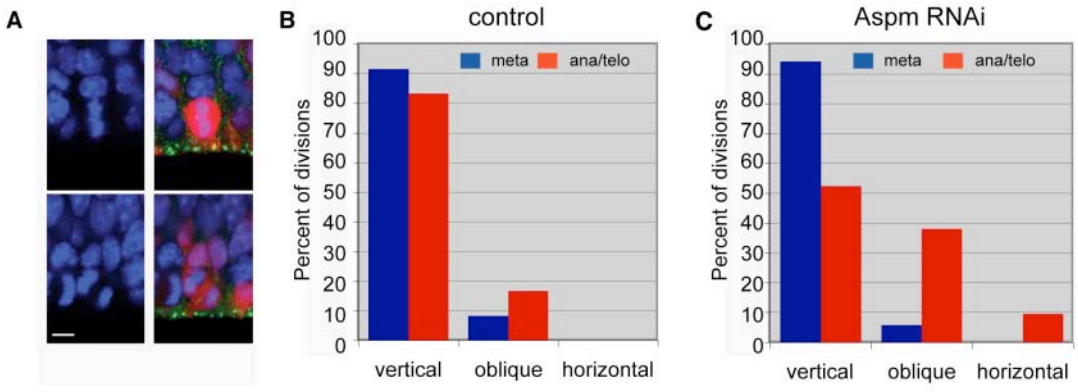

Figure 28: Knock-down of *Aspm* affects the cleavage plane angle of NE cells in anaphase. **A**, NE cells in metaphase (upper panels) and anaphase/telophase (lower panels) from mouse E10.5 dorsal telencephalon of *Tis21*-GFP knock-in mice after co-electroporation with Aspm esiRNAs and pCAGGS-Cherry plasmid and 24 h whole-embryo culture. Dapi is shown in blue, Cherry is shown in red, and γ-tubulin is shown in green. All cells analyzed were *Tis21*-GFP negative (not shown). The apical surface is down. Scale bar in lower left panel, 5 μm. **B**, **C**, Quantification of cleavage plane angle in NE cells of control (**B**) and Aspm RNAi (**C**) embryos. **B**, In the control condition, metaphase (blue bars, n=12) and anaphase/telophase (red bars, n=12) are predominantly vertical. **C**, Upon Aspm RNAi, the cleavage plane of anaphase/telophase (red; n=21) NE cells tends to deviate from vertical, consistent with previous findings. However, the majority of metaphase (blue; n=19) NE cells are vertical, similar to control conditions. Cleavage plane angle was predicted by measuring the angle of the chromatids to the ventricular surface. Vertical = 90-80°, oblique = 79-40°, horizontal = 40-0°.

II – 1.9. Model for Aspm function during symmetric NE cell divisions

How could Aspm be involved in the maintenance of spindle position? The data presented here suggest that suggest that Aspm exerts a critical role at the spindle poles of NE cells in maintaining spindle position through mitosis and, consequently, in ensuring the precise cleavage plane orientation required for symmetric, proliferative divisions (Figure 29). In particular, Aspm may be required to maintain the tight association of kinetochore microtubules to the centrosome. This association becomes particularly important in anaphase when forces are generated on the spindle in order to separate the sister chromatids (Alberts et al. 1994; Mitchison & Salmon 2001).

In the absence of Aspm, the interaction between centrosomes and kinetochore microtubules may weaken, causing spindle position to deviate from its precise alignment. This deviation would not have to be great in order for it to be significant. Since NE cells are highly elongated, the requirement to bisect their small apical membrane for symmetric, proliferative division implies not only that the mitotic spindle has to adopt an axis exactly perpendicular to the NE cell apical-basal axis by the end of metaphase. It also necessitates that this spindle axis is maintained during

anaphase and telophase to ensure that the basal-to-apical ingression of the cleavage furrow occurs precisely along the apical-basal NE cell axis.

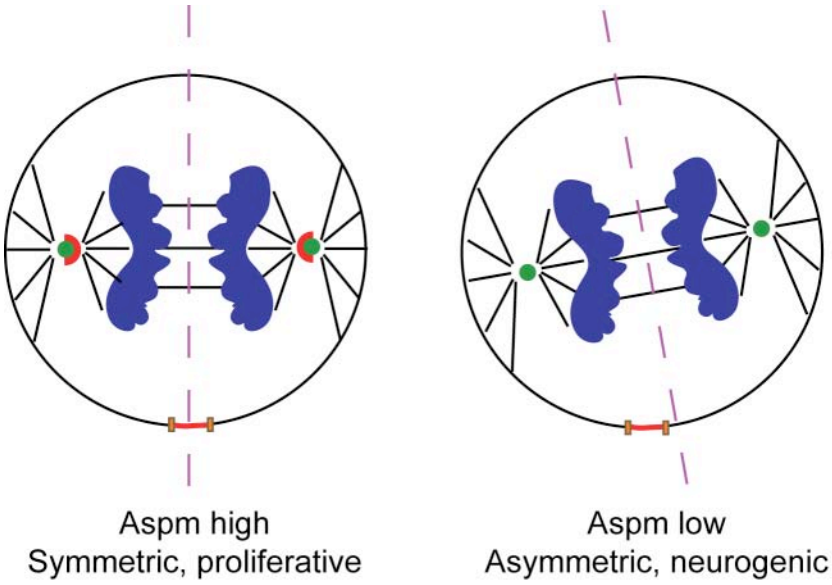

Figure 29: **Model of Aspm function in mammalian NE cells.** A schematic diagram of NE cells in anaphase. In proliferating cells (left), *Aspm* expression is high. Aspm (red crescents) localizes to the centrosome (green circles) where it maintains the precise alignment of the spindle along the apical-basal axis, contributing to the bisection of the apical membrane (red line) and junctional complexes (brown boxes). In neurogenic divisions (right), *Aspm* expression is low. In the absence of Aspm at the spindle poles, precision of the spindle along the apical-basal axis is not maintained, contributing to the cleavage furrow bypassing the apical membrane and junctional complexes.

II – 1.10. Strategy for testing ASPM in an evolutionary context

Our results can only provide a possible explanation for the *ASPM* loss of function phenotypes observed in humans. However, our data does suggest that evolutionary changes in *ASPM* have been selected to increase the number of symmetric, proliferative cell divisions, thus increasing the precursor pool. If this is true, human ASPM should promote more symmetric, proliferative cell divisions than mouse Aspm. In order to assess if expression of human *ASPM* provides a gain of function, we have generated a "humanized" mouse. The humanized mouse is a transgenic animal in which a copy of the human *ASPM* gene has been added to the genome. Expression of the human gene in the developing neuroepithelium of our humanized mouse was confirmed by *in situ* hybridization (Figure 30). *ASPM* appears to be properly expressed in the VZ, as expected. Further characterization of *ASPM* expression, localization and function in the humanized mouse is necessary to

determine if ASPM confers any gain of function that might have led to evolutionary selection. This project is currently being pursued by another student in our laboratory.

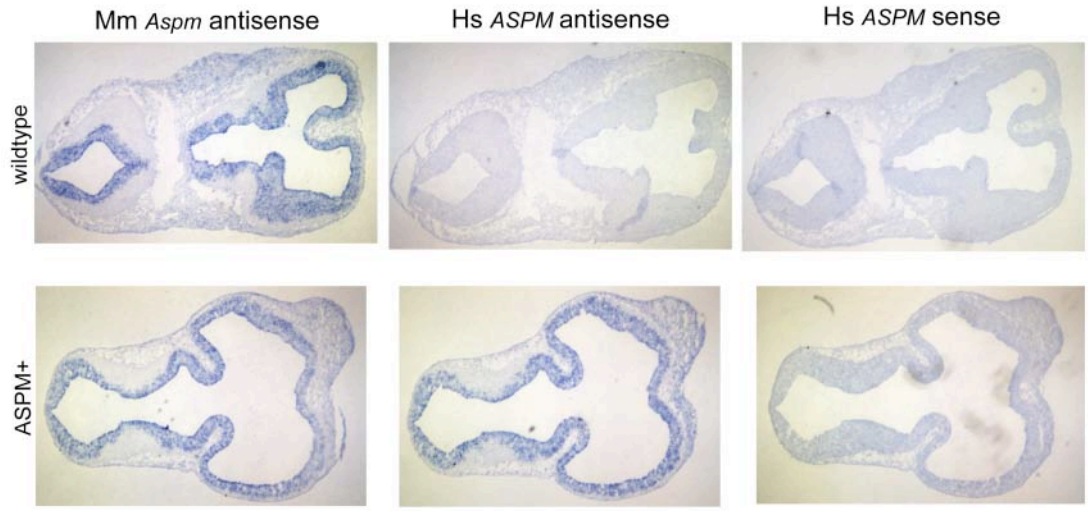

Figure 30: Expression of *ASPM* in the "humanized" mouse. *In situ* hybridization on E10.5 transverse cryosections of NMRI mouse brains. Two littermate embryos from a cross between a heterozygous transgenic mouse carrying a copy of the human *ASPM* gene and a wildtype mouse. Consecutive cryosections from an embryo negative for the human *ASPM* gene are shown in the upper panels. The lower panels display consecutive cryosections from an embryo positive for the human ASPM gene. Both embryos express the mouse *Aspm* gene (left panels). The positively transgenic embryo also expresses human *ASPM*, which is absent in the negative embryo (middle panels). A sense probe against the human *ASPM* gene is negative for both embryos (right panels).

II – 2. Comparative Analysis: Primate and Rodent Progenitors

II – 2.1. Pax6 and Tbr2 in rodent neuronal progenitors

In the rodent CNS, two distinct pathways of neuron generation have been described (see Figure 6): 1) asymmetric cell division at the apical surface of the VZ yielding one post-mitotic neuron and one cell that continues to cycle (apical progenitors), and 2) symmetric cell division in the SVZ yielding two post-mitotic neurons (IPCs, basal progenitors). Based on mitotic position (apical or basal), the abundance of these two progenitors was quantified in the mouse at early developmental times (Haubensak et al. 2004). More recently, the transcription factors Pax6 and Tbr2 have been shown to be reliable lineage markers distinguishing these neuronal progenitors. Pax6 is expressed in apical mitotic cells whereas Tbr2 marks basal mitotic cells (Englund et al. 2005).

For the purposes of the analysis presented here, it was important to determine the specificity of Tbr2 and Pax6 as markers for different progenitor populations in rodents. The mouse neuroepithelium was immunostained for Tbr2 or Pax6 together with Phosphohistone H3 (Figure 31). As predicted, Tbr2 is largely present in the SVZ (Figure 31A), and Pax6 is widely expressed in the VZ (Figure 31B). In the case of Tbr2, its co-localization with *Tis21*-GFP could also be visualized, allowing its expression in neurogenic versus proliferating cells to be determined. This analysis was not possible for Pax6 because the immunostaining protocol requires special treatment for antigen retrieval, which destroys the GFP signal.

Tbr2 and Pax6 positive mitotic cells, both basal and apical, were counted and assessed for the presence or absence of these markers (Figure 31C). Basal mitotic cells are almost always Tbr2+ regardless of *Tis-21*-GFP expression (80/82 cells; the two negative cells were negative for both markers). In contrast, apical mitotic cells are predominantly negative for Tbr2. Instead, apical mitotic cells appear to be exclusively labeled by Pax6 (128/128). Pax6 is also present in approximately one-third of basal mitotic cells (9/32), although the immunoflourescence is weaker relative to apical mitotic cells. This data indicates that *Tbr2* is more broadly expressed in basal mitotic cells than *Tis21* (which is only expressed in 90% of basal mitotic cells), at least at early developmental times.

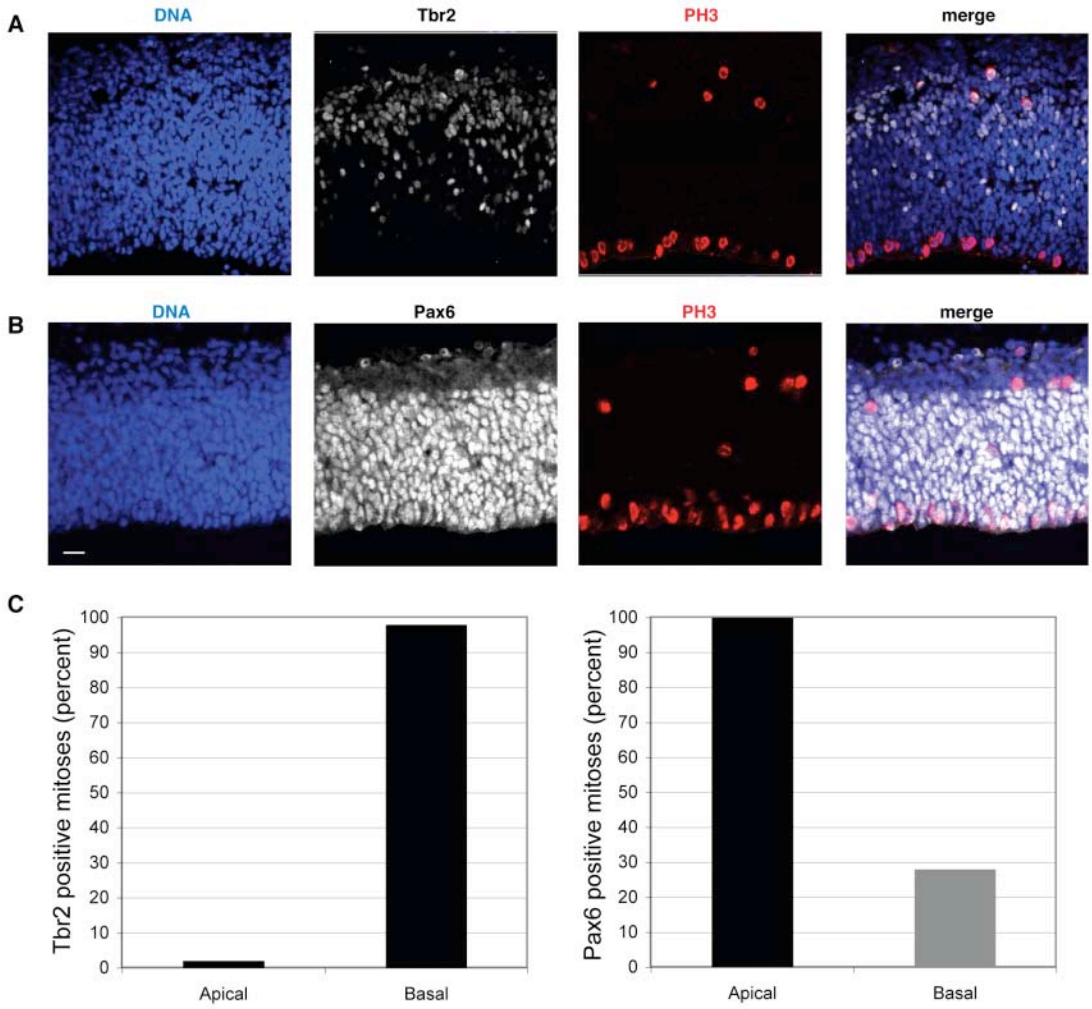

Figure 31: Tbr2 and Pax6 in rodent apical and basal mitotic cells. **A,** Cryosections of E13.5 mouse telencephalon were analyzed for DNA staining using DAPI (blue), and Tbr2 (white) and PhosphoHistone-H3 (red) immunofluorescence. **B,** Cryosections of E12.5 mouse telencephalon were analyzed for DNA staining using DAPI (blue), and Pax6 (white) and PhosphoHistone-H3 (red) immunofluorescence. **A**, **B**, The apical surface is down. Scale bar in lower left panel, 20 µm. **C,** Mitotic cells, represented by PhosphoHistone-H3 positive immunostaining, were scored for their localization (apical or basal) and the presence of Tbr2 (left) or Pax6 (right). Nearly all basal mitoses are positive for Tbr2 (80/82), while less than one-third of basal mitoses are Pax6 (9/32) positive. Pax6+ basal mitoses are weaker than Pax6+ apical mitoses (represented by grey versus black bars). In contrast, apical mitotic cells are almost exclusively Pax6 positive (128/128) and Tbr2 negative (11/408). Data come from E12.5 (n=4) and E13.5 (n=4) embryos.

Recently, a transgenic mouse carrying a bacterial artificial chromosome (BAC) coding for GFP under the control of the Tbr2 locus was generated (Gong et al. 2003). Characterization of this mouse has been undertaken with the intent of determining the fate of the Tbr2+/*Tis21*-GFP– basal mitotic cells. First, to ensure that the cells identified by Tbr2 immunostaining were also GFP+ in the transgenic mouse, co-localization of Tbr2 immunoreactivity and *Tbr2*-GFP expression in E10.5 mouse telencephalon was assessed (Figure 32A). Early developmental times were chosen in order to reduce the number of cells that would be GFP+ due to inheritance of the

protein rather than due to activation of the Tbr2 locus. However, the fact that GFP is inherited by the daughter cells of the progenitor that expressed Tbr2 allows the progeny of all Tbr2+ progenitors to be followed. Interestingly, throughout development, the neuronal layer of *Tbr2*-GFP knock-in mice is completely GFP+ (Figure 32B). This data suggests that either Tbr2 is expressed in neurons or that all neurons derive from a Tbr2+ progenitor. Since it has been shown that many neurons are born from apically dividing NE cells, which are largely Tbr2–, we suggest that Tbr2 may, in fact, be an early neuronal marker. This hypothesis is supported by the recent study of Tbr2 mutations in humans that indicated a role for Tbr2 in neuronal migration (Baala et al. 2007).

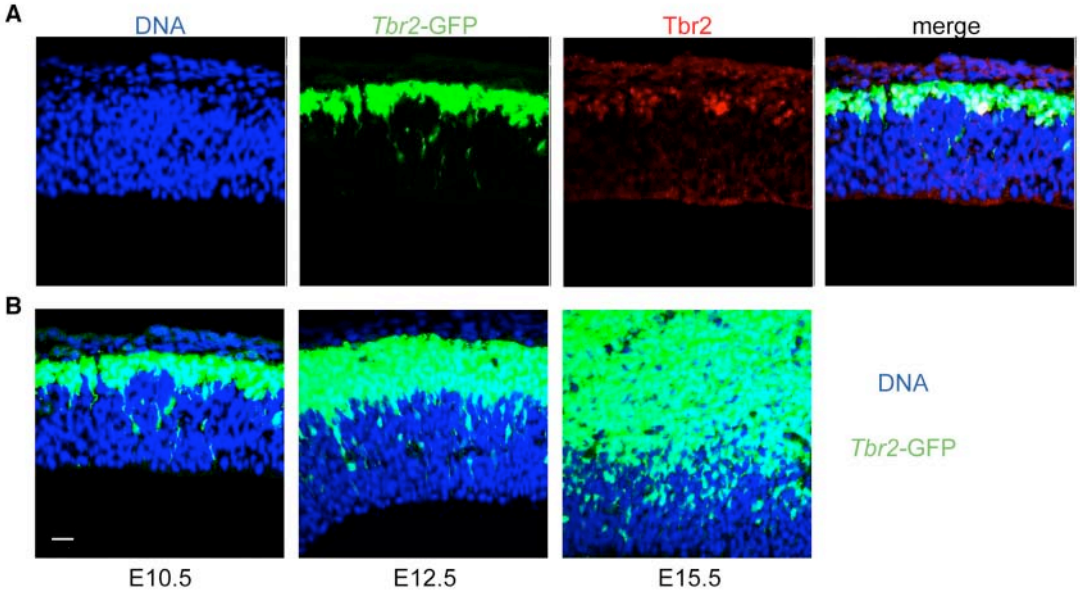

Figure 32: *Tbr2* expression in the *Tbr2*-GFP knock-in mouse. **A,** Dorsal telencephalon of E10.5 *Tbr2*-GFP knock-in mice was stained with DAPI (DNA, blue), and immunostained for Tbr2 (red). Intrinsic GFP–fluorescence driven from the Tbr2 locus is shown in green. Tbr2 immunofluorescence colocalizes with *Tbr2*-GFP–fluorescence, although *Tbr2*-GFP– fluorescence is also seen in neurons that are not positively immunostained. **B**, *Tbr2*-GFP– fluorescence in E10.5, E12.5, and E15.5 telencephali, showing Tbr2-GFP–positive cells in the VZ and the neuronal layer. All cells in the neuronal layer appear positive for Tbr2-GFP. The apical surface is down. Scale bar in lower left panel, 20 μm.

That Tbr2 is not a general marker for basal mitotic cells, but rather may be specific to the neuronal lineage, is suggested by its absence in basal mitotic cells at late developmental times. We found that most basal mitotic cells at E18.5 are *Tbr2*-GFP– (Figure 33). At this developmental time point, neurogenesis is largely complete, and gliogenesis has begun (Sauvageout 2002).

Consistent with previous observations (Englund et al. 2005), these data suggest that *Pax6* is expressed in apically dividing NE and RG cells in the VZ, the polarized epithelial progenitors, and down-regulated in cells that have lost their epithelial characteristics. Conversely, Tbr2 immunoreactivity identifies SVZ progenitors, the non-epithelial IPCs. That *Tbr2*-GFP is found in all neurons suggests that *Tbr2* is transiently expressed in newborn neurons.

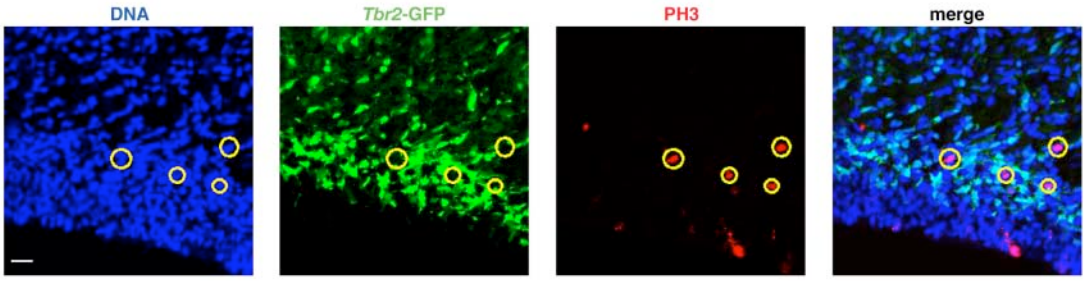

Figure 33: *Tbr2* is not expressed in basal mitotic cells at late developmental stages. Dorsal telencephalon of E18.5 *Tbr2*-GFP knock-in mice was stained with DAPI (DNA, blue) and immunostained for Phosphohistone H3 (red). At this stage, basal mitotic cells (yellow circles) are negative for *Tbr2*-GFP. Scale bar in lower left panel, 20 μm. The apical surface is down.

II – 2.2. Pax6 in primate basal neuronal progenitors

Following from the observation that Pax6 and Tbr2 immunoreactivity identify distinct neuronal progenitors in rodents, the pattern of these markers in primate neuronal progenitors may reflect evolutionary changes in one of these two progenitor populations. In order to perform this analysis, monkey telencephalic tissue was obtained as part of a collaboration with the lab of Collette Dehay in the Department of Stem Cell and Cortical Development at the Université Claude Bernard Lyon I in Lyon, France. Several slices of E80 (late-mid-neurogenesis) macaque brain, representing cortical areas 17 and 18, were analyzed. Unfortunately, Tbr2 immunostaining in this tissue was weak to absent (data not shown). It is not yet clear if this reflects an absence of expression at this developmental time point or technical limitations due to the method of preservation. However, Pax6 immunoreactivity in this tissue provided some interesting results. The OSVZ, as well as the VZ, contains many Pax6+ cells (Figure 34). Most of the mitotic figures in the VZ and OSVZ were Pax6 positive. Under the immunostaining conditions employed, mitotic cells are more highly immunoreactive, most likely due to the lack of a nuclear envelope that

may make them more accessible to the antibody. Thus, it is possible that most, if not all of the cells of the OSVZ are Pax6+.

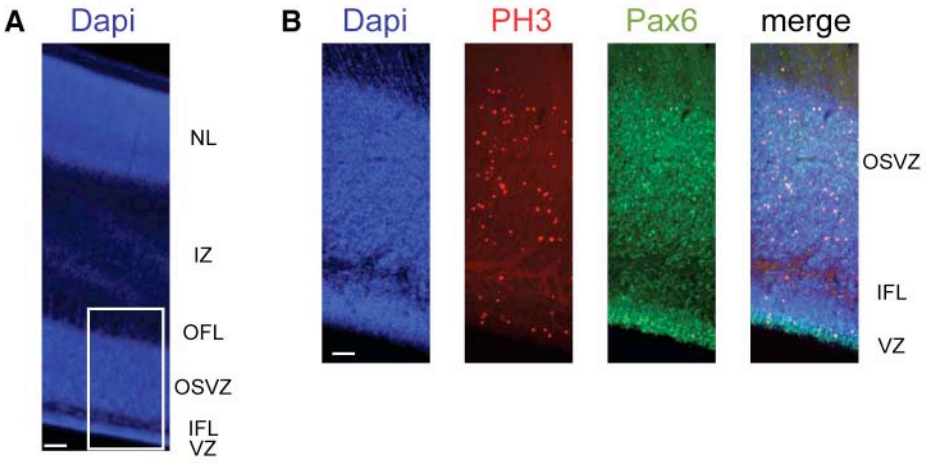

Figure 34: Pax6 in primate basal mitotic cells. Dorsal telencephalon of E80 macaque was stained with DAPI (DNA, blue) and immunostained for Phosphohistone H3 (red) and Pax6 (green). **A**, Low power view of the entire neuroepithelium indicating the major layers. The area inside the white box is magnified in **B**. Scale bar in lower left panel, 250 µm. The apical surface is down. **B**, Mitotic cells at the apical surface in the VZ as well as basal mitosis in the OSVZ are Pax6 positive. Scale bar in lower left panel, 100 µm. The apical surface is down.

Mitotic cells of the monkey VZ and OSVZ were compared more precisely in high magnification confocal images. As shown in Figure 35, mitotic cells of the OSVZ are strongly positive for Pax6, with similar or greater immunoreactivity than that of mitotic cells of the VZ. This is interesting to note given that, in rodents, basal mitotic cells that are Pax6+ are much weaker than apical mitotic cells. The difference between mouse and monkey in Pax6 identity of basal mitotic cells is even more striking when considered in quantitative terms. In the mouse, less than one third of the basal mitotic cells were Pax6 positive (Figure 31C). In contrast, 89% of basal mitotic cells in the monkey OSVZ were found to be Pax6 positive (Figure 36). More samples will be required in order to reliably quantify this pattern, but it provides some evidence that basal progenitors of the OSVZ are more similar to the apical progenitors of the rodent VZ than to the basally dividing IPCs.

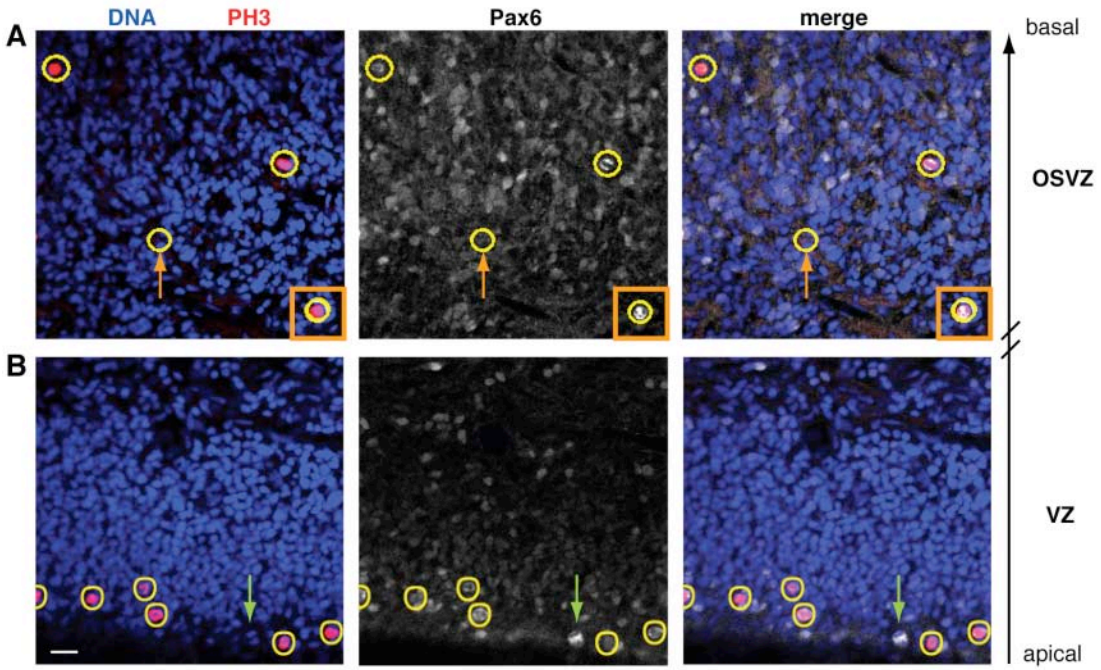

Figure 35: Pax6 in mitotic cells of the primate germinal layers. Dorsal telencephalon of E80 macaque was stained with DAPI (DNA, blue, left panel) and immunostained for Pax6 (white, middle panel) and Phosphohistone H3 (red, right panel). Single optical sections are shown. Mitotic cells identified by Phosphohistone H3 immunofluorescence are highlighted with yellow circles. **A**, Mitotic cells of the OSVZ are positive for Pax6. The orange arrow points to a mitotic cell from a different optical section that is shown in an insert at the bottom right of each panel. The boxed mitotic cell is strongly Pax6 positive. **B**, Mitotic cells of the VZ are also Pax6 positive. The green arrow points to a Pax6 positive telophase cell that was not positive for Phosphohistone H3. Note that Pax6 immunoreactivity is roughly equal in cells of the VZ and OSVZ. Scale bar in lower right panel, 20 μm. The apical surface is down.

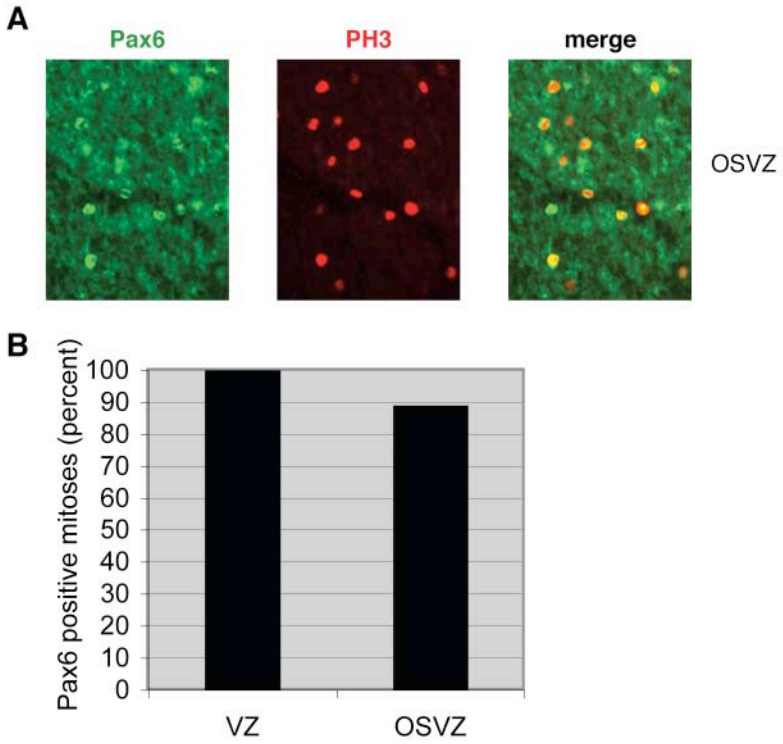

Figure 36: Pax6 in mitotic cells of the primate OSVZ. **A**, Dorsal telencephalon of E80 macaque was immunostained for Pax6 (green, left panel) and Phosphohistone H3 (red, middle panel). Mitotic cells

from a portion of the OSVZ are shown. **B**, Mitotic cells of the VZ (not shown) and OSVZ, represented by PhosphoHistone-H3 positive immunostaining, were scored for the presence of Pax6. All VZ mitoses were Pax6 positive (20/20) and 89% of OSVZ mitoses were Pax6 positive (94/106). Data come from a 60µm thick macaque section.

II – 2.3. Pax6 and Tbr2 in human neuronal progenitors

The implication that basal mitotic cells in monkeys may have different properties than basal mitotic cells in rodents suggests an evolutionary change in progenitors between these two lineages. However, to confirm that this pattern was general for primates rather than specific to monkeys, a second primate species was analyzed. To this end, fetal human telencephalon samples were collected. We established a collaboration with the University Clinic in Dresden, Germany, which provided human fetal tissue coming from legal abortions with parental consent. In total, 41 embryonic samples were collected (Table 2). However, from these 41, only one sample (number 36) was sufficiently preserved to obtain an intact and identifiable telencephalic sample. This sample, aged 10 weeks post conception, was used for immunostaining analyses.

Sample number	Date collected	Sample age	Tissue identified
1	2 June 2004	8 weeks	No CNS
2	4 June 2004	10 weeks	No CNS
3	11 June 2004	11 weeks	Partial SC
4	11 June 2004	11 weeks	Un-ID brain
5	23 June 2004	9 weeks	Partial HB
6	25 June 2004	10 weeks	No CNS
7	25 June 2004	9 weeks	No CNS
8	9 July 2004	10 weeks	No CNS
9	21 July 2004	7 weeks	No CNS
10	6 August 2004	10 weeks	No CNS
11	9 August 2004	11 weeks	Partial SC
12	9 August 2004	10 weeks	Partial SC, HB
13	11 August 2004	11 weeks	SC, 2 un-ID brain
14	24 September 2004	9 weeks	Partial SC
15	4 October 2004	10 weeks	2 partial SC, partial HB
16	8 October 2004	9 weeks	2 partial SC
17	22 October 2004	8 weeks	No CNS
18	10 December 2004	12 weeks	Partial SC, HB
19	21 January 2005	11.5 weeks	Partial SC, HB
20	26 January 2005	10 weeks	Partial SC

21	7 February 2005	7 weeks	Partial SC
22	25 February 2005	12 weeks	Partial SC, HB
23	19 March 2005	12 weeks	Partial HB
24	18 April 2005	11 weeks	No CNS
25	18 April 2005	9 weeks	Partial SC, HB
26	10 June 2005	7 weeks	No CNS
27	13 June 2005	10 weeks	4 Un-ID brain
28	1 July 2005	7 weeks	3 Un-ID brain
29	22 July 2005	10 weeks	Partial HB
30	22 July 2005	10 weeks	Partial SC, MB
31	9 September 2005	7 weeks	Partial HB
32	14 October 2005	11 weeks	2 Un-ID brain
33	17 October 2005	10 weeks	Partial SC, HB
34	5 November 2005	12 weeks	2 Un-ID brain
35	9 December 2005	10 weeks	2 partial HB
36	6 February 2006	10 weeks	Complete brain
37	3 April 2006	9 weeks	No CNS
38	17 May 2006	11 weeks	2 Un-ID brain
39	22 May 2006	10 weeks	No CNS
40	12 February 2007	12 weeks	Partial SC
41	21 February 2007	12 weeks	Partial SC

Table 2: Human tissue samples collected. The number, date, age, and identification of each sample collected are listed.

In contrast to the monkey tissue, the human tissue was positively immunostained for Tbr2. Double-labeling with Tbr2 and Pax6 revealed a pattern that is superficially similar to that in rodents (Figure 37). Pax6 strongly labels the VZ, whereas Tbr2 labels cells of the SVZ (ISVZ). It is not clear if the difference in staining is tissue specific (monkey versus human), related to developmental stage (the human tissue is from a relatively earlier developmental time), or differences in preservation and storage of the tissue. Nonetheless, comparison of the human and mouse Tbr2 and Pax6 immunostainings reveals some interesting differences. First, Pax6 immunoreactivity in humans is more broad, overlapping with Tbr2 immunoreactivity and extending more basally (compare Figure 37A with Figure 31B).

Second, basal mitotic cells in the human are Pax6 positive. In this sample, basal mitotic cells were rare, perhaps due to its early developmental stage, thus limiting quantitative analysis. However, two examples of basal mitotic cells identified by phosphohistone H3 immunostaining that are Pax6 positive and Tbr2 negative are shown in Figure 37 A and B. Tbr2 positive basal mitotic cells could also

be identified by Dapi staining (highlighted by the red arrow in Figure 37B), but as seen in this sample, they are also strongly positive for Pax6. These data suggest that Pax6 expression in basal mitotic cells is a general pattern in primate NE cells that is distinguishes primate basal progenitors from rodent IPCs.

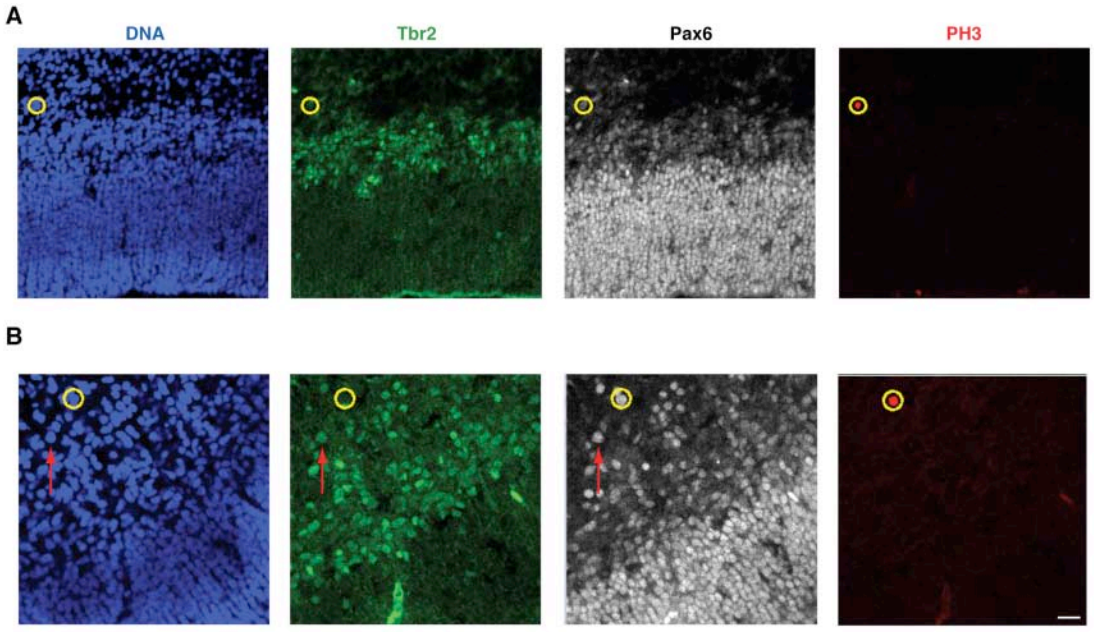

Figure 37: Tbr2 and Pax6 in human basal mitotic cells. **A, B,** Consecutive cryosections of 10wpc human dorsal telencephalon were stained for Dapi (DNA, blue, left panels) and immunostained for Pax6 (**A**) or Tbr2 (**B**) (red, middle panels). Scale bar in lower right panel, 20 µm. The apical surface is down.

II – 2.4. The epithelial characteristics of primate basal neuronal progenitors

In rodents, Pax6 immunoreactivity identifies progenitors with epithelial characteristics, which maintain apical contact. The finding that primate basal progenitors are Pax6 positive suggests that they may also have apical processes (as predicted by Smart and colleagues 2002). Therefore, attempts were made to further evaluate the epithelial characteristics of primate basal mitotic cells. Due to preservation issues, the structural quality of the monkey tissue that we received from the Dehay lab was not sufficient for us to make reliable conclusions about the cellular structure of the cells in the OSVZ. Consequently, this analysis focused on the human tissue. A first attempt to visualize cell processes with DiI labeling of fixed tissue, did not result in any positive labeling (data not shown).

Immunostaining with MPM2, a mitotic protein marker that labels the cytoplasm of mitotic cells including their processes, was slightly more informative. The immunostaining worked quite well on the human tissue, however, the processes were too numerous and thin to follow (Figure 38). An additional problem with this method is that MPM2 also labels neurons, which caused a lot of background in our analysis. Unfortunately, these results cannot contribute to the discussion about apical contact in basal mitotic cells, but they do indicate the extensive processes present in the human germinal layers.

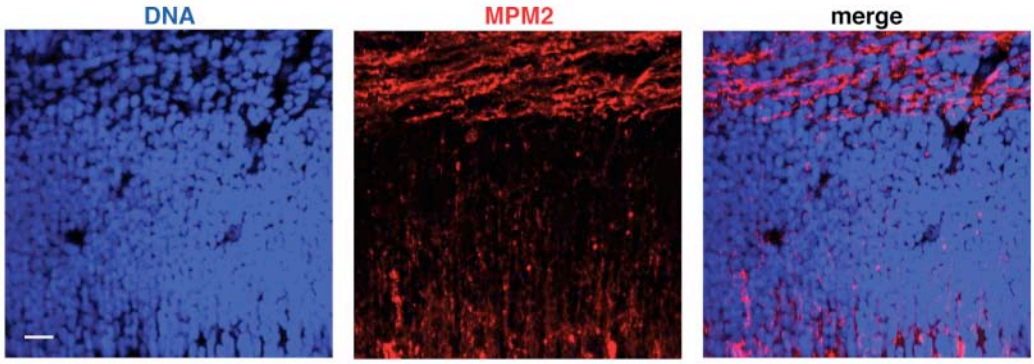

Figure 38: NE cell processes in the human VZ. 10wpc human dorsal telencephalon stained for Dapi (DNA, blue, left panel) and immunostained for MPM2 (red, middle panel). The image is presented as a projection of 8 1µm confocal sections. Note the numerous, thin cell processes. Scale bar in lower left panel, 20 µm. The apical surface is down.

III. Discussion

III – 1. ASPM and the Evolution of NE Cell Division

III – 1.1. Aspm has functionally diverged from Asp

In *Drosophila*, mutations in *asp* cause NBs to arrest in metaphase. However, beside the observation that *Aspm* knocked-down NE cells progressed through telophase (Figure 20, bottom), we did not detect any increase in mitotic NE cells (identified by phosphohistone H3 immunostaining or DAPI staining) upon *Aspm* knock-down (Figure 27). Thus, unlike *asp* mutations in *Drosophila* NBs, *Aspm* knock-down in mouse NE cells does not appear to block mitosis in metaphase.

It is important to note that, in *Drosophila*, loss of Asp function only disrupts asymmetric division of NBs. There is no reported function/role for Asp in the symmetric division of *Drosophila* epidermoblasts, although the functional data does not indicate that Asp should be specific for asymmetric division. Our data indicate that, in mammals, *Aspm* is expressed in both proliferating and neurogenic NE cells, with a specific role in maintaining symmetric NE cell divisions. These observations demonstrate that there has been some functional evolution separating Aspm and Asp.

III – 1.2. The role of *Aspm* in mammalian development and evolution

Our results provide a cell biological explanation for the function of Aspm in mammalian neocortical development. The need of the highly elongated, polarized NE cells to bisect their small apical membrane for symmetric, proliferative division implies not only that the mitotic spindle has to adopt an axis exactly perpendicular to the NE cell apical-basal axis by the end of metaphase. It also necessitates that this spindle axis is maintained during anaphase and telophase to ensure that the basal-to-apical ingression of the cleavage furrow occurs precisely along the apical-basal NE cell axis. Our observations suggest that Aspm exerts a critical role at the spindle poles of NE cells in maintaining spindle position through mitosis and, consequently, in ensuring the precise cleavage plane orientation required for symmetric, proliferative divisions.

Loss of Aspm upon knock-down results in a deviation of spindle position, and hence an alteration in cleavage plane orientation, thereby increasing the probability of

asymmetric division of NE cells, with only one daughter cell inheriting apical membrane and adherens junctions and thus remaining epithelial. In other words, loss of Aspm reduces the expansion of the NE progenitor pool. This would explain why humans with mutations in *ASPM* suffer from primary microcephaly (Bond et al. 2002). Similar considerations may hold true for mutations in other genes encoding centrosomal proteins that cause primary microcephaly (Bond et al. 2005). The observation that only the brain is affected in these patients (Woods et al. 2005), despite the expression of *Aspm* in other developing epithelia (Kouprina et al. 2005), likely reflects the highly elongated shape of NE cells and their small apical membrane, which make them more vulnerable to any perturbations in spindle position when undergoing symmetric, proliferative divisions. A corollary of this is that with the increase in brain size during primate evolution, the further reduction in the apical membrane of NE cells, which predicts the need for even greater accuracy of cleavage plane orientation, offers a potential reason for the positive selection of *ASPM* observed in the primate lineage (Zhang et al. 2003; Kouprina et al. 2004).

III – 1.3. Evolution of the regulation of asymmetric division

All vertebrates studied (e.g., turtles, fish, birds, lizards, rodents, carnivores, primates) have a multi-layered cortex that develops from a pseudo-stratified neuroepithelium (Nakai & Fujita 1994; Aboitiz et al. 1999). In contrast, invertebrates, such as *Drosophila*, have a simple brain that develops from a stratified epithelium. After losing their junctional complexes, *Drosophila* NBs delaminate from the overlying neuroectodermal epithelium. Asymmetric division in *Drosophila* NBs occurs via a horizontal cleavage plane that results from a 90° rotation of the spindle away from the apical-basal axis. In contrast, vertebrate neurogenic progenitors maintain junctional contact with proliferating NE cells and both divide vertically (Figure 11). It is interesting to note that progenitor cells of non-nervous epithelial tissues of the mouse, such as the epidermis (Smart 1970a; Lechler & Fuchs 2005) and esophagus (Smart 1970b) also develop from a stratified epithelium, which involves rotation of the spindle for asymmetric divisions.

Given that *Drosophila* NBs and non-nervous epithelial tissue share a developmental pattern where asymmetric divisions are associated with a 90°rotation

of the spindle, the question then arises: why is the mammalian neuroepithelium different? One hypothesis is that the pattern of spindle orientation in mammalian NE cells is related to the increase in the size of their brain. Since epithelial cells are polarized along their apical-basal axes, any developmental change that increased the number of vertical cleavages along the polarized axis would contribute to an increase in symmetric, proliferative divisions, and consequently an increase in overall tissue size.

III – 1.4. Evolution of the regulation of spindle orientation

As detailed in the introduction, spindle alignment is largely controlled by factors operating at the cell cortex. In particular, the mammalian ternary complex of the NuMA/LGN/Gα proteins regulates the attachment of aster microtubules to the cell cortex during mitosis (Du and Macara 2004). This complex appears to be evolutionarily conserved, as the *Drosophila* (Mud/Pins) and *C. elegans* (Lin-5/GPR1/2) homologues of NuMA and LGN also attach the spindle to the cell cortex in a G-protein dependent manner (Yu et al. 2003; Srinivasan et al. 2003, 2006; Bowman et al. 2006; Izumi et al. 2006; Siller et al. 2006).

The factors responsible for determining where on the cell cortex this complex associates, and consequently the orientation of spindle alignment, are less clear. In *Drosophila*, Insc is necessary and sufficient for spindle rotation (Kraut et al. 1996; Kaltschmidt et al. 2000). Insc is expressed specifically in NBs, and its ablation leads to randomization of spindle orientation (Kaltschmidt et al. 2000). Further, ectopic expression of Insc in epidermoblasts, leads to spindle rotation and horizontal cleavage (Kraut et al. 1996). Importantly, in wildtype conditions, cleavage in epidermoblasts is not random, but vertical. However, loss of adherens junctions in *Drosophila* epidermoblasts does cause randomization of spindle orientation and cleavage plane (Lu et al. 2001). These observations lead to the hypothesis that junctional complexes provide a signal for vertical cleavage while Insc directs horizontal cleavage, with Insc being the dominant factor. In the absence of either signal (junctional complexes signaling vertical cleavage or Insc mediating horizontal cleavage), cells divide randomly.

In mammals, the vertical cleavage signal provided by junctional complexes appears to be conserved, however, horizontal cleavages are exceptionally rare. In

neural progenitors of the SVZ (which lack apical contact), cleavage plane is randomized (Attardo et al., in prep). Additionally, in mice with mutations that cause NE cells to lose apical membrane attachment, there is an increase in abventricular mitoses and randomization of cleavage plane (e.g., aPKC, Imai et al. 2006; Cdc42, Cappello et al. 2006). Insc expression has been reported in the mammalian neuroepithelium (Zigman et al. 2005), however the rarity of horizontal divisions in this tissue suggests that Insc is not acting in a dominant fashion.

III – 1.5. Evolution of spindle precision

The most parsimonious explanation for these data is that there is a conserved pattern of spindle orientation regulation in epithelial derived animal tissues, where vertical cleavage planes are associated with symmetric divisions and horizontal cleavage planes are associated with asymmetric divisions. The difference in the mammalian neuroepithelium could be explained by a prolongation of the proliferative phase of cell division (most likely via signaling pathways), which includes maintaining a vertical cleavage plane orientation, with a loss of the response to the horizontal cleavage signal.

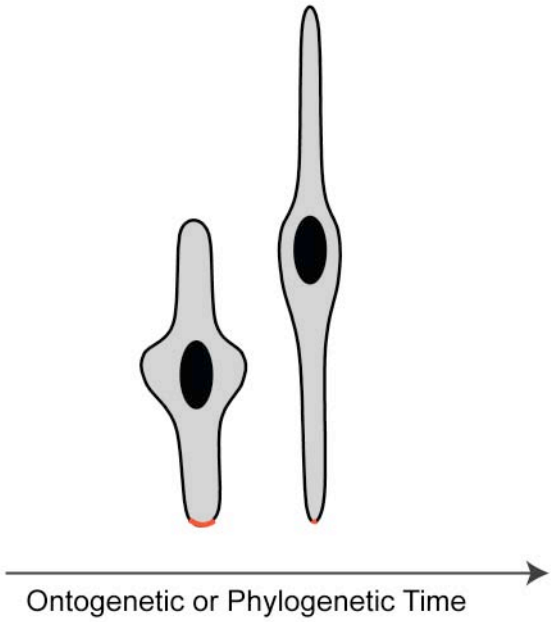

Figure 39: Elongation of NE cells during ontogenetic or phylogenetic time. A schematic representation of NE cells elongating over time. Across ontogenetic or phylogenetic time, the neuroepithelium thickens and NE cells elongate. As a consequence, the apical membrane (shown in red) is reduced in size.

A consequence of an increase in NE cell proliferation is the pseudo-stratification of the neuroepithelium, which in turn results in increasingly elongated NE cells. As NE cells become more elongated, the total size of their apical membrane shrinks, requiring increasing spindle precision in order to bisect it during symmetric divisions (Figure 39). Because only a slight deviation from the apical-basal axis during cytokinesis can result in bypassing, rather than bisecting, the apical membrane, imprecision of spindle orientation can result in an asymmetric division even with a vertically orientated cleavage plane.

Based on the available data, we propose an hypothesis for the two-step evolution of NE cell division in vertebrates, leading to an increase in brain size:

1. Maintenance of junctional complexes in neurogenic progenitors leading to a prolongation of vertical cleavages, with loss of the response to the horizontal cleavage signal leading to pseudo-stratification and increased progenitor number.
2. Evolution of precision proteins as pseudo-stratification increases and the apical membrane shrinks, leading to an increase in symmetric, proliferative divisions.

In this model, symmetry versus asymmetry of division in mammalian NE cells would be modulated by spindle *precision* along the apical-basal axis, rather than spindle *position* perpendicular or parallel to the apical-basal axis. We suggest that Aspm may have evolved as a "precision protein" functioning to maintain spindle position from the time it is set at the end of metaphase through anaphase and telophase until cytokinesis is completed.

Regarding the first point, it is interesting to consider the evolutionary history of the Reelin signaling pathway. If the neuronal layer is no longer created by delamination into a stratified tissue, there will have to be a mechanism for neurons to properly migrate out of the germinal zone. Reelin is important for neuronal migration and the condensation of the cortical plate (radial and laminar CP organization). Importantly, Reelin is present in all vertebrates, but absent in the invertebrates *Drosophila* and *C. elegans* (Bar et al. 2000). In the absence of Reelin, the developing mouse cortex is poorly organized, with neurons that are obliquely rather than radially aligned and less densely packed than in wildtype animals (Bar et al. 2000). Thus, the

establishment and elaboration of the Reelin signaling pathway may have been important to the advent of pseudo-stratification.

With regard to the second point, it has been noted that NuMA mutants have a similar phenotype to Asp mutants (Compton 1998). That is, that mutations in NuMA block mitosis. Consequently, it was suggested that Asp was the *Drosophila* NuMA homologue. Now it is established that Mud is the NuMA homologue in *Drosophila* and that Asp is the homologue of Aspm. However, these data indicate that there may be some functional redundancy between Asp and Mud. The recent discovery of an essential role for NuMA at the cell cortex (Du & Macara 2004) in addition to its previously defined role at the spindle poles (Fant et al. 2004), may have led to conservation of NuMA/Mud structure and function. Consequently, any redundancy of function between Mud and Asp at the spindle poles could have contributed to relaxation of selective constraints on Aspm, allowing it to diverge functionally.

III – 1.6. *ASPM* evolution: Selection for other cellular roles?

It follows from the functional study in mouse NE cells presented here that selection for changes in *ASPM* in the primate and human lineages could have promoted an increase in symmetric, proliferative divisions, resulting in an increase in brain size. We suspect that the role of ASPM gains increasing importance as proliferation of NE cells increases, due to their increased elongation during ontogenetic and phylogenetic time (see Figure 39). However, while our data is consistent with this inference, we have yet to demonstrate any gain of function associated with ASPM that would be necessary to support our hypothesis.

Ponting (2006) has argued that selection on ASPM may not have been for its role during mitosis of NE cells, but rather for a role in ciliary function. While our data cannot exclude this hypothesis, particularly as it relates to sperm flagella, we consider it unlikely. First, we did not observe Aspm associating with the centrosome during interphase when it serves as the basal body of the cilium. Second, our *in situ* hybridization data indicate that *Aspm* is not expressed in the neuronal layer, which would reduce the possibility of it directing neuronal migration. We cannot exclude that Aspm is inherited by newborn neurons where it could then be involved in cell migration. However, the fact that *Aspm* is down-regulated as NE cells switch from

proliferative to neurogenic divisions makes a critical role for Aspm in neurons unlikely.

III – 2. Constraints on NE Cell Proliferation

III – 2.1. The apical membrane as a cell fate determinant

The data presented here indicates that expansion of the pool of proliferating NE cells can be inhibited by artificial alteration of the cleavage plane away from the apical-basal axis. Similar results were also reported for Nde1 (Feng & Walsh 2004). Despite this, it is still unknown if and how daughter cell fate may be determined. For example, the inheritance of apical plasma membrane may be important to maintain the proliferative state. At the same time, loss of apical contact and junctional complexes might be a critical step to initiate the differentiation process in newborn neurons.

The difference in cell fate observed in *Drosophila* NBs upon horizontal cleavage is predicated upon the segregation of cell fate determinants along the apical basal axis. For example, the Prospero, Brat, and Miranda proteins localize to the basal side of the NB and are inherited only by the GMC. In contrast, the vertical cleavages of epidermoblasts equally distribute cell fate determinants, generating daughter cells of similar cell fate. In *Drosophila* NBs, Numb is asymmetrically localized to the basal cortex and is inherited only by the GMC (Knoblich et al. 1995). In contrast, mammalian numb (mNUMB) localizes to the apical cortex of NE cells, and is variably inherited between daughter cells (Zhong et al. 1996). This suggests that the localization of and/or response to cell fate determinants has diverged between *Drosophila* NBs and mammalian NE cells.

Instead, the critical cell fate determinants in mammalian NE cells appear to be the apical plasma membrane and junctional components (Huttner & Kosodo 2005). Mouse mutants that disrupt apical contact lead to premature neurogenesis and disordered cortices (e.g., cdc42, aPKC, Pax6). Constitutive over-expression of beta-catenin, an integral component of adherens junctions, leads to increased cell-cycle re-entry of progenitors, resulting in an expansion of the progenitor pool (Chenn & Walsh

2002). All of these data are consistent with Smart's hypothesis (1972) that limited apical membrane space is a constraint on proliferation.

III – 2.2. Basal mitotic populations and the SVZ

It is readily accepted in the literature that the SVZ is the source of upper layer neurons. Further, the expansion of the SVZ correlates with the expansion of upper layer neurons in primates. From these data, it is inferred that IPCs increase in number and evolutionary importance. But what is the evidence that the size of the SVZ is equivalent to the number of IPCs, or that the gene expression of the SVZ represents gene expression of IPCs? In addition to IPCs, the SVZ contains many newborn and young neurons that are migrating through this layer towards the cortical plate. The correlation of IPC marker identity with SVZ identity is largely based on *in situ* hybridization data that cannot distinguish between mitotic cells and other cells that might be in the SVZ, such as migrating neurons.

One study that specifically evaluated mitotic cells concluded that Tbr2 is a marker of the IPC lineage (Englund et al. 2005). However, data presented in this thesis, while preliminary, suggests that Tbr2 might be more generally a neuronal marker. The finding that basal mitotic cells in rodents have a higher Tbr2 expression than apical progenitors could be explained by the hypothesis that IPCs are more primed from neurogenesis (Haubensak et al. 2004; Miyata et al. 2004; Noctor et al. 2004).

Related to the hypothesis of the apical membrane being important to proliferation is the possibility that something in the apical membrane inhibits differentiation. That is, apical membrane contact is not only important to receive signals at the junctions or from the lumen for cell cycle re-entry, but that differentiation is actively inhibited. Thus, *Tbr2*, and perhaps other neuronal markers may be more obviously expressed in IPCs, because their expression is no longer inhibited once apical contact and junctions are lost. This hypothesis may also hold for *Cux2* and *Svet1*, which have already been clearly described as neuronal markers. Further, since these genes are known to be neuronal markers, their expression in the SVZ may also be accounted for by newborn neurons migrating through the SVZ rather than reflecting an increase in progenitors from this layer.

Finally, an important finding reported in this thesis is that basal mitotic cells in primates are Pax6 positive, similar to apical progenitors in rodents (Figure 40). If Tbr2 is a marker of the IPC lineage, then the data presented here suggest that the Tbr2 lineage does not increase in primates as hypothesized by Kriegstein and colleagues (2006). Instead, it supports the hypothesis that basal mitotic cells of the primate OSVZ are derived from rodent VZ progenitors. Confirmation of epithelial characteristics in primate basal mitotic cells, specifically maintenance of apical processes, was not achieved by the results reported here. However, it should be noted that basal Tbr2 positive cells increase in the mice with mutations that disrupt apical contact (e.g., Cdc42, Cappello et al. 2006), suggesting that Tbr2 is a reliable marker of cells that have lost their apical processes. Together, these data favor the hypothesis that basal mitotic cells in the primate maintain apical contact as proposed by Smart and colleagues (2002).

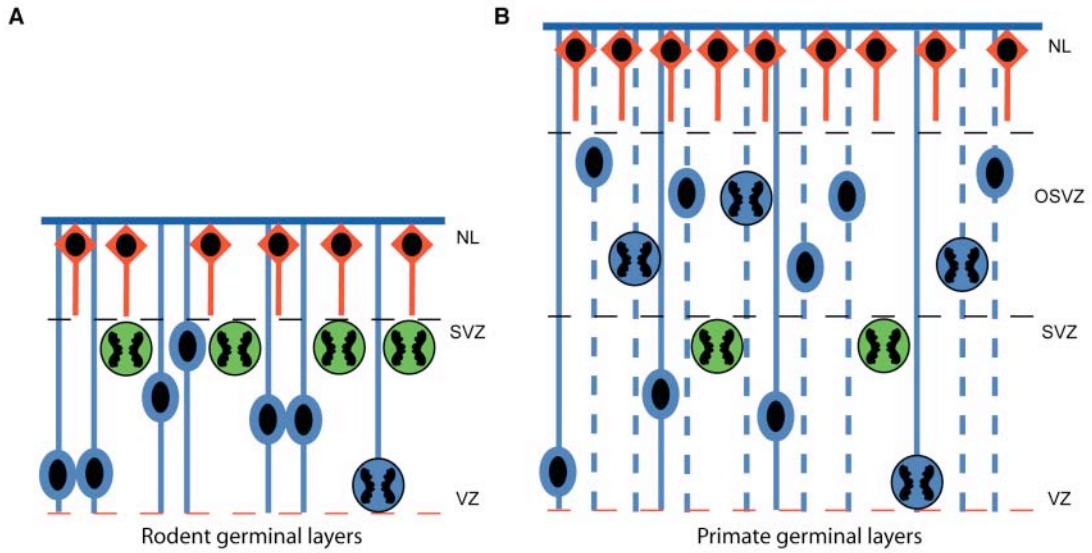

Figure 40: Tbr2 and Pax6 in primate and rodent basal mitotic cells. A schematic representation of the germinal layers of rodents (**A**) and primates (**B**). **A**, In rodents, NE/RG progenitors of the VZ (blue nuclei) have elongated processes, divide at the apical surface, and express Pax6. In contrast, SVZ progenitors (IPCs, green nuclei) lack apical processes, divide basally, and express Tbr2. **B**, In primates, the Tbr2 positive mitotic cell population (green nuclei) is reduced. Moreover, both basal and apical dividing progenitors express Pax6 (blue nuclei). Dashed lines represent the hypothesized epithelial nature of basal mitotic cells in primates.

III – 2.3. Epithelial versus non-epithelial progenitors

An impressive feature of the isocortex is its highly organized morphology. This contrasts starkly with the ganglionic eminences of the ventral telencephalon.

Why is it then, that the isocortex forms a thin, tightly compact, radially organized sheet of cells whereas the GE appears as a globular lump of cells (Rakic 1995)? One phenomenon that correlates with these structures is mitotic populations. In the cortex, most progenitors divide apically, from a radial precursor. In the GE, most progenitors are basal, arising from cells without apical membrane. This correlation, together with previously mentioned increasing role of the Reelin signaling pathway, indicate the importance of radial guidance to cortical structure and function. Further, most data from mammals indicates that the apical membrane is important for continued proliferation (see above discussion).

It is unclear how a vast increase in non-epithelial cells would allow for the maintenance of radial organization. The increased number of neurons generated from such IPCs, could, in principle, contribute to increased thickness of the CP by hopping onto a neighboring radial guide, but a mechanism by which non-epithelial precursors could contribute to an ordered, radial lateral expansion of the brain has not been offered. Thus, although the hypothesis of non-epithelial progenitor expansion cannot yet be rejected, it is not the most parsimonious explanation for lateral expansion of the primate brain because it requires multiple evolutionary changes.

In contrast, there is at least some direct evidence in favor of the epithelial nature of SVZ progenitors in primates. First, GFP labeling of OSVZ progenitors in monkey tissue slices clearly shows elongated apical and basal processes extending from OSVZ nuclei (Lukaszewicz et al. 2006). The number of OSVZ nuclei with processes was not quantified, but comparative morphological studies on primates and rodents reveal a difference in shape and organization between the OSVZ and the rodent SVZ (Smart et al. 2002). In this work, I tried to quantify the epithelial nature of basal mitotic cells in monkey and human tissue, but I was limited by tissue availability and quality. The processes of the human VZ cells are too thin and too abundant to reliably trace their identity to individual nuclei. Future work in which live cells are labeled in a slice culture system may allow quantitative data to be obtained.

III – 2.4. Delayed versus extended differentiation

A related point that is not specifically addressed in this thesis, but is nonetheless relevant to the discussion, is the issue of the kinetics of the switch from

symmetric to asymmetric divisions. Both Smart's two rules and Rakic's two phases emphasize expansion of the proliferative pool via delayed differentiation. This is undubitably true in the mathematical sense that more progenitors make more neurons. However, this mathematical model refers to the average onset of neurogenesis. That is, to say that primates have a delay in neurogenesis compared to rodents means that the time that the majority of progenitors are generating neurons rather than undergoing symmetric, proliferative divisions is relatively later in primates than in rodents. While true, this conceptualization diminishes the importance of another potentially critical component contributing to lateral expansion- that is, the potential early onset of neurogenesis in primates.

MPM2 immunostaining which was used to look for processes in mitotic cells of the human VZ, revealed a striking amount of positive staining throughout the whole VZ (see Figure 38). At the same time, there is already a well-developed neuronal layer at 10 weeks post-conception. These observations lead to the consideration that neurogenesis is occurring relatively earlier in the humans than it does in mouse. Recently, it was reported that "predecessor" neurons are found in the human isocortex prior to neural tube closure (Bystron et al. 2006). To date, this type of cortical neurons appear unique to humans, both in their molecular characteristics and early birthdate.

Thus, it could be that the onset of neurogenesis is earlier in primates than in rodents, even if "on average" neurogenesis is delayed. Why is this important? If apical membrane space is a constraint on proliferation, there will be a finite number of progenitors that can exist at one time per given apical membrane area. At some point, it will be mechanically impossible to put more progenitors in the same area. Still the neuron generating potential of this apical membrane area can be increased by allowing some of the progenitors to undergo neurogenesis early, generate their allotment of neurons, and then be consumed, thus freeing some apical membrane space for new progenitors which continue to be generated.

The effects of the kinetics of the switch from symmetric to asymmetric division are presented in Figure 41. In this example, it can be seen that an early onset of neurogenesis with a slow rate of progression (green line) can ultimately lead to more progenitors in the same number of generations than a late onset of neurogenesis with a fast switch (red line).

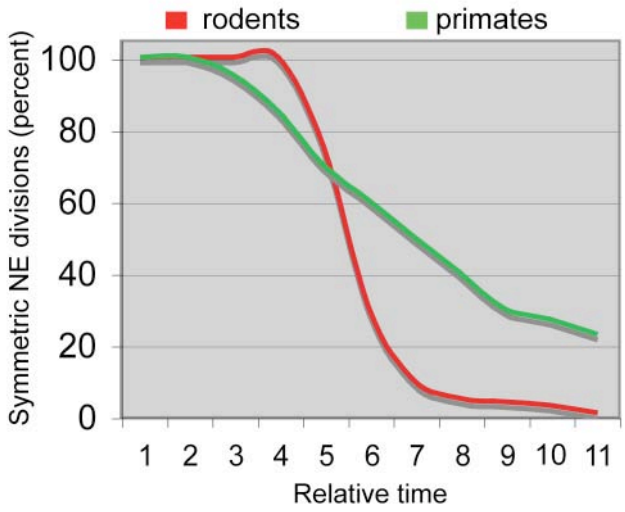

Figure 41: Delayed versus extended differentiation. Graph displaying a hypothetical change in the kinetics of the switch from symmetric, proliferative to asymmetric, neurogenic cell divisions. An earlier, but slow switch in primates may allow more lateral expansion than a later, but fast switch.

As an hypothesis, one could add a third rule to Smart's two: *In order to maximally optimize the neuronal production over a given apical membrane space, the duration of neurogenesis should be increased, with some progenitors initiating neurogenesis early and the rate at which subsequent progenitors switch to neurogenic divisions decreased*. This point has not been explicitly emphasized in the literature, and it is not trivial when considering the evolutionary mechanisms generating increases in brain size. It suggests that whatever mechanisms are triggering the onset of neurogenesis must be induced *earlier* rather than later, maintained for a longer time, and regulated with a slower rate. It changes the question from how to delay neurogenesis to how to extend neurogenesis. This hypothesis also suggests that progenitors may escape the apical crunch by dividing basally, and/or dividing apically over a more extended period.

III – 3. Future Perspectives

The mouse model system provides a powerful tool for genetic manipulation and functional studies. As exemplified by our study on *Aspm*, cell biological mechanisms can be dissected, and their role in embryonic development studied. These studies allow us to generate hypotheses about evolutionary processes. However, the mouse model system is restricted in the sense that it cannot account for

developmental processes that are specific to primates (see Molnar et al. 2005 for review). In the case of *Aspm*, its evolutionary importance might only be relevant in the highly elongated cells of the OSVZ that do not exist in the mouse neuroepithelium. For this and other reasons, comparative studies in primate tissue are essential. Further, more live imaging and genetic manipulation via viral infection in slice culture of primate tissue will be necessary to understand primate neurogenesis. A more complete picture of primate neural development will help elucidate the important changes in this lineage and contribute to our understanding of its evolution.

One of the most obvious open questions is whether or not the progenitors of the OSVZ divide in a symmetric, proliferative manner, and the percentage of these progenitors that maintain apical contact. It is known that the OSVZ generates the majority of neurons in the primate cortex (Lukaszewicz et al. 2005), however, it is not known if these cells also proliferate. It would also be interesting to know the mechanics of how these cells divide. If OSVZ progenitors do proliferate, this would imply that they can symmetrically distribute their apical membrane to both daughters or that one daughter can "re-grow" apical membrane in a similar manner that has been proposed for the basal processes of apical progenitors in rodents (Miyata et al. 2001). Answering these questions about the cell biology of the developing primate brain will provide invaluable insight into the molecular genetics behind the evolutionary changes that generated the large brains of primates.

IV – 1. Materials

IV - 1.1. Antibodies

Antibody I	*Kind*	*Dilution*	*Source*
α-Aspm	Rabbit, polyclonal, IgG	1:1000	(generated in house)
α-βIII-tubulin	Mouse, monoclonal, IgG	1:400	Sigma
α-BrdU	Mouse, monoclonal, IgG	1:500	Hybridoma cell line (in house)
α-Cadherin	Mouse, monoclonal, IgG	1:200	Sigma
α-Cadherin	Rabbit, polyclonal, IgG	1:200	Sigma
α-γ-tubulin	Mouse, monoclonal, IgG	1:200	Alexis Biochemicals
α-γ-tubulin	Rabbit, polyclonal, IgG	1:200	Sigma
α-MPM2	Mouse , Monoclonal, IgG	1:6000	Upstate
α-Pax6	Rabbit, polyclonal, IgG	1:200	Covance
α-PH3	Rabbit, polyclonal, IgG	1:400	Upstate
α-Tbr2	Rabbit, polyclonal	1:250	AbCam

Antibody II	*Kind*	*Dilution*	*Source*
α-Mouse A532	Goat, polyclonal IgG	1:1000	Jacksons immunoresearch
α-Mouse Cy3	Goat, polyclonal IgG	1:1000	Jacksons immunoresearch
α-Mouse Cy5	Goat, polyclonal IgG	1:1000	Jacksons immunoresearch
α-Rabbit A532	Goat, polyclonal IgG	1:1000	Jacksons immunoresearch
α-Rabbit Cy3	Goat, polyclonal IgG	1:1000	Jacksons immunoresearch
α-Rabbit Cy5	Goat, polyclonal IgG	1:1000	Jacksons immunoresearch

IV - 1.2. Mouse strains and tissue samples

IV-1.2.1 Mouse strains

All experiments with *Tis21*-GFP knock-in mice were performed on heterozygous embryos obtained from crossing homozygous males with C57BL/6J females. Wildtype embryos were obtained from NMRI mice. The vaginal plug was defined as embryonic day E0.5. All experiments with *Tbr2*-GFP knock-in mice were performed on heterozygous embryos obtained from crossing homozygous males with CD1 females.

IV-1.2.2 Monkey tissue

Fixed 60μm thick sections of E80 macaque brain (areas 17 and 18) were obtained from the laboratory of Collette Dehay in the Department of Stem Cell and Cortical Development at the Université Claude Bernard Lyon I in Lyon, France. The samples were shipped and stored in 1ml of anti-freeze solution. Sections were washed 3 times for a total of 24 hours in PBS + 0.1% Tween prior to proceeding with immunostaining.

IV-1.2.3 Human tissue

Human embryonic tissue age 7-12 weeks was obtained from the Frauenklinik, Dresden, Germany after legal abortions. All tissue was received with consent of the mother and obtained following national ethics guidelines under German law. Tissue

was fixed in 4% paraformaldehyde at 4°C for 24 hours, embedded in Tissue Tek, and stored at -80°C until used.

IV - 1.3. Buffers and culture media

10X DNA loading buffer	50mM Tris/Hcl, pH7.6 2.5mg/ml Bromophenol Blue 2.5mg/ml Xylene Cyanol 60% Glycerol in H_2O
10X TBE	0.89 Tris 0.89 Boric Acid 20mM EDTA pH8.0 in H_2O

Western Blot:

High Molecular Weight Transfer Buffer:	25mM Tris- 190mM Glycine, pH 8.2-8.5 20% EtOH
Buffer 1	0.3M Tris 20%MeOH pH 10.4 with NaOH
Buffer 2	0.025M Tris 20%MeOH pH 10.4 with NaOH
Buffer 3	0.025M Tris 20%MeOH 0.04M 6-Aminohexane acid pH 9.4

Immunofluorescence:

(i)	Permeabilization	0.3% Triton X 100 in PBS
(ii)	Quenching	0.1M Glycine in PBS, pH 7.4
(iii)	Tx Buffer	0.2%gelatin 300mM NaCl 0.3% Triton X 100 in PBS

Moviol	6.9g Glycerol 2.4g Moviol 120ul 200mM Tris/Hcl pH8.5 in 6ml H_2O

In situ Hybridization:

Ripa buffer	150mM NaCl 1% NP-40 0.5% Na Deoxycholate 0.1% SDS 1mM EDTA 50 mM Tris, pH 8.0

Triethanolamine buffer	100mM Triethanolamine Acetic Acid to pH 8.0
Hybridization buffer	50% Formamide 5X SSC 5X Denhardts 500µg/ml Herring sperm DNA 250µg/ml Yeast RNA
Post-hybridization buffer	50% Formamide 2X SSC 0.1% Tween
Buffer B1	100mM Maleic Acid, pH 7.5 150mM NaCl 0.1% Tween
Buffer B3	100mM Tris, pH9.5 50mM $MgCl_2$ 100mM NaCl 0.1% Tween
Bacteria:	
LB	10mg/ml NaCl 10mg/ml Bacto-Tryptone (Difco) 5mg/ml Bacto-Yeast extract (Difco)
LB-Agar	15mg/ml Bacto-Agar (Difco) in LB
Embryo culture and dissection:	
PBS	137mM NaCl 2.7mM KCl 8mM Na_2HPO_4 1.5mM KH_2PO_4
Penicillin/Streptomycin (100X)	10.000U/ml Penicillin 10.000U/ml Streptomycin in PBS
Tyrod	16g NaCl 0.4g KCl 0.4g $CaCl_2$ 0.42g $MgCl_2 \cdot 6H_2O$ 0.114g $NaH_2PO_4 \cdot 2H_2O$ 2g $NaHCO_3$ 2g Glucose pH 7.4 in H_2O

Whole embryo culture Medium Japan)	Freshly centrifuged rat serum (Charles River 1X Penicillin/Streptomycin 2mg/ml Glucose

IV - 1.4. Chemicals, enzymes, DNA standards and films

For routine work, standard chemicals from the companies Merck, Roth and Sigma were used.

Digoxygenin labeling and detection systems	Roche
DNA standards	NEB
Films	Amersham Hyperfilm
Penicillin/Streptomycin	GibcoBRL
Restriction enzymes and ligases	MBI Fermentas NEB Roche

IV - 1.5. Devices and computer applications

Computer software	Adobe	Photoshop Illustrator Image ready
	Microsoft	Office for Mac
	Scanalytics Inc.	IpLab 3.5.5
	Zeiss	LSM image examiner
Centrifuges	Eppendorf	5417R 5415R
	Beckmann Coulter	Avanti J-25
Cryostat	Microm	HM560
Developer	Kodak	M35X-OMAT-Processor
Electroporator	Genetronics	BTX®-ECM®830
Electrophoresis chambers	EMBL	
Heating block	Eppendorf	Thermostat 5320
Heating chamber	Saur	Bachoffer Chamber
Microscopes	Olympus	BX61 SZX12 Fluoreview FV1000
	Zeiss	LSM510
	Nikon	TE300
pH Meter	Radiometer Analytical	MeterLab PHM210
Spectrophotometer	Pharmacia	Ultrospec III
Sterile Hood	The Baker Company	SteriGard Hood
Thermal Cycler	MJ Research	PTC-200

IV - 1.6. Commercial Kits

Digoxygenin labeling and detection systems	Roche
DNA preparation	

(i)	Maxiprep	Quiagen	Endofree Plasmid Maxi Kit
(ii)	Miniprep	Quiagen	QUIAprep spin Miniprep Kit
(iii)	Tail preparation	Quiagen	DNAeasy Tissue Kit
	DNA transfer	Schlecker & Schuell	Turbo blotter

IV - 1.7. Oligonucleotides

Aspm cloning
ASPMex3-s2: GGC TCG AGGG CCA GCC TCT TCA AAA CAT AC (585-604)
ASPMex3-a2: CCA GAA TTC GGC TGC TTA TCC GCT TTG (1932-1915)

Aspm esiRNAs
Aspm esi sense T7 promoter sequence
5'-CGTAATACGACTCACTATA**G**GG TCTGGCTATGAGTGAATGCTC (695-715)
anti-sense T7 promoter sequence
5'-CGTAATACGACTCACTATA**G**GG ACCTACTAGACCTTCGAGAC (1628-1609)

Aspm in situ:
5'-AATTAACCCTCACTAAA**G**GG AACGGGATTGACGGACTTG (1250-1232)

IV- 1.8. Plasmids

Clontech EGFP C1	EGFP mammalian expression vector (CMV promoter)
pCAGGS-mRFP	mRFP mammalian expression vector (CAGGs promoter)
pCAGGS-Cherry	Cherry mammalian expression vector (CAGGs promoter)

IV – 2. Methods

IV - 2.1. DNA preparation

Plasmid and genomic DNA from mouse tails was prepared using commercially available Kits from Quiagen, according to the manufacturer instructions. For details and buffer composition refer to the manufacturer handbooks.

IV - 2.1.1. Miniprep (QUIAKprep spin Miniprep Kit)

A single bacterial colony was selected with a sterile toothpick and used to inoculate 5ml of LB, supplemented with the appropriate concentration of the appropriate antibiotic. The culture was grown overnight in a shaking incubator at 37°C. The bacteria were harvested by centrifugation (5' at 13,000 rpm, room temperature) and re-suspended in 250µl of buffer P1, then lysed by the addition of 250µl of buffer P2. The lysed suspension was neutralized after 5' by the addition of 350µl of buffer N3 and centrifuged for 10' at 13,000 rpm. The supernatant was applied to the QUIAprep column and centrifuged for 1' at 13,000 rpm. The column was washed twice by the addition of 750µl of buffer PE followed by centrifugation for 1' at 13,000 rpm. The DNA was eluted by the addition of 50µl of buffer EB and centrifugation for 1' at 13,000 rpm.

IV - 2.1.2. Maxiprep (Endofree Plasmid Maxi Kit)

A single bacterial colony was selected with a sterile toothpick and used to inoculate 5ml LB, supplemented with the appropriate concentration of the appropriate antibiotic. The culture was grown overnight in a shaking incubator at 37°C. 500µl of the culture was used to inoculate 250ml LB, supplemented with the appropriate concentration of the appropriate antibiotic. The bacteria were harvested by centrifugation (15' at 6,000g, 4°C) and re-suspended in 10ml of buffer P1, then lysed by the addition of 10ml of buffer P2. The lysate was neutralized after 5' by the addition of 10ml of cold buffer P3. The lysate was then poured into the QUIAfilter cartridge and filtered after 10' incubation. The filtered lysate was incubated for 30' with the endotoxin removal buffer ER, then applied onto the QIAGEN-tip 500 column and allowed to elute by gravity flow. The column was washed twice by the addition of 30ml of buffer QC. The DNA was eluted into a corex tube by the addition of 15ml of buffer QN. The eluate was precipitated by the addition of 10.5ml (0.7 volumes) of isopropanol followed by centrifugation (30' at 15,000g, 4°C). The DNA pellet was washed with 5ml of 70% endotoxin free ethanol, followed by centrifugation (15' at 15,000g, 4°C). The pellet was air-dried and re-suspended in 100µl of cell culture-grade PBS. The DNA solution was centrifuged once more for 10' at 13,000 rpm to clear it from possible debris.

IV - 2.2. Genomic cloning via the polymerase chain reaction

An aliquot of genomic DNA obtained from mouse tails was used for amplification via Polymerase Chain Reaction. The recombinant TAQ DNA polymerase, made in house by D. Drechsel, has a proofreading activity. Amplification products were run on a 2% agarose gel containing Ethidium Bromide at 0.5mg/ml. The gel was prepared in TBE and gel run in TBE buffer.

PCR Mix		*Thermal Cycler Program*	
Reaction Buffer (10x)	3ul	Cycle(s)	Temperature
			Time

dNTPs (10mM)	0.3ul	1	95^0C	5’
Oligonucleotides (100um)	0.3ul	10	95^0C	30”
Template DNA	5ul		0.1^0C/ second down to	
“super” TAQ (5U/ul)	0.3ul		55^0- 65^0C	45”
ddH_2O up to	30ul		72^0 C	
1’/Kb				
		20	95^0C	30”
			55^0- 65^0C	45”
			72^0 C	
1’/Kb				
		1	72^0 C	10’

The amplified band corresponding to Mouse Aspm exon 3 was excised from the gel and purified using a Qiagen kit protocol. Prior to ligation, both the PCR product (Aspm exon 3) and the target vector (EGFP-C1) are digested with Xho1 and EcoR1 enzymes at 37°C. The PCR product is digested overnight, and the vector is digested for one hour. After digestion, the nucleic acids are purified by phenol extraction. Digested PCR products and vector are ligated at 16°C for 16 hours. The ligation reaction mix contains 100ng of vector, 10ng PCR product, 1µl 10X reaction buffer, 1µl 10mM ATP, 0.1 unit of T4 DNA ligase, and water up to 10µl total volume. The ligated vector is then transformed into Top10 competent cells. 3µl of the ligation mix is added to 50µl bacteria and transformed by heat shock at 45°C for 90 seconds. After transformation, the bacteria is amplified in a shaking incubator at 37°C for 3 hours. Bacteria are then plated on drug resistant agar plates to obtain transformed colonies.

IV - 2.3. Aspm antibody

GST-tagged recombinant protein from mouse *Aspm* exon 3, representing amino acids 150-263, was used as an immunogen in rabbits. The resulting antisera were affinity-purified. Antisera and affinity-purified Aspm antibodies were first tested in immunoblots of total protein of Cos7 cells overexpressing a GFP-$Aspm_{150-263}$ fusion protein. The specificity of the affinity-purified Aspm antibodies was further corroborated in immunoblots of total protein from mouse E12.5-13.5 heads, in which a band >300 kDa and 3 smaller bands were recognized.

IV - 2.4. Embryo electroporation

Using a glass capillary, wild type or transgenic mice embryos (from 10.5 to E12.5) were injected (*in* or *ex* utero) into the developing telencephalic vesicle with 1-2ul of an endotoxin-free DNA solution (, pCAGGs-mRFP, or pCAGGs-Cherry, or Aspm esiRNAs; concentrations ranging from 0.3ug/ul to 1ug/ul in PBS) containing a vital dye (Fastgreen in PBS, 10%). 5 unidirectional squared electrical pulses (30V for *in utero*, 42V for *ex utero*, 50 ms each at 1-s intervals), were delivered through platinum electrodes (2 mm diameter, 1 mm space between the electrodes), using a BTX®-ECM®830 electroporator. The orientation of the electric field was used to direct the uptake of the plasmid to cortical cells with an apical contact. The embryos were allowed to develop 24h to 1 day, then collected and checked for fluorescence prior to fixation.

IV - 2.4.1. *In* utero electroporation

In utero electroporation of mouse embryos was performed as described in (Takahashi 2002) except that the topology of the embryos was determined using illumination and a dissecting microscope rather than ultrasound microscopy. Pregnant mice 12 days post coitum were anesthetized with isofluorane vapor and their uteri exposed. 1-2 µl of the DNA solution described above were injected through the uterine wall into the lumen of the telencephalic vesicles. Immediately after injection, electrical pulses were delivered as described above. After electroporation, the uterus was relocated into the peritoneal cavity and the abdomen sutured. The mice were sacrificed either 24h or 48h after this procedure and embryos collected for further analysis.

IV - 2.4.2. *Ex utero* electroporation and whole embryo culture

Ex utero electroporation and whole embryo culture were performed as previously described (Eto, 1995; Calegari et al. 2004). The uteri were collected from time-mated females killed by cervical dislocation, and dissected in Tyrod solution. E10.5 embryos were freed from uterine walls, decidua capsularis and Reichert's membrane. They were then cultured with their open amnion, yolk sac and ectoplacental cone for approximately one hour to allow equilibration with the culture conditions. The culture was carried out in glass bottles (one embryo per bottle) containing 1.5 ml of whole embryo culture medium. To ensure proper oxygenation, the bottles were kept in continuous rotation (25 rpm) with a continuous oxygen flow (from 60% to 95% O_2, 5% CO_2 in N_2) going from 50cm^3/min (60% O_2) to 50 cm^3/min (95% O_2) according to the developmental stage. After equilibration, the embryos were transferred to the electroporation station and immobilized . 1-2 µl of the DNA solution described above were injected into the lumen of the telencephalic vesicles. Immediately after injection, electrical pulses were delivered as described above. The embryos were transferred back to the culture bottle and analyzed 24 hrs later.

IV - 2.4.3. *Aspm* knock-down

Following previously established methods (Yang et al. 2002; Calegari et al. 2004), Aspm esiRNAs (0.6 µg/µl) generated from double-stranded RNA complementary to nucleotides 585-1932 of exon 3 of mouse *Aspm*, together with an mRFP plasmid (0.75 µg/µl), were injected and directionally electroporated into one half of the dorsal telencephalon of E10.5 embryos *ex utero* or E12.5 embryos *in utero*, which were then allowed to develop in whole-embryo culture for 24 h or *in utero* for 24-48 h, respectively. The contralateral side of the dorsal telencephalon and/or dorsal telencephalon electroporated with mRFP plasmid only were used as controls. The mRFP plasmid was a pCAGGS vector expressing mRFP (kind gift of Dr. Roger Tsien) under the control of the chicken β-actin promoter coupled to the CMV enhancer.

IV - 2.5. Immunofluorescence

Cryosections were surrounded with a layer of hydrophobic compound (PAP-pen). Then kept in a humidified chamber and treated according to the following protocol. The

stained slides were mounted in moviol and stored in the dark at 4° C. Monkey slices (60µm) were stained while floating in a 1.5ml microfuge tube according to the following protocol and then mounted on coated glass slides (Histobond Marienfeld).

Wash	2x 5' incubation in PBS, 0.3% TritonX100
Permeabilization	30' incubation in PBS, 0.3% TritonX100
Quenching	30' incubation in PBS, 0.1M glycine
Wash	3x 10' in Tx Buffer
Primary antibody	2h at room temperature in Tx Buffer
Wash	5x 5' in Tx Buffer
Secondary antibody and Dapi	1h at room temperature in Tx Buffer
Wash	5x 5' in Tx Buffer
Wash	3x 1' in PBS
Wash	1x in ddH_2O

For BrdU immunostaining, 5 U DNAse per ml of TX buffer were added to the primary antibody incubation. GFP and mRFP were detected by their intrinsic fluorescence.

For Pax6 immunostaining, the slides are boiled in 0.1M Sodium Citrate for 10 minutes prior to the primary antibody incubation. After boiling, the slides are washed 3 times for 5 minutes in PBS and then the regular protocol can be followed.

IV - 2.6. *In situ* hybridization

Non-radioactive *in situ* hybridization using digoxigenin-labeled cRNA antisense and sense probes corresponding to nucleotides 585-1932 of exon 3 of mouse *Aspm* was carried out on 10 µm cryosections by standard methods. Slides were washed with PBS and treated 2x 10min with RIPA buffer. Postfix for 10min in 4% PFA in PBS at RT (without a washing step after RIPA treatment). Wash the slides 3x 5min with PBS. Treat 15min with triethanolamine buffer and dropwise add acetic anhydride (0.25% final concentration). Wash 3x 5min with PBS-Tween 0,1%. Prehybridise the slides 15min to *1h* at 70°C using hybridization solution.

Hybridization (hybridization buffer + 50-1000ng/ml of cold probe) could be done directly on the slides, using 250-300µl/slide or in a bath, using a 5 slides container (17ml). Hybridization is done overnight in a humidified chamber (or in a bath) at 70°C. If needed, stringency of the hybridization can be lowered by decreasing the temperature or the percentage of formamide or by increasing the salt concentration. Heat the probe at least for 10min. Rinse quickly 1x with the pre-heated hybridisation buffer (@70°C) and then wash the slides 2x 1h at 70°C in the post-hybridization solution.

Slides are washed 2x 5min and 1x 20min at RT in buffer B1. Then block in B2 buffer (10% FCS or Goat Serum in B1) for 30min to 1h at RT directly on the slides (200µl/slide). Anti-DIG antibody diluted 1/2000 in B2 buffer is incubated overnight at 4°C (directly on the slides with 250µl/slide). Put the antibody on the slides in the 4°C. Wash the slides 2x 5min with B1 and then incubate the slides in B3 buffer for 30min.

Overlay each slide with 250-300µl of NBT-BCIP (filter the ready-to-use solution and add 0.1% of Tween-20). The colour reaction is developed in the dark for 30min to one day at RT or overnight at 4°C. When one tests a new probe, it should first be done at room temperature, and the coloring of the sample should be checked

after 1h. If everything is OK, the samples are left overnight at 4°C. The reaction is stopped with PBST (PBS + 0.1% Tween-20); wash 3-5x for 5min in PBST. If no more reaction is to be done briefly wash the slides in water and let them dry. Then mount in aqueous mounting medium.

IV - 2.6.1 Preparation of DIG labeled probe

The plasmid (20µg) is linearized via enzyme digestion on a reaction mix with a total volume of 100μl. The reaction mix included 10μl 10x buffer, 2μl of the appropriate enzyme, 20µg of plasmid DNA, and sdH_20 up to 100μl. The reaction mix is incubated at 37°C for 1 hour. The digested DNA is recovered by phenol extraction. An equal volume of phenol/chloroform is added to the reaction mix, it is vortexed for 1 minute, and then spun in a microfuge at 13,000rpm for 10 minutes. The upper phase is then transferred to a new tube. Two volumes of 100% ethanol and 0.1 volume 3M sodium acetate are added to the upper phase. The solution is briefly vortexed and the DNA is precipitated by incubation at -20°C for at least 1 hour. The DNA is collected by centrifugation at 13,000rpm for 30 minutes at 4°C. The digested DNA can now be used for DIG labeling. The reaction mix is as follows:

DNA	10µl (1µg)
10X Buffer	2µl
sdH_20	4µl
10X DIG label mix	2µl
RNA polymerase	2µl

Total volume = 20µl

This reaction is mixed and incubated at 37°C for 2 hours. The in vitro transcribed RNA is collected by precipitation with 2.5µl pre-chilled 4M LiCl and 75µl pre-chilled EtOH. The mix is precipitated at -20°C overnight. RNA is collected by centrifugation at 13,000rpm for 30 minutes at 4°C and then re-suspended in 50µl sdH_20. RNAse inhibitors should be added for long term storage. RNA concentration was quantified on an agarose gel.

IV - 2.7. Western Blot

Pour stacking gel. The volume for a minigel is ~6ml. Leave ~1cm below comb for stacking gel. Pour separation gel and gently add ~1ml isopropanol to top of gel with blue tip. Allow separation gel to polymerize. Pour isopropanol off, rinse with water 3X, then use 3M paper to get most of the water off the gel. Pour stacking gel. Allow the gel to polymerize. Prepare and load samples: Boil samples 3-5 minutes in a 95°C heating block. Spin samples down. All samples should have same amount of protein in the same loading volume. All wells must be loaded- use equal volume loading buffer. Load sample placing the pipette tip at the bottom of the well and move up. Run the gel at 15mA until dye front is at the end. Transfer the gel a PVDF nylon membrane. The membrane should be the size of the gel (8x7cm). Cut 10 pieces of 3M Whatman paper slightly larger than the membrane (8x9cm). Rehydrate the membrane in 100% EtOH for 1minute. Move membrane to buffer 2. Wash the gels in water. Remove the stacking gel from the separation gel and rinse in water again. Rinse the gel in buffer 2. Wash blotting apparatus with water and leave humid. Individually wet three 3M papers in Buffer 1 and place then on the transfer apparatus. Remove air bubbles with a pipette. Individually wet two more 3M papers in Buffer 2 and add to other

papers in a stack. Remove air bubbles with pipette. Place the membrane on top of the stacked 3M papers using forceps, and avoiding bubbles. With a pencil, label one corner of the membrane. Place the gel on top of the membrane, avoiding lots of movements. Individually wet five more 3M papers in Buffer 3. Stack these on top of the gel, membrane and other papers. Two first, remove air bubbles, then the last three. Remove air bubbles. Put on apparatus lid. Add 2 (1)-Liter bottles as weights. Run at 150mAmp for 1 hour. After the transfer, cut the corner of the gel and membrane for orientation. Put the gel into commassie buffer to confirm the transfer. Put the membrane into a container with blocking buffer (5% milk in PBS; 0.1% Tween 20) and incubate overnight at +4°C. The following day, incubate the membrane with the primary antibody diluted in blocking buffer (5% milk in PBS; 0.05% Tween 20) for 2 hours at RT. (Blocking buffer can also be diluted 1:1 in PBS/Tween (0.1%)). Wash for 1 hour at RT in PBS/Tween 20 (0.1%). Incubate with secondary antibody in blocking buffer (5% milk in PBS; 0.05% Tween 20) for 1 hour at RT. Wash for 1 hour at RT in PBS/Tween 20 (0.1%). After washing, expose the membrane. Mix the ECL compounds 1:1 (200μl: 200μl). Incubate immediately with the membrane for 5 minutes. Put the membrane between two transparent sheets. Remove air bubbles. Tape the membrane into place inside a dark cassette. Develop for 10 seconds, 30 seconds, one minute, and longer if necessary.

Proteins from over-expressing cells were separated on a 12% acrylamide gel and transferred as described above. Proteins from the embryo extract were separated on a 4% agarose gel. Since the proteins from the embryo extract are of a high molecular weight, the transfer of proteins to the membrane was done overnight (16 hours) at 4°C. The transfer buffer (high molecular weight transfer buffer) was continuously circulated overnight.

IV - 2.8. Mouse handling, embryo collection, and fixation

The mice were always handled according to German legal standards. For embryo collection, the pregnant females were killed by cervical dislocation. Embryos were removed from the mother and fixed in freshly depolymerized 4% PFA overnight, then transferred in a sucrose solution (30% in PBS) for cryopreservation. For cryosectioning, the brains were embedded in Tissue Tek (Sakura), deep frozen (on dry ice) then stored at -20^0 C until used. Cryosections (10-16µm-thick) were cut with a cryostat (Microm, HM560) and collected on coated glass slides (Histobond Marienfeld). Slides were kept at -20°C in the dark until used.

IV - 2.9. Confocal microscopy

Confocal microscopy on cryosections of paraformaldehyde-fixed E10.5-E14.5 mouse brains from wildtype or heterozygous *Tis21*-GFP knock-in mouse embryos was performed according to standard procedures. Two different confocal microscopes were used for imaging. The different fluorophores in the 16µm-thick sections were excited with the following laser lines. Pinhole size was 1 airy unit, except for detection of the cadherin hole, where a pinhole of 0.75 airy unit was used.

Dapi	405 or 364
GFP	488
A532	532
mRFP	594
Cherry	594

Cy3	633
Cy5	688

IV - 2.10. Quantitative data analysis

IV - 2.10.1 Assessment of Aspm immunofluorescence intensity in *Tis21*-GFP–negative *versus Tis21*-GFP–positive NE cells

Neighboring NE cells in the same mitotic phase (prophase or metaphase as revealed by DAPI staining) in E14.5 *Tis21*-GFP knock-in mice, of which at least one cell was *Tis21*-GFP–negative and one was *Tis21*-GFP–positive, were analyzed. The cells were scored in print-outs of the confocal scans showing either Aspm immunostaining or GFP fluorescence. For each mitotic cell, the centrosome-specific Aspm immunostaining was evaluated relative to the non-specific background staining and then given an intensity assessment (strong, medium, or weak) by an investigator who was unaware of the absence or presence of *Tis21*-GFP expression in the respective neuroepithelial cell. Each mitotic cell was then scored separately for *Tis21*-GFP expression as positive or negative. Scoring for Aspm and GFP intensity was performed by two independent investigators, with essentially identical results.

IV - 2.10.2 Analysis of cleavage plane orientation and apical membrane distribution

Cleavage plane orientation and apical plasma membrane distribution were determined in optical sections of mitotic NE cells stained for DNA and cadherin as previously described (Kosodo et al. 2004). Briefly, cryosections labeled for DNA and cadherin from electroporated *Tis21*–GFP knock-in mouse embryos were first examined for the pattern of DNA to identify mitotic NE cells in anaphase / early telophase. Only mitotic cells that were both *Tis21*-GFP–negative and mRFP–positive were considered for this analysis. The cleavage plane was deduced from the orientation of the sister chromatids. Cleavage planes were classified into groups +/-5°. Following the determination of the position of the cadherin hole relative to the predicted cleavage plane, divisions with cleavage planes passing through the cadherin hole were defined as symmetric in terms of distribution of apical membrane, and those with cleavage planes bypassing the cadherin hole as asymmetric, irrespective of whether the cleavage plane was vertical or oblique to the ventricular surface.

IV - 2.10.3 Quantification of abventricular centrosomes

After identification of the electroporated region via RFP fluorescence, at least eight consecutive optical sections (1 μm) were obtained from γ-tubulin– and βIII-tubulin–immunostained 16 μm-thick cryosections. For each cryosection, abventricular γ-tubulin–immunostained centrosomes in the VZ of the targeted and non-targeted side were counted in three separate optical sections (with one non-counted optical section in between) within a 200x50 μm field which excluded the strip containing the apical mitotic cells and the βIII-tubulin–immunostained neuronal layers. The number of centrosomes was summed for the 3 optical sections within each cryosection, and the ratio of targeted over non-targeted side was calculated. In the case of BrdU-labeled samples, centrosomes revealed by γ-tubulin–immunostaining were assigned to DAPI-

stained nuclei by an investigator who was unaware of the BrdU immunostaining.

IV - 2.10.4 Quantification of *Tis21*-GFP–negative *versus Tis21*-GFP–positive NE cell progeny

Cryosections from E10.5 *Tis21*-GFP knock-in mice electroporated with either Aspm esiRNAs plus mRFP plasmid or mRFP plasmid only and developed for further 24 h in whole-embryo culture were analyzed. Cells in the neuronal layer adjacent to the VZ were scored as follows. Cells derived from electroporated NE cells were first identified by their RFP fluorescence in the cell body. RFP-positive cell bodies were then scored for the absence or presence of *Tis21*-GFP fluorescence. Scoring of cells was performed by an investigator who was unaware of whether the various cryosections derived from the control or Aspm knock-down condition. *Tis21*-GFP–negative and *Tis21*-GFP–positive, RFP-positive cell bodies were finally analyzed for βIII-tubulin immunofluorescence.

V References

Aaku-Saraste, E., Hellwig, A. and Huttner, W.B. (1996) Loss of occludin and functional tight junctions, but not ZO-1, during neural tube closure - remodeling of the neuroepithelium prior to neurogenesis. Dev. Biol., 180, 664-679.

Aaku-Saraste, E., Oback, B., Hellwig, A. and Huttner, W.B. (1997) Neuroepithelial cells downregulate their plasma membrane polarity prior to neural tube closure and neurogenesis. Mech. Dev., 69, 71-81.

Aboitiz, F. (1999) Evolution of isocortical organization. A tentative scenario including roles of reelin, p35/cdk5 and the subplate zone. Cereb Cortex, 9, 655-661.

Aboitiz, F. (2001) The origin of isocortical development. Trends Neurosci, 24, 202-203.

Aboitiz, F., Montiel, J. and López, J. (2002) Critical steps in the early evolution of the isocortex: insights from developmental biology. Braz J Med Biol Res, 35, 1455-1472.

Anderson, S., Mione, M., Yun, K. and Rubenstein, J.L. (1999) Differential origins of neocortical projection and local circuit neurons: role of Dlx genes in neocortical interneuronogenesis. Cereb Cortex, 9, 646-654.

Anderson, S.A., Eisenstat, D.D., Shi, L. and Rubenstein, J.L. (1997) Interneuron migration from basal forebrain to neocortex: dependence on Dlx genes. Science, 278, 474-476.

Attardo, A., Calegari, F., Haubensak, W., Naumann, R. and Huttner, W.B. Groundbreaking imaging of neuron generation in the mouse telencephalon. In prep.

Baala, L., Briault, S., Etchevers, H.C., Laumonnier, F., Natiq, A., Amiel, J., Boddaert, N., Picard, C., Sbiti, A., Asermouh, A., Attié-Bitach, T., Encha-Razavi, F., Munnich, A., Sefiani, A. and Lyonnet, S. (2007) Homozygous silencing of T-box transcription factor EOMES leads to microcephaly with polymicrogyria and corpus callosum agenesis. Nat Genet, 39, 454-456.

Bachmann, A., Schneider, M., Theilenberg, E., Grawe, F. and Knust, E. (2001) Drosophila Stardust is a partner of Crumbs in the control of epithelial cell polarity. Nature, 414, 638-643.

Bar, I., Lambert de Rouvroit, C. and Goffinet, A.M. (2000) The evolution of cortical development. An hypothesis based on the role of the Reelin signaling pathway. Trends Neurosci, 23, 633-638.

Barth, A.I., Nüthke, I.S. and Nelson, W.J. (1997) Cadherins, catenins and APC protein: interplay between cytoskeletal complexes and signaling pathways. Curr Opin Cell Biol, 9, 683-690.

Basto, R., Lau, J., Vinogradova, T., Gardiol, A., Woods, C.G., Khodjakov, A. and Raff, J.W. (2006) Flies without centrioles. Cell, 125, 1375-1386.

Bellaiche, Y. and Gotta, M. (2005) Heterotrimeric G proteins and regulation of size asymmetry during cell division. Curr Opin Cell Biol, 17, 658-663.

Betschinger, J., Mechtler, K. and Knoblich, J.A. (2003) The Par complex directs asymmetric cell division by phosphorylating the cytoskeletal protein Lgl. Nature, 422, 326-330.

Bond, J., Roberts, E., Mochida, G.H., Hampshire, D.J., Scott, S., Askham, J.M., Springell, K., Mahadevan, M., Crow, Y.J., Markham, A.F., Walsh, C.A. and Woods, C.G. (2002) ASPM is a major determinant of cerebral cortical size. Nat Genet, 32, 316-320.

Bond, J., Roberts, E., Springell, K., Lizarraga, S.B., Lizarraga, S., Scott, S., Higgins, J., Hampshire, D.J., Morrison, E.E., Leal, G.F., Silva, E.O., Costa, S.M., Baralle, D., Raponi, M., Karbani, G., Rashid, Y., Jafri, H., Bennett, C., Corry, P., Walsh, C.A. and Woods, C.G. (2005) A centrosomal mechanism involving CDK5RAP2 and CENPJ controls brain size. Nat Genet, 37, 353-355.

Bond, J., Scott, S., Hampshire, D.J., Springell, K., Corry, P., Abramowicz, M.J., Mochida, G.H., Hennekam, R.C., Maher, E.R., Fryns, J.P., Alswaid, A., Jafri, H., Rashid, Y., Mubaidin, A., Walsh, C.A., Roberts, E. and Woods, C.G. (2003) Protein-truncating mutations in ASPM cause variable reduction in brain size. Am J Hum Genet, 73, 1170-1177.

Bond, J. and Woods, C.G. (2006) Cytoskeletal genes regulating brain size. Curr Opin Cell Biol, 18, 95-101.

Bowman, S.K., Neumüller, R.A., Novatchkova, M., Du, Q. and Knoblich, J.A. (2006) The Drosophila NuMA Homolog Mud regulates spindle orientation in asymmetric cell division. Dev Cell, 10, 731-742.

Buchman, J.J. and Tsai, L.H. (2007) Spindle regulation in neural precursors of flies and mammals. Nat Rev Neurosci, 8, 89-100.

Bystron, I., Rakic, P., Molnár, Z. and Blakemore, C. (2006) The first neurons of the human cerebral cortex. Nat Neurosci, 9, 880-886.

Cai, Y., Yu, F., Lin, S., Chia, W. and Yang, X. (2003) Apical complex genes control mitotic spindle geometry and relative size of daughter cells in Drosophila neuroblast and pI asymmetric divisions. Cell, 112, 51-62.

Calegari, F., Haubensak, W., Haffner, C. and Huttner, W.B. (2005) Selective lengthening of the cell cycle in the neurogenic subpopulation of neural progenitor cells during mouse brain development. J Neurosci, 25, 6533-6538.

Calegari, F., Haubensak, W., Yang, D., Huttner, W.B. and Buchholz, F. (2002) Tissue-specific RNA interference in postimplantation mouse embryos with endoribonuclease-prepared short interfering RNA. Proc Natl Acad Sci U S A, 99, 14236-14240.

Calegari, F. and Huttner, W.B. (2003) An inhibition of cyclin-dependent kinases that lengthens, but does not arrest, neuroepithelial cell cycle induces premature neurogenesis. J Cell Sci, 116, 4947-4955.

Cappello, S., Attardo, A., Wu, X., Iwasato, T., Itohara, S., Wilsch-Bräuninger, M., Eilken, H.M., Rieger, M.A., Schroeder, T.T., Huttner, W.B., Brakebusch, C. and Götz, M. (2006) The Rho-GTPase cdc42 regulates neural progenitor fate at the apical surface. Nat Neurosci, 9, 1099-1107.

Casal, J., Gonzalez, C., Wandosell, F., Avila, J. and Ripoll, P. (1990) Abnormal meiotic spindles cause a cascade of defects during spermatogenesis in asp males of Drosophila. Development, 108, 251-260.

Caviness. (1973) Time of neuron origin in the hippocampus and dentate gyrus of normal and reeler mutant mice: an autoradiographic analysis. J Comp Neurol, 151, 113-120.

Chang, C.J., Goulding, S., Adams, R.R., Earnshaw, W.C. and Carmena, M. (2006) Drosophila Incenp is required for cytokinesis and asymmetric cell division during development of the nervous system. J Cell Sci, 119, 1144-1153.

Chenn, A. and McConnell, S.K. (1995) Cleavage orientation and the asymmetric inheritance of Notch1 immunoreactivity in mammalian neurogenesis. Cell, 82, 631-641.

Chenn, A. and Walsh, C.A. (2002) Regulation of cerebral cortical size by control of cell cycle exit in neural precursors. Science, 297, 365-369.

Chenn, A. and Walsh, C.A. (2003) Increased neuronal production, enlarged forebrains and cytoarchitectural distortions in beta-catenin overexpressing transgenic mice. Cereb Cortex, 13, 599-606.

Chenn, A., Zhang, Y.A., Chang, B.T. and McConnell, S.K. (1998) Intrinsic polarity of mammalian neuroepithelial cells. Mol Cell Neurosci, 11, 183-193.

Compton, D.A. (1998) Focusing on spindle poles. J Cell Sci, 111 (Pt 11), 1477-1481.

Copp, A.J., Greene, N.D. and Murdoch, J.N. (2003) The genetic basis of mammalian neurulation. Nat Rev Genet, 4, 784-793.

Cox, J., Jackson, A.P., Bond, J. and Woods, C.G. (2006) What primary microcephaly can tell us about brain growth. Trends Mol Med, 12, 358-366.

Craig, R. and Norbury, C. (1998) The novel murine calmodulin-binding protein Sha1 disrupts mitotic spindle and replication checkpoint functions in fission yeast. J Cell Sci, 111 (Pt 24), 3609-3619.

D'Arcangelo, G., Miao, G.G., Chen, S.C., Soares, H.D., Morgan, J.I. and Curran, T. (1995) A protein related to extracellular matrix proteins deleted in the mouse mutant reeler. Nature, 374, 719-723.

David, N.B., Martin, C.A., Segalen, M., Rosenfeld, F., Schweisguth, F. and Bellaïche, Y. (2005) Drosophila Ric-8 regulates Galphai cortical localization to promote Galphai-dependent planar orientation of the mitotic spindle during asymmetric cell division. Nat Cell Biol, 7, 1083-1090.

Dehay, C., Giroud, P., Berland, M., Smart, I. and Kennedy, H. (1993) Modulation of the cell cycle contributes to the parcellation of the primate visual cortex. Nature, 366, 464-466.

Dehay, C., Savatier, P., Cortay, V. and Kennedy, H. (2001) Cell-cycle kinetics of neocortical precursors are influenced by embryonic thalamic axons. J Neurosci, 21, 201-214.

do Carmo Avides, M. and Glover, D.M. (1999) Abnormal spindle protein, Asp, and the integrity of mitotic centrosomal microtubule organizing centers. Science, 283, 1733-1735.

do Carmo Avides, M., Tavares, A. and Glover, D.M. (2001) Polo kinase and Asp are needed to promote the mitotic organizing activity of centrosomes. Nat Cell Biol, 3, 421-424.

Doe, C.Q., Chu-LaGraff, Q., Wright, D.M. and Scott, M.P. (1991) The prospero gene specifies cell fates in the Drosophila central nervous system. Cell, 65, 451-464.

Dorus, S., Vallender, E.J., Evans, P.D., Anderson, J.R., Gilbert, S.L., Mahowald, M., Wyckoff, G.J., Malcom, C.M. and Lahn, B.T. (2004) Accelerated evolution of nervous system genes in the origin of Homo sapiens. Cell, 119, 1027-1040.

Doudney, K. and Stanier, P. (2005) Epithelial cell polarity genes are required for neural tube closure. Am J Med Genet C Semin Med Genet, 135, 42-47.

Du, Q. and Macara, I.G. (2004) Mammalian Pins is a conformational switch that links NuMA to heterotrimeric G proteins. Cell, 119, 503-516.

Enard, W., Khaitovich, P., Klose, J., Zöllner, S., Heissig, F., Giavalisco, P., Nieselt-Struwe, K., Muchmore, E., Varki, A., Ravid, R., Doxiadis, G.M., Bontrop, R.E. and Pääbo, S. (2002) Intra- and interspecific variation in primate gene expression patterns. Science, 296, 340-343.

Englund, C., Fink, A., Lau, C., Pham, D., Daza, R.A., Bulfone, A., Kowalczyk, T. and Hevner, R.F. (2005) Pax6, Tbr2, and Tbr1 are expressed sequentially by radial glia, intermediate progenitor cells, and postmitotic neurons in developing neocortex. J Neurosci, 25, 247-251.

Eto, K. and Osumi-Yamashita, N. (1995) Whole embryo culture and the study of postimplantation mammalian development. Develop. Growth Differ., 37, 123-132.

Evans, P.D., Anderson, J.R., Vallender, E.J., Choi, S.S. and Lahn, B.T. (2004a) Reconstructing the evolutionary history of microcephalin, a gene controlling human brain size. Hum Mol Genet, 13, 1139-1145.

Evans, P.D., Anderson, J.R., Vallender, E.J., Gilbert, S.L., Malcom, C.M., Dorus, S. and Lahn, B.T. (2004b) Adaptive evolution of ASPM, a major determinant of cerebral cortical size in humans. Hum Mol Genet, 13, 489-494.

Evans, P.D., Gilbert, S.L., Mekel-Bobrov, N., Vallender, E.J., Anderson, J.R., Vaez-Azizi, L.M., Tishkoff, S.A., Hudson, R.R. and Lahn, B.T. (2005) Microcephalin, a gene regulating brain size, continues to evolve adaptively in humans. Science, 309, 1717-1720.

Evans, P.D., Vallender, E.J. and Lahn, B.T. (2006) Molecular evolution of the brain size regulator genes CDK5RAP2 and CENPJ. Gene, 375, 75-79.

Fant, X., Merdes, A. and Haren, L. (2004) Cell and molecular biology of spindle poles and NuMA. Int Rev Cytol, 238, 1-57.

Feng, Y. and Walsh, C.A. (2004) Mitotic spindle regulation by Nde1 controls cerebral cortical size. Neuron, 44, 279-293.

Fish, J.L., Kosodo, Y., Enard, W., Pääbo, S. and Huttner, W.B. (2006) Aspm specifically maintains symmetric proliferative divisions of neuroepithelial cells. Proc Natl Acad Sci U S A, 103, 10438-10443.

Fluckiger, A.C., Marcy, G., Marchand, M., N√©gre, D., Cosset, F.L., Mitalipov, S., Wolf, D., Savatier, P. and Dehay, C. (2006) Cell cycle features of primate embryonic stem cells. Stem Cells, 24, 547-556.

Gilbert, S.L., Dobyns, W.B. and Lahn, B.T. (2005) Genetic links between brain development and brain evolution. Nat Rev Genet, 6, 581-590.

Goffinet, A.M. (1983) The embryonic development of the cortical plate in reptiles: a comparative study in Emys orbicularis and Lacerta agilis. J Comp Neurol, 215, 437-452.

Gonzalez, C., Saunders, R.D., Casal, J., Molina, I., Carmena, M., Ripoll, P. and Glover, D.M. (1990) Mutations at the asp locus of Drosophila lead to multiple free centrosomes in syncytial embryos, but restrict centrosome duplication in larval neuroblasts. J Cell Sci, 96 (Pt 4), 605-616.

Gotta, M., Dong, Y., Peterson, Y.K., Lanier, S.M. and Ahringer, J. (2003) Asymmetrically distributed C. elegans homologs of AGS3/PINS control spindle position in the early embryo. Curr Biol, 13, 1029-1037.

Gul, A., Hassan, M., S, C., W, R., S, N., Dellefave, L., Muhammad, N., Rafiq, A., M, C., Ali, G., Siddique, T. and Ahmad, W. (2006) Genetic studies of autosomal

recessive primary microcephaly in 33 Pakistani families: novel sequence variants in ASPM gene. Neurogenetics, (null), (null).

Gupta, A., Wang, Y. and Markram, H. (2000) Organizing principles for a diversity of GABAergic interneurons and synapses in the neocortex. Science, 287, 273-278.

Götz, M. and Huttner, W.B. (2005) The cell biology of neurogenesis. Nat Rev Mol Cell Biol, 6, 777-788.

Hampoelz, B., Hoeller, O., Bowman, S.K., Dunican, D. and Knoblich, J.A. (2005) Drosophila Ric-8 is essential for plasma-membrane localization of heterotrimeric G proteins. Nat Cell Biol, 7, 1099-1105.

Haubensak, W., Attardo, A., Denk, W. and Huttner, W.B. (2004) Neurons arise in the basal neuroepithelium of the early mammalian telencephalon: a major site of neurogenesis. Proc Natl Acad Sci U S A, 101, 3196-3201.

Haydar, T.F. and Ang, R. (2003) Mitotic spindle rotation and mode of cell division in the developing telencephalon. Proc Natl Acad Sci U S A, 100, 2890-2895.

Hendry, S.H., Huntsman, M.M., Viñuela, A., Möhler, H., de Blas, A.L. and Jones, E.G. (1994) GABAA receptor subunit immunoreactivity in primate visual cortex: distribution in macaques and humans and regulation by visual input in adulthood. J Neurosci, 14, 2383-2401.

Hill, R.S. and Walsh, C.A. (2005) Molecular insights into human brain evolution. Nature, 437, 64-67.

Hirata, J., Nakagoshi, H., Nabeshima, Y. and Matsuzaki, F. (1995) Asymmetric segregation of the homeodomain protein Prospero during Drosophila development. Nature, 377, 627-630.

Hong, Y., Stronach, B., Perrimon, N., Jan, L.Y. and Jan, Y.N. (2001) Drosophila Stardust interacts with Crumbs to control polarity of epithelia but not neuroblasts. Nature, 414, 634-638.

Horvath, S., Zhang, B., Carlson, M., Lu, K.V., Zhu, S., Felciano, R.M., Laurance, M.F., Zhao, W., Qi, S., Chen, Z., Lee, Y., Scheck, A.C., Liau, L.M., Wu, H., Geschwind, D.H., Febbo, P.G., Kornblum, H.I., Cloughesy, T.F., Nelson, S.F. and Mischel, P.S. (2006) Analysis of oncogenic signaling networks in glioblastoma identifies ASPM as a molecular target. Proc Natl Acad Sci U S A, 103, 17402-17407.

Howell, B.W., Gertler, F.B. and Cooper, J.A. (1997) Mouse disabled (mDab1): a Src binding protein implicated in neuronal development. EMBO J, 16, 121-132.

Huttner, W.B. and Kosodo, Y. (2005) Symmetric versus asymmetric cell division during neurogenesis in the developing vertebrate central nervous system. Curr Opin Cell Biol, 17, 648-657.

Iacopetti, P., Michelini, M., Stuckmann, I., Oback, B., Aaku-Saraste, E. and Huttner, W.B. (1999) Expression of the antiproliferative gene TIS21 at the onset of neurogenesis identifies single neuroepithelial cells that switch from proliferative to neuron-generating division. Proc Natl Acad Sci U S A, 96, 4639-4644.

Ikeshima-Kataoka, H., Skeath, J.B., Nabeshima, Y., Doe, C.Q. and Matsuzaki, F. (1997) Miranda directs Prospero to a daughter cell during Drosophila asymmetric divisions. Nature, 390, 625-629.

Imai, F., Hirai, S., Akimoto, K., Koyama, H., Miyata, T., Ogawa, M., Noguchi, S., Sasaoka, T., Noda, T. and Ohno, S. (2006) Inactivation of aPKClambda results in the loss of adherens junctions in neuroepithelial cells without affecting neurogenesis in mouse neocortex. Development, 133, 1735-1744.

Izumi, Y., Ohta, N., Hisata, K., Raabe, T. and Matsuzaki, F. (2006) Drosophila Pins-binding protein Mud regulates spindle-polarity coupling and centrosome organization. Nat Cell Biol, 8, 586-593.

Jackson, A.P., Eastwood, H., Bell, S.M., Adu, J., Toomes, C., Carr, I.M., Roberts, E., Hampshire, D.J., Crow, Y.J., Mighell, A.J., Karbani, G., Jafri, H., Rashid, Y., Mueller, R.F., Markham, A.F. and Woods, C.G. (2002) Identification of microcephalin, a protein implicated in determining the size of the human brain. Am J Hum Genet, 71, 136-142.

Jones, B.E. (1993) The organization of central cholinergic systems and their functional importance in sleep-waking states. Prog Brain Res, 98, 61-71.

Kaltschmidt, J.A., Davidson, C.M., Brown, N.H. and Brand, A.H. (2000) Rotation and asymmetry of the mitotic spindle direct asymmetric cell division in the developing central nervous system. Nat Cell Biol, 2, 7-12.

Kaushik, R., Yu, F., Chia, W., Yang, X. and Bahri, S. (2003) Subcellular localization of LGN during mitosis: evidence for its cortical localization in mitotic cell culture systems and its requirement for normal cell cycle progression. Mol Biol Cell, 14, 3144-3155.

Kittler, R., Surendranath, V., Heninger, A.K., Slabicki, M., Theis, M., Putz, G., Franke, K., Caldarelli, A., Grabner, H., Kozak, K., Wagner, J., Rees, E., Korn, B., Frenzel, C., Sachse, C., Sönnichsen, B., Guo, J., Schelter, J., Burchard, J., Linsley, P.S., Jackson, A.L., Habermann, B. and Buchholz, F. (2007) Genome-wide resources of endoribonuclease-prepared short interfering RNAs for specific loss-of-function studies. Nat Methods, 4, 337-344.

Knoblich, J.A., Jan, L.Y. and Jan, Y.N. (1995) Asymmetric segregation of Numb and Prospero during cell division. Nature, 377, 624-627.

Kornack, D.R. and Rakic, P. (1995) Radial and horizontal deployment of clonally related cells in the primate neocortex: relationship to distinct mitotic lineages. Neuron, 15, 311-321.

Kornack, D.R. and Rakic, P. (1998) Changes in cell-cycle kinetics during the development and evolution of primate neocortex. Proc Natl Acad Sci U S A, 95, 1242-1246.

Kosodo, Y., Röper, K., Haubensak, W., Marzesco, A.M., Corbeil, D. and Huttner, W.B. (2004) Asymmetric distribution of the apical plasma membrane during neurogenic divisions of mammalian neuroepithelial cells. EMBO J, 23, 2314-2324.

Kouprina, N., Pavlicek, A., Collins, N.K., Nakano, M., Noskov, V.N., Ohzeki, J., Mochida, G.H., Risinger, J.I., Goldsmith, P., Gunsior, M., Solomon, G., Gersch, W., Kim, J.H., Barrett, J.C., Walsh, C.A., Jurka, J., Masumoto, H. and Larionov, V. (2005) The microcephaly ASPM gene is expressed in proliferating tissues and encodes for a mitotic spindle protein. Hum Mol Genet, 14, 2155-2165.

Kouprina, N., Pavlicek, A., Mochida, G.H., Solomon, G., Gersch, W., Yoon, Y.H., Collura, R., Ruvolo, M., Barrett, J.C., Woods, C.G., Walsh, C.A., Jurka, J. and Larionov, V. (2004) Accelerated evolution of the ASPM gene controlling brain size begins prior to human brain expansion. PLoS Biol, 2, E126.

Kraut, R., Chia, W., Jan, L.Y., Jan, Y.N. and Knoblich, J.A. (1996) Role of inscuteable in orienting asymmetric cell divisions in Drosophila. Nature, 383, 50-55.

Kreitman, M. (2000) Methods to detect selection in populations with applications to the human. Annu Rev Genomics Hum Genet, 1, 539-559.

Kriegstein, A., Noctor, S. and Martínez-Cerdeño, V. (2006) Patterns of neural stem and progenitor cell division may underlie evolutionary cortical expansion. Nat Rev Neurosci, 7, 883-890.

Kumar, A., Blanton, S.H., Babu, M., Markandaya, M. and Girimaji, S.C. (2004) Genetic analysis of primary microcephaly in Indian families: novel ASPM mutations. Clin Genet, 66, 341-348.

Kumar, A., Markandaya, M. and Girimaji, S.C. (2002) Primary microcephaly: microcephalin and ASPM determine the size of the human brain. J Biosci, 27, 629-632.

Lambert de Rouvroit, C., de Bergeyck, V., Cortvrindt, C., Bar, I., Eeckhout, Y. and Goffinet, A.M. (1999) Reelin, the extracellular matrix protein deficient in reeler mutant mice, is processed by a metalloproteinase. Exp Neurol, 156, 214-217.

Lambert de Rouvroit, C. and Goffinet, A.M. (1998) The reeler mouse as a model of brain development. Adv Anat Embryol Cell Biol, 150, 1-106.

Lechler, T. and Fuchs, E. (2005) Asymmetric cell divisions promote stratification and differentiation of mammalian skin. Nature, 437, 275-280.

Lee, C.Y., Wilkinson, B.D., Siegrist, S.E., Wharton, R.P. and Doe, C.Q. (2006) Brat is a Miranda cargo protein that promotes neuronal differentiation and inhibits neuroblast self-renewal. Dev Cell, 10, 441-449.

Letinic, K. and Rakic, P. (2001) Telencephalic origin of human thalamic GABAergic neurons. Nat Neurosci, 4, 931-936.

Letinic, K., Zoncu, R. and Rakic, P. (2002) Origin of GABAergic neurons in the human neocortex. Nature, 417, 645-649.

Lin, D., Edwards, A.S., Fawcett, J.P., Mbamalu, G., Scott, J.D. and Pawson, T. (2000) A mammalian PAR-3-PAR-6 complex implicated in Cdc42/Rac1 and aPKC signalling and cell polarity. Nat Cell Biol, 2, 540-547.

Lu, B., Roegiers, F., Jan, L.Y. and Jan, Y.N. (2001) Adherens junctions inhibit asymmetric division in the Drosophila epithelium. Nature, 409, 522-525.

Lu, B., Rothenberg, M., Jan, L.Y. and Jan, Y.N. (1998) Partner of Numb colocalizes with Numb during mitosis and directs Numb asymmetric localization in Drosophila neural and muscle progenitors. Cell, 95, 225-235.

Lukaszewicz, A., Cortay, V., Giroud, P., Berland, M., Smart, I., Kennedy, H. and Dehay, C. (2006) The concerted modulation of proliferation and migration contributes to the specification of the cytoarchitecture and dimensions of cortical areas. Cereb Cortex, 16 Suppl 1, i26-34.

Lukaszewicz, A., Savatier, P., Cortay, V., Giroud, P., Huissoud, C., Berland, M., Kennedy, H. and Dehay, C. (2005) G1 phase regulation, area-specific cell cycle control, and cytoarchitectonics in the primate cortex. Neuron, 47, 353-364.

Lüers, G.H., Michels, M., Schwaab, U. and Franz, T. (2002) Murine calmodulin binding protein 1 (Calmbp1): tissue-specific expression during development and in adult tissues. Mech Dev, 118, 229-232.

Macara, I.G. (2004) Parsing the polarity code. Nat Rev Mol Cell Biol, 5, 220-231.

Manabe, N., Hirai, S., Imai, F., Nakanishi, H., Takai, Y. and Ohno, S. (2002) Association of ASIP/mPAR-3 with adherens junctions of mouse neuroepithelial cells. Dev Dyn, 225, 61-69.

Martínez-Cerdeño, V., Noctor, S.C. and Kriegstein, A.R. (2006) Estradiol stimulates progenitor cell division in the ventricular and subventricular zones of the embryonic neocortex. Eur J Neurosci, 24, 3475-3488.

Marín-Padilla, M. (1998) Cajal-Retzius cells and the development of the neocortex. Trends Neurosci, 21, 64-71.

McDonald, J.H. and Kreitman, M. (1991) Adaptive protein evolution at the Adh locus in Drosophila. Nature, 351, 652-654.

Mekel-Bobrov, N., Gilbert, S.L., Evans, P.D., Vallender, E.J., Anderson, J.R., Hudson, R.R., Tishkoff, S.A. and Lahn, B.T. (2005) Ongoing adaptive evolution of ASPM, a brain size determinant in Homo sapiens. Science, 309, 1720-1722.

Mitchison, T.J. and Salmon, E.D. (2001) Mitosis: a history of division. Nat Cell Biol, 3, E17-21.

Miyata, T., Kawaguchi, A., Okano, H. and Ogawa, M. (2001) Asymmetric inheritance of radial glial fibers by cortical neurons. Neuron, 31, 727-741.

Miyata, T., Kawaguchi, A., Saito, K., Kawano, M., Muto, T. and Ogawa, M. (2004) Asymmetric production of surface-dividing and non-surface-dividing cortical progenitor cells. Development, 131, 3133-3145.

Mochida, G.H. and Walsh, C.A. (2001) Molecular genetics of human microcephaly. Curr Opin Neurol, 14, 151-156.

Molnár, Z., Métin, C., Stoykova, A., Tarabykin, V., Price, D.J., Francis, F., Meyer, G., Dehay, C. and Kennedy, H. (2006) Comparative aspects of cerebral cortical development. Eur J Neurosci, 23, 921-934.

Morales-Mulia, S. and Scholey, J.M. (2005) Spindle pole organization in Drosophila S2 cells by dynein, abnormal spindle protein (Asp), and KLP10A. Mol Biol Cell, 16, 3176-3186.

Muller, M., W.E. and Campos-Ortega, J.A. (1996) Expression domains of a zebrafish homologue of the Drosophila pair-rule gene hairy correspond to primordia of alternating somites. Development, 122, 2071-2078.

Nakai, J. and Fujita, S. (1994) Early events in the histo- and cytogenesis of the vertebrate CNS. Int J Dev Biol, 38, 175-183.

Narumiya, S., Oceguera-Yanez, F. and Yasuda, S. (2004) A new look at Rho GTPases in cell cycle: role in kinetochore-microtubule attachment. Cell Cycle, 3, 855-857.

Narumiya, S. and Yasuda, S. (2006) Rho GTPases in animal cell mitosis. Curr Opin Cell Biol, 18, 199-205.

Nelson, W.J. (2003) Adaptation of core mechanisms to generate cell polarity. Nature, 422, 766-774.

Nishihara, H., Hasegawa, M. and Okada, N. (2006) Pegasoferae, an unexpected mammalian clade revealed by tracking ancient retroposon insertions. Proc Natl Acad Sci U S A, 103, 9929-9934.

Noctor, S.C., Martínez-Cerdeño, V., Ivic, L. and Kriegstein, A.R. (2004) Cortical neurons arise in symmetric and asymmetric division zones and migrate through specific phases. Nat Neurosci, 7, 136-144.

Noonan, J.P., Coop, G., Kudaravalli, S., Smith, D., Krause, J., Alessi, J., Chen, F., Platt, D., Pääbo, S., Pritchard, J.K. and Rubin, E.M. (2006) Sequencing and analysis of Neanderthal genomic DNA. Science, 314, 1113-1118.

Palazzo, A.F., Joseph, H.L., Chen, Y.J., Dujardin, D.L., Alberts, A.S., Pfister, K.K., Vallee, R.B. and Gundersen, G.G. (2001) Cdc42, dynein, and dynactin regulate MTOC reorientation independent of Rho-regulated microtubule stabilization. Curr Biol, 11, 1536-1541.

Parnavelas, J.G., Lieberman, A.R. and Webster, K.E. (1977) Organization of neurons in the visual cortex, area 17, of the rat. J Anat, 124, 305-322.

Petronczki, M. and Knoblich, J.A. (2001) DmPAR-6 directs epithelial polarity and asymmetric cell division of neuroblasts in Drosophila. Nat Cell Biol, 3, 43-49.

Pichon, B., Vankerckhove, S., Bourrouillou, G., Duprez, L. and Abramowicz, M.J. (2004) A translocation breakpoint disrupts the ASPM gene in a patient with primary microcephaly. Eur J Hum Genet, 12, 419-421.

Ponting, C. and Jackson, A.P. (2005) Evolution of primary microcephaly genes and the enlargement of primate brains. Curr Opin Genet Dev, 15, 241-248.

Ponting, C.P. (2006) A novel domain suggests a ciliary function for ASPM, a brain size determining gene. Bioinformatics, 22, 1031-1035.

Rakic, P. (1988) Specification of cerebral cortical areas. Science, 241, 170-176.

Rakic, P. (1995) A small step for the cell, a giant leap for mankind: a hypothesis of neocortical expansion during evolution. Trends Neurosci, 18, 383-388.

Rakic, P. and Caviness. (1995) Cortical development: view from neurological mutants two decades later. Neuron, 14, 1101-1104.

Rakic, S. and Zecevic, N. (2003) Emerging complexity of layer I in human cerebral cortex. Cereb Cortex, 13, 1072-1083.

Rhyu, M.S. and Knoblich, J.A. (1995) Spindle orientation and asymmetric cell fate. Cell, 82, 523-526.

Riparbelli, M.G. and Callaini, G. (2005) The meiotic spindle of the Drosophila oocyte: the role of centrosomin and the central aster. J Cell Sci, 118, 2827-2836.

Riparbelli, M.G., Callaini, G., Glover, D.M. and Avides, M.C. (2002) A requirement for the Abnormal Spindle protein to organise microtubules of the central spindle for cytokinesis in Drosophila. J Cell Sci, 115, 913-922.

Riparbelli, M.G., Massarelli, C., Robbins, L.G. and Callaini, G. (2004) The abnormal spindle protein is required for germ cell mitosis and oocyte differentiation during Drosophila oogenesis. Exp Cell Res, 298, 96-106.

Roberts, E., Hampshire, D.J., Pattison, L., Springell, K., Jafri, H., Corry, P., Mannon, J., Rashid, Y., Crow, Y., Bond, J. and Woods, C.G. (2002) Autosomal recessive

primary microcephaly: an analysis of locus heterogeneity and phenotypic variation. J Med Genet, 39, 718-721.

Rolls, M.M., Albertson, R., Shih, H.P., Lee, C.Y. and Doe, C.Q. (2003) Drosophila aPKC regulates cell polarity and cell proliferation in neuroblasts and epithelia. J Cell Biol, 163, 1089-1098.

Rowitch, D.H. and McMahon, A.P. (1995) Pax-2 expression in the murine neural plate precedes and encompasses the expression domains of Wnt-1 and En-1. Mech Dev, 52, 3-8.

Sanada, K. and Tsai, L.H. (2005) G protein betagamma subunits and AGS3 control spindle orientation and asymmetric cell fate of cerebral cortical progenitors. Cell, 122, 119-131.

Saunders, R.D., Avides, M.C., Howard, T., Gonzalez, C. and Glover, D.M. (1997) The Drosophila gene abnormal spindle encodes a novel microtubule-associated protein that associates with the polar regions of the mitotic spindle. J Cell Biol, 137, 881-890.

Sauvageot, C.M. and Stiles, C.D. (2002) Molecular mechanisms controlling cortical gliogenesis. Curr Opin Neurobiol, 12, 244-249.

Schaefer, M., Petronczki, M., Dorner, D., Forte, M. and Knoblich, J.A. (2001) Heterotrimeric G proteins direct two modes of asymmetric cell division in the Drosophila nervous system. Cell, 107, 183-194.

Schaefer, M., Shevchenko, A., Shevchenko, A. and Knoblich, J.A. (2000) A protein complex containing Inscuteable and the Galpha-binding protein Pins orients asymmetric cell divisions in Drosophila. Curr Biol, 10, 353-362.

Schober, M., Schaefer, M. and Knoblich, J.A. (1999) Bazooka recruits Inscuteable to orient asymmetric cell divisions in Drosophila neuroblasts. Nature, 402, 548-551.

Schwarz, M., Alvarez-Bolado, G., Dressler, G., Urb√°nek, P., Busslinger, M. and Gruss, P. (1999) Pax2/5 and Pax6 subdivide the early neural tube into three domains. Mech Dev, 82, 29-39.

Sheldon, M., Rice, D.S., D'Arcangelo, G., Yoneshima, H., Nakajima, K., Mikoshiba, K., Howell, B.W., Cooper, J.A., Goldowitz, D. and Curran, T. (1997) Scrambler and yotari disrupt the disabled gene and produce a reeler-like phenotype in mice. Nature, 389, 730-733.

Shen, C.P., Jan, L.Y. and Jan, Y.N. (1997) Miranda is required for the asymmetric localization of Prospero during mitosis in Drosophila. Cell, 90, 449-458.

Shen, J., Eyaid, W., Mochida, G.H., Al-Moayyad, F., Bodell, A., Woods, C.G. and Walsh, C.A. (2005) ASPM mutations identified in patients with primary microcephaly and seizures. J Med Genet, 42, 725-729.

Shen, Q., Wang, Y., Dimos, J.T., Fasano, C.A., Phoenix, T.N., Lemischka, I.R., Ivanova, N.B., Stifani, S., Morrisey, E.E. and Temple, S. (2006) The timing of cortical neurogenesis is encoded within lineages of individual progenitor cells. Nat Neurosci, 9, 743-751.

Sidman, R.L. and Rakic, P. (1973) Neuronal migration, with special reference to developing human brain: a review. Brain Res, 62, 1-35.

Siegrist, S.E. and Doe, C.Q. (2005) Microtubule-induced Pins/Galphai cortical polarity in Drosophila neuroblasts. Cell, 123, 1323-1335.

Siller, K.H., Cabernard, C. and Doe, C.Q. (2006) The NuMA-related Mud protein binds Pins and regulates spindle orientation in Drosophila neuroblasts. Nat Cell Biol, 8, 594-600.

Silva, A.O., Ercole, C.E. and McLoon, S.C. (2002) Plane of cell cleavage and numb distribution during cell division relative to cell differentiation in the developing retina. J Neurosci, 22, 7518-7525.

Smart, I.H. (1970a) Changes in location and orientation of mitotic figures in mouse oesophageal epithelium during the development of stratification. J Anat, 106, 15-21.

Smart, I.H. (1970b) Variation in the plane of cell cleavage during the process of stratification in the mouse epidermis. Br J Dermatol, 82, 276-282.

Smart, I.H. (1971) Location and orientation of mitotic figures in the developing mouse olfactory epithelium. J Anat, 109, 243-251.

Smart, I.H. (1972a) Proliferative characteristics of the ependymal layer during the early development of the mouse diencephalon, as revealed by recording the number, location, and plane of cleavage of mitotic figures. J Anat, 113, 109-129.

Smart, I.H. (1972b) Proliferative characteristics of the ependymal layer during the early development of the spinal cord in the mouse. J Anat, 111, 365-380.

Smart, I.H. (1973) Proliferative characteristics of the ependymal layer during the early development of the mouse neocortex: a pilot study based on recording the number, location and plane of cleavage of mitotic figures. J Anat, 116, 67-91.

Smart, I.H. (1976) A pilot study of cell production by the ganglionic eminences of the developing mouse brain. J Anat, 121, 71-84.

Smart, I.H. (1982) Radial unit analysis of hippocampal histogenesis in the mouse. J Anat, 135, 763-793.

Smart, I.H. (1983) Three dimensional growth of the mouse isocortex. J Anat, 137 (Pt 4), 683-694.

Smart, I.H., Dehay, C., Giroud, P., Berland, M. and Kennedy, H. (2002) Unique morphological features of the proliferative zones and postmitotic compartments of the

neural epithelium giving rise to striate and extrastriate cortex in the monkey. Cereb Cortex, 12, 37-53.

Spana, E.P. and Doe, C.Q. (1995) The prospero transcription factor is asymmetrically localized to the cell cortex during neuroblast mitosis in Drosophila. Development, 121, 3187-3195.

Srinivasan, D.G., Fisk, R.M., Xu, H. and van den Heuvel, S. (2003) A complex of LIN-5 and GPR proteins regulates G protein signaling and spindle function in C elegans. Genes Dev, 17, 1225-1239.

Takahashi, M., Sato, K., Nomura, T. and Osumi, N. (2002) Manipulating gene expressions by electroporation in the developing brain of mammalian embryos. Differentiation, 70, 155-162.

Takahashi, T., Nowakowski, R.S. and Caviness. (1995) Early ontogeny of the secondary proliferative population of the embryonic murine cerebral wall. J Neurosci, 15, 6058-6068.

Tan, S.S., Kalloniatis, M., Sturm, K., Tam, P.P., Reese, B.E. and Faulkner-Jones, B. (1998) Separate progenitors for radial and tangential cell dispersion during development of the cerebral neocortex. Neuron, 21, 295-304.

Tanaka, T., Serneo, F.F., Higgins, C., Gambello, M.J., Wynshaw-Boris, A. and Gleeson, J.G. (2004) Lis1 and doublecortin function with dynein to mediate coupling of the nucleus to the centrosome in neuronal migration. J Cell Biol, 165, 709-721.

Tang, B.L. (2006) Molecular genetic determinants of human brain size. Biochem Biophys Res Commun, 345, 911-916.

Tang, C.J., Hu, H.M. and Tang, T.K. (2004) NuMA expression and function in mouse oocytes and early embryos. J Biomed Sci, 11, 370-376.

Tarabykin, V., Stoykova, A., Usman, N. and Gruss, P. (2001) Cortical upper layer neurons derive from the subventricular zone as indicated by Svet1 gene expression. Development, 128, 1983-1993.

Thiéry, M., Racine, V., Pépin, A., Piel, M., Chen, Y., Sibarita, J.B. and Bornens, M. (2005) The extracellular matrix guides the orientation of the cell division axis. Nat Cell Biol, 7, 947-953.

Trommsdorff, M., Borg, J.P., Margolis, B. and Herz, J. (1998) Interaction of cytosolic adaptor proteins with neuronal apolipoprotein E receptors and the amyloid precursor protein. J Biol Chem, 273, 33556-33560.

Trommsdorff, M., Gotthardt, M., Hiesberger, T., Shelton, J., Stockinger, W., Nimpf, J., Hammer, R.E., Richardson, J.A. and Herz, J. (1999) Reeler/Disabled-like disruption of neuronal migration in knockout mice lacking the VLDL receptor and ApoE receptor 2. Cell, 97, 689-701.

Urbach, R. and Technau, G.M. (2004) Neuroblast formation and patterning during early brain development in Drosophila. Bioessays, 26, 739-751.

Wakefield, J.G., Bonaccorsi, S. and Gatti, M. (2001) The drosophila protein asp is involved in microtubule organization during spindle formation and cytokinesis. J Cell Biol, 153, 637-648.

Walther, C. and Gruss, P. (1991) Pax-6, a murine paired box gene, is expressed in the developing CNS. Development, 113, 1435-1449.

Ware, M.L., Fox, J.W., González, J.L., Davis, N.M., Lambert de Rouvroit, C., Russo, C.J., Chua, G., Am, W. and Ca. (1997) Aberrant splicing of a mouse disabled homolog, mdab1, in the scrambler mouse. Neuron, 19, 239-249.

Weigmann, A., Corbeil, D., Hellwig, A. and Huttner, W.B. (1997) Prominin, a novel microvilli-specific polytopic membrane protein of the apical surface of epithelial cells, is targeted to plasmalemmal protrusions of non-epithelial cells. Proc. Natl. Acad. Sci. USA, 94, 12425-12430.

Wodarz, A. (2005) Molecular control of cell polarity and asymmetric cell division in Drosophila neuroblasts. Curr Opin Cell Biol, 17, 475-481.

Wodarz, A. and Huttner, W.B. (2003) Asymmetric cell division during neurogenesis in Drosophila and vertebrates. Mech Dev, 120, 1297-1309.

Wodarz, A., Ramrath, A., Grimm, A. and Knust, E. (2000) Drosophila atypical protein kinase C associates with Bazooka and controls polarity of epithelia and neuroblasts. J Cell Biol, 150, 1361-1374.

Wodarz, A., Ramrath, A., Kuchinke, U. and Knust, E. (1999) Bazooka provides an apical cue for Inscuteable localization in Drosophila neuroblasts. Nature, 402, 544-547.

Wood, B. and Collard, M. (1999) The human genus. Science, 284, 65-71.

Woods, C.G. (2004) Human microcephaly. Curr Opin Neurobiol, 14, 112-117.

Woods, C.G., Bond, J. and Enard, W. (2005) Autosomal recessive primary microcephaly (MCPH): a review of clinical, molecular, and evolutionary findings. Am J Hum Genet, 76, 717-728.

Woods, R.P., Freimer, N.B., De Young, J.A., Fears, S.C., Sicotte, N.L., Service, S.K., Valentino, D.J., Toga, A.W. and Mazziotta, J.C. (2006) Normal variants of Microcephalin and ASPM do not account for brain size variability. Hum Mol Genet, 15, 2025-2029.

Yang, D., Buchholz, F., Huang, Z., Goga, A., Chen, C.Y., Brodsky, F.M. and Bishop, J.M. (2002) Short RNA duplexes produced by hydrolysis with Escherichia coli RNase III mediate effective RNA interference in mammalian cells. Proc. Natl. Acad. Sci. USA, 99, 9942-9947.

Ybot-Gonzalez, P., Savery, D., Gerrelli, D., Signore, M., Mitchell, C.E., Faux, C.H., Greene, N.D. and Copp, A.J. (2007) Convergent extension, planar-cell-polarity signalling and initiation of mouse neural tube closure. Development, 134, 789-799.

Yu, F., Kuo, C.T. and Jan, Y.N. (2006) Drosophila neuroblast asymmetric cell division: recent advances and implications for stem cell biology. Neuron, 51, 13-20.

Yu, F., Morin, X., Cai, Y., Yang, X. and Chia, W. (2000) Analysis of partner of inscuteable, a novel player of Drosophila asymmetric divisions, reveals two distinct steps in inscuteable apical localization. Cell, 100, 399-409.

Yu, F., Morin, X., Kaushik, R., Bahri, S., Yang, X. and Chia, W. (2003) A mouse homologue of Drosophila pins can asymmetrically localize and substitute for pins function in Drosophila neuroblasts. J Cell Sci, 116, 887-896.

Zamenhof, S. and Marthens, E. (1976) Neonatal and adult brain parameters in mice selected for adult brain weight. Dev. Psychobiol., 9, 587-593.

Zecevic, N. and Rakic, P. (2001) Development of layer I neurons in the primate cerebral cortex. J Neurosci, 21, 5607-5619.

Zhang, J. (2003) Evolution of the human ASPM gene, a major determinant of brain size. Genetics, 165, 2063-2070.

Zhang, J., Webb, D.M. and Podlaha, O. (2002) Accelerated protein evolution and origins of human-specific features: Foxp2 as an example. Genetics, 162, 1825-1835.

Zhong, W., Feder, J.N., Jiang, M.M., Jan, L.Y. and Jan, Y.N. (1996) Asymmetric localization of a mammalian numb homolog during mouse cortical neurogenesis. Neuron, 17, 43-53.

Zhong, X., Liu, L., Zhao, A., Pfeifer, G.P. and Xu, X. (2005) The abnormal spindle-like, microcephaly-associated (ASPM) gene encodes a centrosomal protein. Cell Cycle, 4, 1227-1229.

Zigman, M., Cayouette, M., Charalambous, C., Schleiffer, A., Hoeller, O., Dunican, D., McCudden, C.R., Firnberg, N., Barres, B.A., Siderovski, D.P. and Knoblich, J.A. (2005) Mammalian inscuteable regulates spindle orientation and cell fate in the developing retina. Neuron, 48, 539-545.

Zimmer, C., Tiveron, M.C., Bodmer, R. and Cremer, H. (2004) Dynamics of Cux2 expression suggests that an early pool of SVZ precursors is fated to become upper cortical layer neurons. Cereb Cortex, 14, 1408-1420.

VI Acknowledgements

Was wir alleine nicht schaffen, schaffen wir dann zusammen. Without question, this work would not have been accomplished without the assistance and advise of many people. I am indebted to the whole Huttner lab for their intelligence, experience, and willingness to share their knowledge.

In particular, I must acknowledge my thesis supervisor Professor Wieland B. Huttner who provided me with unequaled opportunities to pursue my research interests. Additionally, Wieland's attention to detail was critical for the advancement of this work, in which he provided many critical insights. I have grown a lot as a scientist during my time in Dresden, and Wieland and his lab environment have been greatly responsible.

I am eternally grateful to "Super" Yoichi Kosodo for his guidance in the field of cell biology. He helped me transfer the techniques I learned into tools to answer cell biological questions. His patience, intelligence, and wonderful personality will always be remembered.

My intellectual guides, Véronique Dubreuil and Alessio Attardo, with whom I've shared many interesting conversations about science (and life), have been essential to the development of my thought process during the past few years. I am thankful that they always had an ear for my questions, tried to reel me in when I went too far, while encouraging me to go farther.

The inspiration for the ASPM project, as well as many other unique and interesting ideas, came from our collaborators in Leipzig, Svante Pääbo and Wolfgang Enard. Many great ideas over excellent coffee, have been harvested from our interactions with the Leipzig team. Thanks also to Jeremy Pulvers and Jarek Bryk, the other members of the evolution team.

Life in the Huttner Lab runs smoothly thanks to the diligent work of our technicians, Katja Langenfeld and Christiane Haffner. They take care of every need, problem, empty buffer bottle, and all the details that we tend to forget.

Advice and feedback on this project was provided by my TAC members Francis Stewart and Andy Oates, as well as by Elly Tanaka and her group during our joint group meetings.

Essential tissue was provided by our collaborators, Collete Dehay in Lyon, France and Drs. Distler and Riehn at the Frauenklinik in Dresden, Germany.

Thanks to those who contributed to the preparation of this work with advice, comments, or encouragement. Specifically, I would like to thank the "eldor" students, Alessio and Anna, and helpful post-docs Zoltan, Véronique, and Michaela W-B for their time.

Last, but not least, many thanks go to the multiple in house facilities that have made work in the MPI-CBG a luxury. Especially Jussi, Anke, and the animal house staff

who take care of our mice. Jan and the LMF team that keep the microscopes running, and the protein and antibody facilities.

VII List of Abbreviations

aPKC	atypical protein kinase C
ApoER2	Apolipoprotein E receptor type-2
Asp	abnormal spindle protein
Aspm	abnormal spindle-like microcephaly associated
BAC	Bacterial artificial chromosome
BrdU	Bromo-deoxy-Uridine
CAM	Cell adhesion molecule
CNS	Central nervous system
C-R	Cajal-Retzius
GABA	Gamma Amino Butirric Acid
Dab1	Disabled 1
DNA	Deoxyribonucleic acid
E	Embryonic day
esiRNAs	endoribonuclease-prepared short interfering RNAs
GFP	Green fluorescent protein
HB	Hindbrain
IFL	Inner fiber layer
INM	Interkinetic nuclear migration
Insc	Inscuteable
IPC	Intermediate progenitor cell
ISVZ	Inner subventricular zone
IUP	*In utero* electroporation
IZ	Intermediate zone
kDa	KiloDalton
MAP	Microtubule-associated protein
MCPH	Microcephaly
mRFP	Monomeric red fluorescent protein
Mud	Mushroom body defect
MZ	Marginal zone
NE	Intraepithelial
NB	Neuroblast
NL	Neuronal layer
NuMA	Nuclear mitotic apparatus protein
OSVZ	Outer subventricular zone
PBS	Phosphate Buffered Saline
PCR	Polymerase chain reaction
PH3	Phospho-Histone H3
Pins	Partner of Inscuteable
RG	Radial glia
RNAi	Ribonuclei Acid interference
SC	Spinal cord
SP	Subplate
SVZ	Subventricular zone
VLDLR	Very low density lipoprotein receptor
VZ	Ventricular zone
WEC	Whole embryo culture

VIII List of Publications

Fish, JL, Kosodo, K, Enard, W, Pääbo, S, and Huttner WB. Aspm specifically maintains symmetric proliferative divisions of neuroepithelial cells. *Proceedings of the National Academy of Sceinces USA*, (2006), **103**(27):10438-43.

Communications to scientific conferences:

American Assoication of Physical Anthropologists, 2005.
Evolution of primate brains: A cell biological perspective. **J.L. Fish**, Y. Kosodo, W. Enard, S. Pääbo, W.B. Huttner.

European Society for Evolutionary Developmental Biology, 2006.
Cell Biological Evolution of Neurogenesis in Mammalian Brains. **J.L. Fish**, J.N. Pulvers, Y. Kosodo, W. Enard, S. Pääbo, W.B. Huttner.

Symposium of the Priority Programme "Cell Polarity," 2006
The role of Aspm in maintaining symmetric cell divisions in polarized NE cells. **J.L. Fish**, Y. Kosodo, W. Enard, S. Pääbo, W.B. Huttner.

IX Declaration

I hereby declare that I have produced this thesis without the prohibited assistance of any third party or other aid, except where noted. Concepts taken directly or indirectly from other sources are duly noted. This thesis has not previously been presented in an identical or similar form to any other German or foreign board of examiners.

This thesis work was conducted from the 1st of November, 2003 until the 30th of April, 2007 under the supervision of Professor Dr. Wieland B. Huttner at the Max Planck Institute of Molecular Cell Biology and Genetics in Dresden, Germany.

Dresden, 30th April 2007